DEVELOPMENT OF A SIMULATOR FOR PLASMA DISPLAY PANEL

By

Amit Vijay

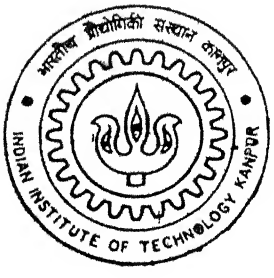

DEPARTMENT OF MATERIALS AND METALLURGICAL ENGINEERING

Indian Institute of Technology Kanpur

July, 2002

DEVELOPMENT OF A SIMULATOR FOR PLASMA DISPLAY PANEL

A Thesis Submitted
in partial Fulfillment of the Requirements
for the Degree of

MASTER OF TECHNOLOGY

by

AMIT VIJAY

to the

DEPARTMENT OF MATERIALS AND METALLURGICAL ENGINEERING

INDIAN INSTITUTE OF TECHNOLOGY, KANPUR

JULY, 2002

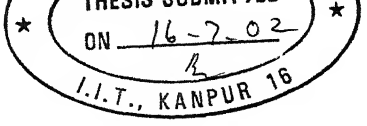

CERTIFICATE

This is to certify that the work contained in the thesis entitled "Development of a Simulator for Plasma Display Panel" by Mr. Amit Vijay has been carried out under my guidance and that this work has not been submitted elsewhere for a degree.

Dr. Deepak Gupta

Department of Material and
Metallurgical Engineering,
Indian Institute of Technology,
Kanpur.

ACKNOWLEDGEMENT

With a profound sense of gratitude, I express my sincere thanks to my thesis supervisor, Dr. Deepak Gupta, for his invaluable guidance. I am really grateful for his encouragement throughout the work and for providing me all the facilities and extended help in every possible way at IIT Kanpur.

I would also like to acknowledge thanks to my labmates Anshu, Amitesh, Surendra, Pawan, Aditya, Rohit and Asha, who have helped me throughout the work. Thanks are due to all my friends Sudhir, Siddharth, Sunil, Madhuri, Indrani, Rajil, Sankaran and Amboo who have extended their helping hand and made my presence in IIT a memorable one.

Last but not the least, I would like to thank my parents who have been a constant source of moral support and inspiration to me.

Amit Vijay

Abstract

A one dimensional model of the discharge occurring in the alternating current plasma display panel cell is developed. The model includes a continuity equation for each species and Poisson's equation. The space and time variation of the charge particle densities, electric potential, electric field and surface charge densities are described. Results are presented in a 90% Neon-10% Xenon gas mixture, for a gap length of 100 μm and a gas pressure of 560 Torr at ambient temperature. Both single pulse and multipulse simulation is done. The duration of discharge pulse is taken to be 2μs or 4μs, depending on the applied voltage. The code shows a reasonable good agreement with the published literature. The simulation shows that considering neutral density as fixed or variable does not affect the results. Voltage transfer curves and margin obtained with this model are presented. In case of multipulse simulation, the results are found to be a function of sustain voltage and not of firing voltage.

CONTENTS

Chapter 5 Results and Discussions

Chapter 6 Conclusions

Chapter 1
Introduction

1.1 Introduction

Cathode ray tubes (CRT) are by far the dominant display type in consumer application and provide very good performance at low cost but with the limitation of depth and weight. According to an estimate for a 40 inch display, the depth and weight of CRT would be 100 cm and 150 kg [1], respectively. Plasma addressed liquid crystal (PALC) display, field emission display (FED) and plasma display panel (PDP) are proposed as alternative for CRT's. But PALC and FED's have not been found to be feasible for large size displays, whereas PDP seems to be one of the most promising technologies for large size display. The limitation of PALC lies in the difficulty of producing large size, zero default, thin film transistor matrix. The factor responsible for holding back the wide scale adoption of FEDs as a flat panel display is the processing difficulties. In case of PDP, the processing difficulties are not that much and it has an advantage of small size and weight. For a 40 inch display, the depth and weight of PDP would be 10 cm and 20 kg[1], respectively.

But a considerable improvement in performance, lifetime and cost price of PDP is required. The PDP technology makes use of the light emitted by near atmospheric pressure glow micro discharges. These micro discharges are confined in small areas and provide little access for diagnostic measurements. Even PDP parameters that are measured experimentally are insufficient to provide a quantitative understanding of the discharge dynamics. As a result computer modelling is essential for understanding PDP physics and working. The goal of this work is to use one-dimensional simulation to provide better understanding of the underlying physics and also to study the effect of different parameters on breakdown of the gas mixture.

The remaining chapter deals with plasma physics, principles of PDP operation, properties of gases for discharge and the materials required for manufacturing PDPs.

1.2 Production of Discharge and Plasma.

Plasma is an electrically energized matter in a gaseous state. It is a quasineutral gas, but of unusual kind. In a normal gas, the atoms or molecules are electrically neutral, but in plasma at least few of these particles have either lost or gained an electron, so that plasma consists of free electrons and positively or negatively charged atoms and molecules known as ions along with the neutral particles. The term quasineutral means, it consists of approximately equal number of positive and negative charge. A high temperature must be reached before a normal gas can be transformed into plasma.

In order to consider the evolution of discharge, consider a cylindrical tube filled with a gas and two metal electrodes at its two ends. There are always few free electrons present due to ionization by cosmic rays, radioactive impurities or background radiations. When voltage is applied across the two electrodes, the electrons are accelerated towards the anode. During this process they collide with gas particles. If the energy imparted by these fast moving electrons to the neutral gas particles is sufficient to cause ionisation, ions and electrons are produced. Thus if one electron, during its movement towards anode, ionizes 'n' atoms, it produces 'n' electrons and 'n' ions. These n electrons, accelerated because of the effect of applied voltage, ionizes more neutral particle. This process is called avalanche or charge multiplication.

During this process of charge multiplication, electron scattering also takes place. Some electrons are deflected towards the tube wall where they are held by electrostatic image force or by surface atoms in the lattice thereby forming negative ions. The negative charge so developed grows with time. As the negative wall charge increases, the electron scattering towards the wall is decreased. However the positive ions are accelerated towards the wall. As a result of this, neutralisation between ions and electrons takes place. The neutralised energy gained is transferred to the electrons in the lattice and thus dispersed in the wall, while the newly formed neutral particle returns to the gas. When a steady state is reached, equal number of electrons and positive ions arrives per unit time on the wall, while bulk of the charge moves toward the electrode constituting the discharge current.

Figure (1.1) shows the effect of increasing the applied voltage on the discharge current, for disc electrodes of diameter 5-10 mm.

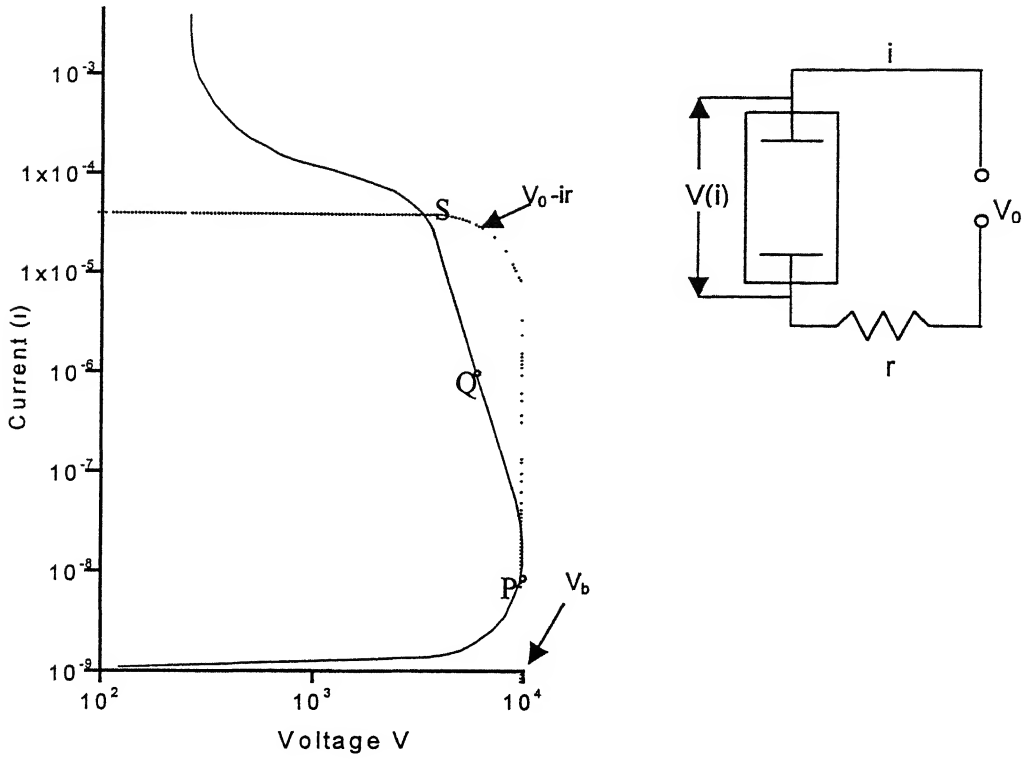

Fig. 1.1[1]: Effect of applied voltage on the discharge current.

It is assumed that the irradiation of cathode with ultra violet light or any other means results in an initial current i_o equal to $10^{-11} - 10^{-9}$ Amp.

The current, i, rises with voltage across electrode, V, first slowly and later faster, up to the point P, where $V=V_b$, the breakdown voltage. The reason for this is that the ionization rate rises as the field $E = f(V/d)$ in the gas is raised.

Beyond point P, voltage V decreases with increasing current i. The reason for this is not very well known. This could be attributed to the fact that i becomes so large that E is no longer a function of applied voltage V only but it also depends on net space charge. The charges of both sign are lost to the wall, at a rate controlled by diffusion and the radial electric field. As a result of this the electrons and ions travel radially from the gas to the wall with a common radial speed if strongly coupled, which is the case near Q. Between P and Q and further up, the

charge loss to the wall gradually drops and hence a smaller E and V with a lower rate of ionization will keep the discharge steady.

Point P divides the curve in two parts. For $V<V_b$, $di/dV >0$ and we have a non self sustaining discharge, since it can be switched off once ultraviolet light is switched off. Beyond point P, when $V>V_b$, $di/dV <0$ and the discharge is self sustaining. Irradiation is no longer needed for discharge to sustain.

The current i can be found from the point of intersection S with the V_o-ir curve, representing V(i), the voltage required across the steady discharge, and is shown as dotted line in figure 1.1, where, V_o is the source voltage and r the external resistance.

The value of breakdown voltage, V_b, depends on the product of pressure of the gas and distance between two electrodes. This is explained by Paschen curve. The Paschen curve is a plot of breakdown voltage for gases as a function of the product of gas pressure and electrode separation.

An analytical expression may be found for the breakdown voltage of a uniform field if it is assumed that breakdown is dependent on secondary emission of electrons at the cathode. The expression[9] is

$$V_b = \frac{B(pd)}{\ln(pd) + \ln\{A/[\ln(1+1/\gamma\}} \qquad (1.1)$$

where,

γ =Number of secondary electrons per ion striking the cathode, i.e secondary electron emission coefficient

p= gas pressure

d= distance between two electrodes

A &B are constant

V_b= Breakdown voltage

For a given gas mixture and cathode material γ is constant. Thus equation 1.1 shows that the breakdown voltage is a function of product of p and d.

The paschen curve is shown in figure 1.2.

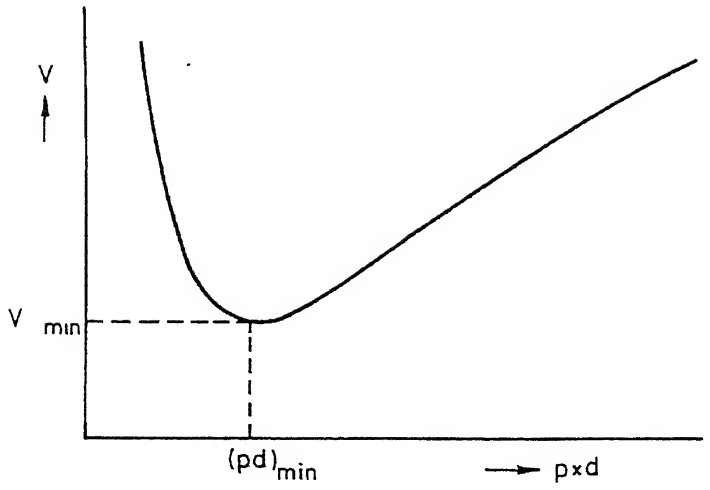

Fig 1.2: Paschen curve

From the curve it is clear that the firing voltage will remain unchanged for differing cathode/anode distances as the pressure is changed so that the product pd is a constant. This curve is mainly utilised by display engineers to minimize cost. In order to reduce drive circuit costs, it is desirable have a low firing voltage. Not much could be done on d, as any change in d will directly affect the resolution. So the display engineer has the freedom to choose p for a given d to minimize the firing voltage.

1.3 Plasma Display Panel

Plasma display panel (PDP) is a flat display in which each picture element consists of microdischarges emitting UV photons. These photons are converted into visible (red, green, blue) by phosphors deposited on the discharge walls. The displays are available in both ac and dc forms.

A large PDP consists of two glass plates, separated by a distance approximately 100 μm. Each glass plate has an array of parallel electrodes deposited on the inner wall, while ensuring transparency of the plate on the viewing side by either using a transparent electrode or a thin film. The plates are sealed together such that their electrodes are at right angle to each other and the gap between them is filled with rare gas mixture. In the case of ac displays, the electrodes are covered with a dielectric usually made up of lead borosilicate glass

and the dielectric layer by another protective coating usually of MgO. The dielectric serves as capacitor in series with the gas capacitor. The protective layer protects dielectric layer against ion sputtering, plus it helps in lowering the firing voltage of gas by emitting secondary electrons. The properties required and material used for a dielectric and protective coating, to be used in PDP, is discussed in a later section.

Figure 1.3 shows a one dimensional schematic of PDP cell. The dielectric layer deposited on the electrode and protective layer, as described above, can be seen in this.

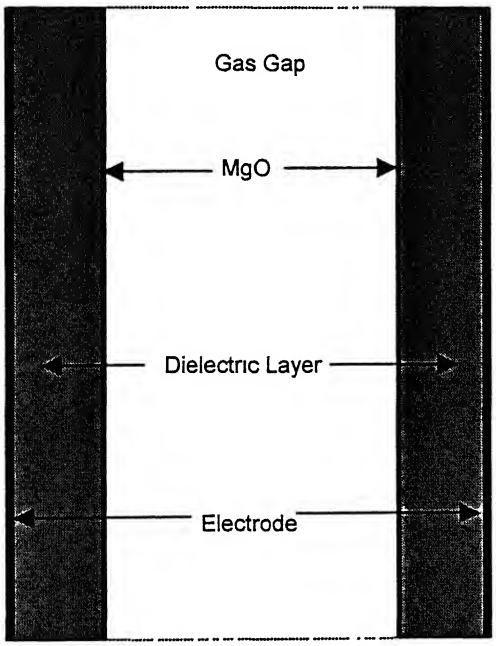

Fig. 1.3 Plasma Display Panel

The picture elements (cells) are defined by the intersection of the perpendicular electrodes. In order to operate a particular cell a voltage pulse is applied between the two electrodes that define the cell. If this applied voltage is greater than the breakdown voltage, a discharge in the gas leads to formation of weakly ionised plasma, which emits visible or UV light. In monochrome displays, the visible light of the discharge, often a orange glow, is used directly. However in colour displays, the UV emission from the discharge is used to excite phosphors in the three fundamental colours, red, blue and green. In the starting phase of development of colour PDP using gas mixture, two gases mixture, usually neon-

xenon[7][15][16] or helium-xenon[13], were used. But now three[18][19] and even four gases[20] mixture is used to improve the luminous efficiency of the colour plasma display panel.

Two kinds of electrode design are being used in plasma displays, matrix electrodes and coplanar electrodes. These are discussed in the subsequent sections.

1.2.1Matrix Plasma Display Panel

Figure 1.4 shows the schematic of a matrix plasma display panel.

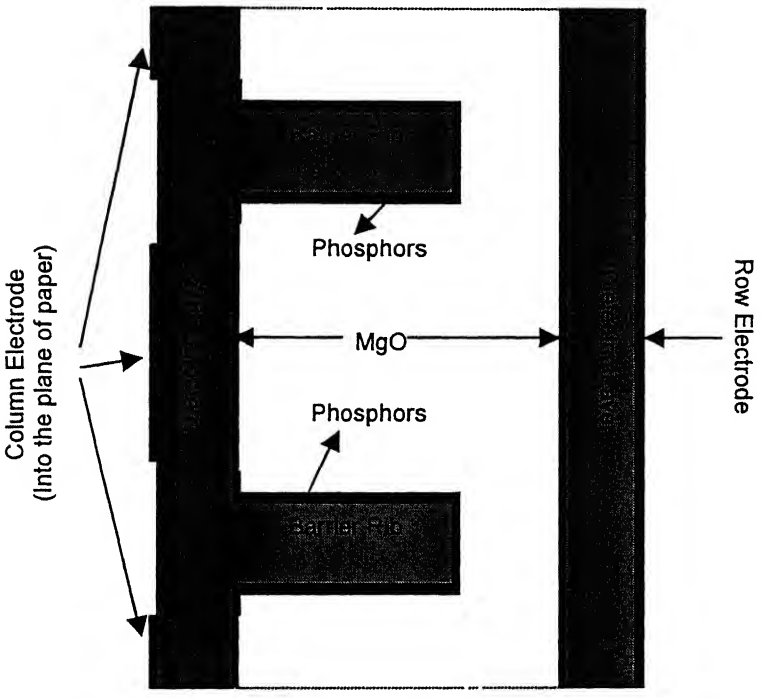

Fig 1.4 Schematic of matrix plasma display panel

In case of matrix plasma display panel the electrodes deposited on each of the two glass plates form perpendicular rows and columns of matrix. A discharge cell is formed between a row and column electrode. The dielectric barrier rib is deposited on the dielectric layer and parallel to electrode on one of the two plates. This barrier rib prevents optical interaction between the adjacent cells. A protective coating is deposited on the dielectric layer above the electrode. Phosphors are deposited on the walls of the barrier ribs. Phosphors are used to convert UV light, emitted by the discharge, into visible photons, to be used for

displaying information. The properties required and material used for a dielectric, protective coating and phosphors, used in PDP, is discussed in a later section.

Figure 1.5 describes the working of a PDP cell.

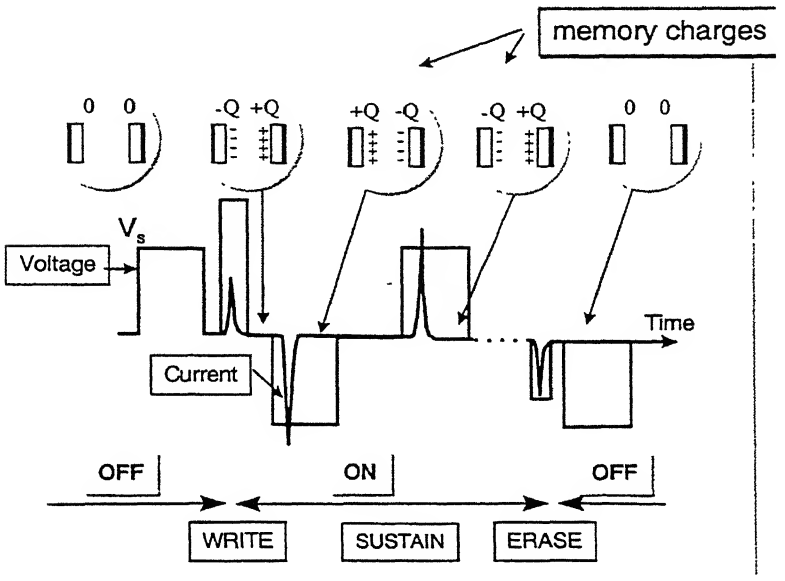

Figs 1.5[2]: Sequence of sustain, write and erase pulse.

A sustaining voltage (square wave with a frequency of 50-100 kHz), as shown in the figure 1.5, marked by V_s, is constantly applied between the row and column electrodes. The amplitude of this voltage is chosen below the breakdown voltage. During this phase the charge stored on the dielectric above two electrodes is almost zero. This is shown in the figure 1.5. This state of the cell is termed as OFF state.

In order to initiate a discharge in a specific cell, a writing voltage pulse is superimposed on the sustaining voltage such that the resulting gap voltage is larger than the breakdown voltage. Gap voltage is the voltage across the gas gap. Therefore on application of write pulse, breakdown of gas occurs usually within few tens of nanoseconds. This results in the formation of plasma, consisting of positive ions, electrons and neutral (ground state, metastable and excited) species. The positive ions move in the direction of electric field and electron moves opposite to the direction of electric field. This results in the build up of charge on

the dielectric layers deposited on the electrodes, as shown in figure 1.5. These charges deposited are called "memory charges". This is called writing of the cell.

It is seen that once discharge is initiated the discharge current density increases and reaches a peak in few nanoseconds. This is shown below in figure1.6 for Neon-10% Xenon gas mixture and for other parameters same as used in this thesis.

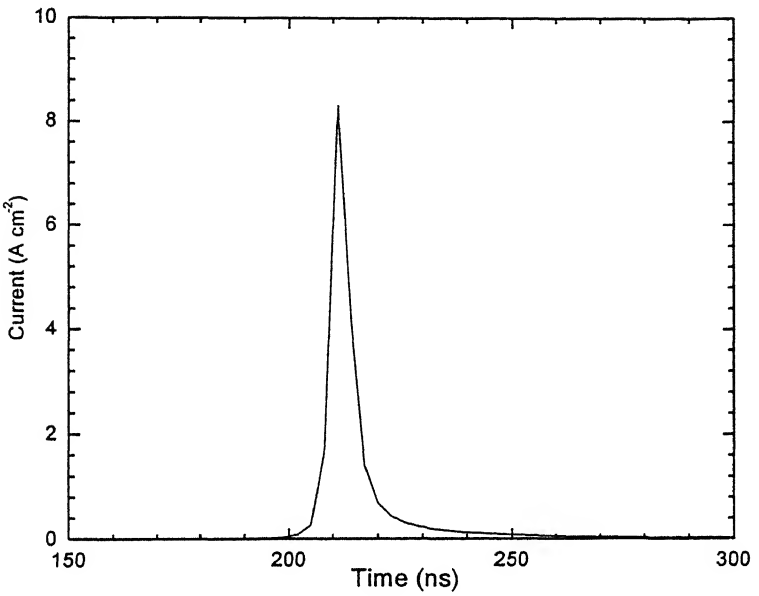

Fig 1.6 Discharge current as a function of time

The current density then decreases rapidly and reaches a value close to zero in few nanoseconds. The decrease in current density is due to the charging of the dielectric layers by electrons and ions generated in the discharge volume and flowing to the walls. The voltage induced by the charging of the dielectric layers opposes the applied voltage. This can be seen in figure 1.7 which shows the time evolution of the voltage, V_g, across the gap V_g starts to decrease during the fast current increase and goes to zero at the end of the discharge current pulse.

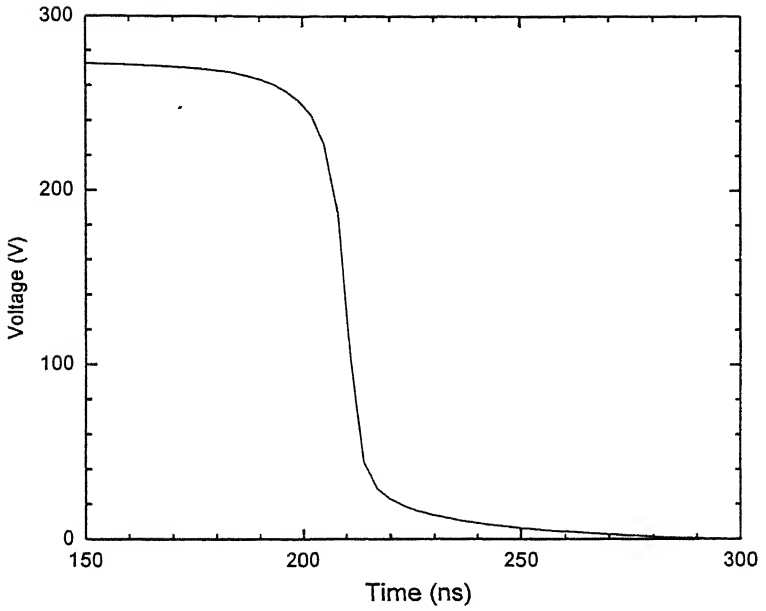

Fig 1.7 Voltage across the cell as a function of time

The dielectric continues to charge during a long time after current peak, and it takes around 100 ns for the gap voltage to drop to zero. During this time a small current density of the order of 0.5 $A.cm^{-2}$ continues to flow through the cell.

During this current pulse, large number of excited atoms is produced. Thus most of the ultra violet emission coincides with the increase in discharge current. However, the decay of UV emission can be different from the current decrease due to the different lifetimes of the excited species.

In the next half cycle the voltage across the electrode changes sign. The voltage due to memory charge in the previous half cycle now adds to the sustaining voltage. This results in another discharge pulse. This goes on for subsequent pulses, as shown in figure 1.5. This state of cell is termed as ON state.

In order to switch the cell to the off state an erasing pulse is superimposed on the sustain voltage. The voltage of the erasing pulse is such that at the end of the erasing pulse the memory charge from the wall is erased, as shown in figure 1.5. Therefore no further discharge occurs until a new write pulse is applied. The cell is switched to OFF state.

The optimum choice of the sustaining, writing and erasing voltage is deduced from voltage transfer curve that is discussed later.

1.2.2Coplanar Plasma Display Panel

Coplanar plasma display panel represents the second type of geometry, which is used in plasma display panels. The typical geometry of coplanar cell is shown in figure 1.8.

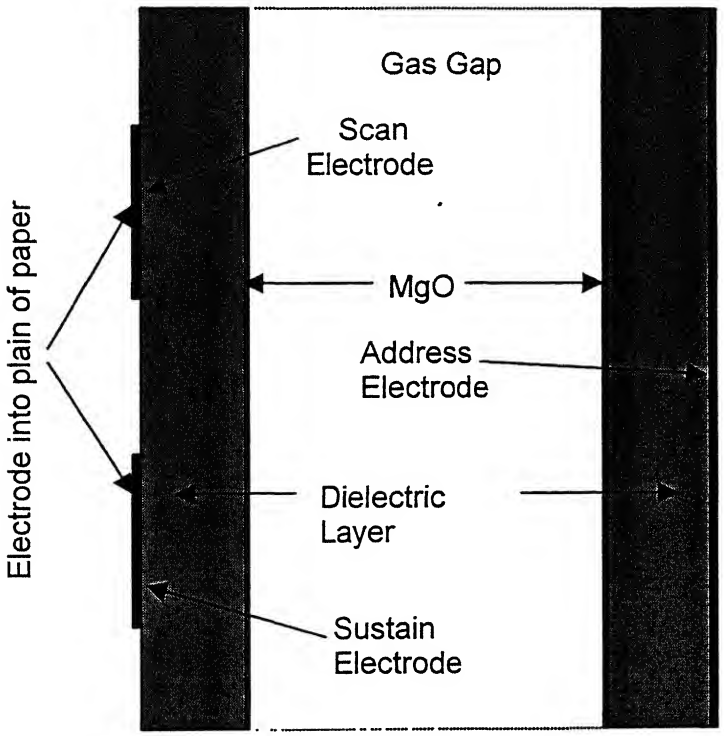

Fig. 1.8 Schematic of Coplanar Plasma Display Panel

In case of coplanar geometry, again the electrodes on the two glass plates are perpendicular to each other. However in a cell, instead of two, now we have three electrodes, with two parallel electrodes lying on one of the glass plates. The difference lies in the application of sustaining voltage. In case of coplanar plasma display panel, the sustain discharge occurs between two parallel electrodes deposited on the same glass plate. A given cell is selected by using a third electrode (address electrode) perpendicular to the coplanar electrodes and deposited on the facing glass plate.

The structure of coplanar plasma display panel is same as that of matrix plasma display panel, but with a difference that in coplanar display cell there are three electrodes. A dielectric layer is deposited on the electrodes that act as a capacitor. A protective coating is given over deposited dielectric. Dielectric barrier ribs separate the column electrodes. They are parallel to the data electrode. Hence is not visible in figure 1.8.

Each of the electrodes, has been given some nomenclature, as shown in the figure above. The electrode that is used to trigger the discharge between the coplanar electrodes is called address electrode or data electrode. The coplanar electrodes are called Scan electrode and Sustain electrode.

Similarly there is nomenclature for voltages applied to the electrode. The voltage applied to address electrode is called address voltage or data voltage. Voltage applied to scan electrode during first pulse is called scan write voltage.

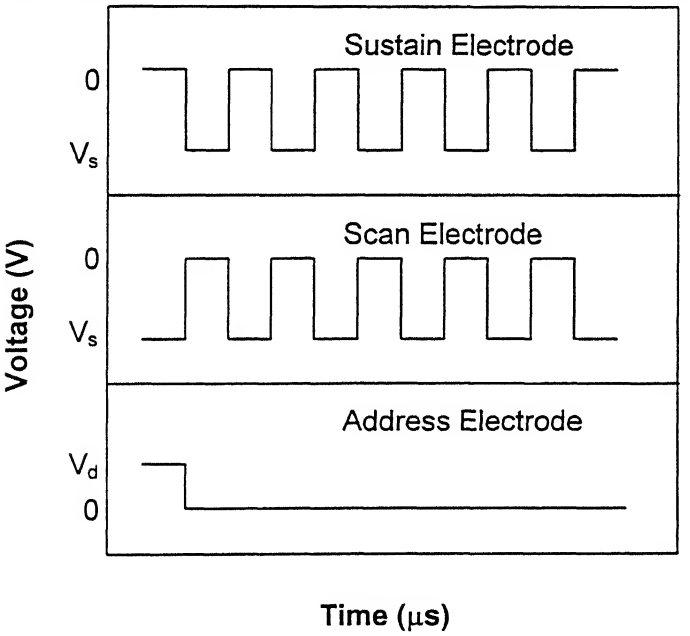

Fig 1.9 Voltage Applied to Different Electrodes

Figure 1.9 shows the voltage applied to various electrodes. V_s is the sustain voltage. V_d is the voltage applied to the address electrode, required to initiate the discharge.

In order to initiate a discharge a voltage pulse (address pulse) is applied between the scan electrode and address electrode. The sustain electrode voltage is set to zero during addressing. On application of address pulse gas breakdown

occurs, resulting in the formation of plasma. At the end of address pulse positive and negative charges are present on the dielectric surfaces above address electrode and scan electrode.

After this address pulse, a succession of sustain voltage pulse is applied between scan electrode and sustain electrode. The voltage of the address electrode is set to zero. The sustain voltage pulse is chosen in such a way, that the voltage across the scan electrode and sustain electrode is less than the breakdown voltage. But because of the charge deposited on the scan electrode the voltage across the electrode reaches a value that is greater then the breakdown voltage of the gas. Thus a discharge is initiated during first sustain pulse. During subsequent sustain pulses the discharge is formed in between sustain and scan electrode.

In order to switch the cell to the off state an erasing pulse is superimposed on the sustain voltage. The voltage of the erasing pulse is such that at the end of the erasing pulse the memory charge from the wall is erased. Therefore no further discharge occurs until a new write pulse is applied.

The optimum choice of the sustaining, writing and erasing voltage is deduced from voltage transfer curve that is discussed in next section.

1.4Voltage Transfer Curve and Stability Criteria

In an AC PDP, a cell can exist in two states, ON state and OFF state. Corresponding to these states, the applied voltage can be termed as ON voltage and OFF voltage. The ON voltage is the voltage at which a pixel comes on, i.e. in each succeeding pulse it exhibits a discharge. The OFF voltage is the voltage at which the pixel that is ON goes OFF and no more discharge occurs in the succeeding pulses. The difference between the ON and OFF voltage is defined as bistable margin.

The bistable margin defines the voltage range that will maintain the state of a pixel in its current state, i.e. pixel that is ON remains ON and a pixel that is OFF remains OFF. This bistable margin can be deduced by voltage transfer curve, which relates change in magnitude of wall voltage during a discharge to the magnitude of the voltage across the discharge site at the beginning of the discharge.

Figure 1.10 shows the essential process for a plasma display discharge site.

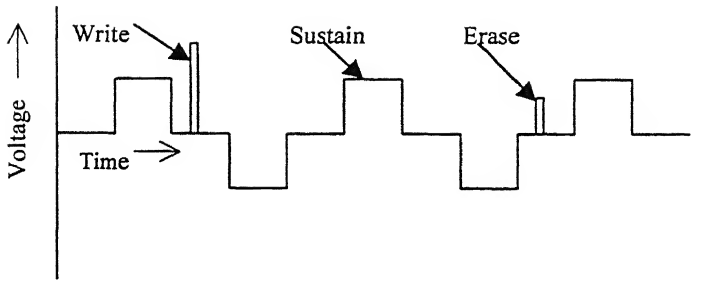

Fig. 1.10 Initiation, maintenance and termination of discharge sequence

From figure 1.10 it can be seen that a gas discharge initiated by a sufficiently high voltage pulse (ON state) reaches equilibrium after number of cycles. Later an erase pulse either terminates the sequence abruptly or establishes condition under which the sequence will terminate itself (OFF state). The behaviour of the discharge sequence is governed by the voltage transfer curve, which is shown in figure 1.11.

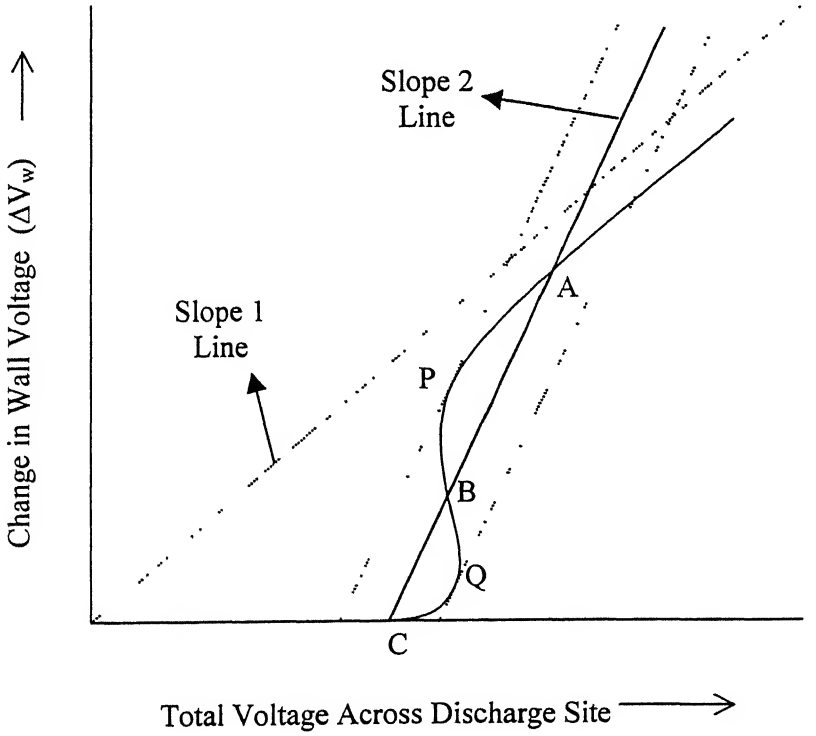

Fig. 1.11 Voltage transfer curve and locus of equilibrium points

In each half cycle the discharge is identical except for sign. Hence the magnitude of change in wall voltage is twice the wall voltage. From this we can deduce that the locus of equilibrium points is a straight line that begins at the applied voltage V_s and extends upward with a slope equal to 2. This is also superimposed in the figure 1.11. The intersection point A, B and C of the two curves are the actual equilibrium points.

When a simple rectangular sustaining voltage is applied, the condition for stability is given by following relationship[3][4][5][6]

$$| -1 + d(\Delta V_w)/d(V_c)| \leq 1$$

Replacing $d(\Delta V_w)/d(V_c)$ with 'm' we can write stability condition as

$$0 \leq m \leq 2.$$

It follows that a stable equilibrium point on the voltage transfer curve is one for which the slope is between 0 and 2. The appropriate value for display applications is m=1 because of least perturbation in the following discharge. As the value becomes different from one, the damping is less rapid.

All operating points above A will move downward toward A, all points between A and B will move upward toward A and away from B and all points between B and C will move downward away from B toward C[6]. This shows that A and C are the stable equilibrium points whereas B is unstable equilibrium point.

Thus writing of a cell (ON state) is nothing but producing wall voltage that corresponds to an operating point on the voltage transfer curve that is above the unstable equilibrium point B. The following sequence of discharge will move the operating point to A where it stabilizes. Similarly erasing a cell (OFF state) is a matter of reducing wall voltage at an ON state to a level that corresponds to an operating point below the unstable equilibrium point B. The following sequence of diminishing discharge move the operating point to C.

The dashed lines, which are tangent to the voltage transfer curve, define the range of bistability for the sustaining voltage V_s[6][7]. The maximum sustaining voltage is typically defined to be 1 V less than the ON voltage. At that maximum sustain voltage a pixel that is OFF remains OFF but at a voltage 1V higher than the maximum sustaining voltage the pixel will turn ON. The minimum sustaining voltage is defined as a voltage 1 V higher than the OFF voltage. At the minimum

sustain voltage a pixel that is ON remain ON but a voltage 1 V lower it will go OFF.

1.5 Materials used

Dielectric layer

In a PDP, a dielectric layer is deposited on a front glass substrate so as to cover the display electrodes. When a discharge occurs, positive ions are attracted towards cathode and electrons towards anode. The charges are deposited on the dielectric deposited over the electrodes. As discharge continues, charge build up takes place. This charge build up induces a potential opposing the applied potential. When the net potential, sum of applied potential and that due to charge build up, reaches a value less then the breakdown voltage of the gas, the discharge ceases. But during next part of cycle when voltage polarity is reversed, this potential due to charge build up adds to the applied voltage and thus the net potential is larger than the applied potential. Hence the discharge can occur, inspite of applied voltage lower than the gas breakdown voltage. Thus, the dielectric used plays an important role in defining the applied voltage.

For the development of a reasonable dielectric layer for a PDP, several properties are required: high transparency, high breakdown voltage, a low firing temperature, a dielectric constant below 15 and a reasonable thermal expansion coefficient to match the glass substrate (soda lime silica glass).

Pb based frits, such as $PbO\text{-}B_2O_3\text{-}SiO_2\text{-}ZnO$ glasses, are the most commonly used glass materials. They have low melting temperature, optical transparency, temperature coefficient of expansion and good discharge characteristics. However there are number of problems associated with their use. The most common problem is that the PbO present is deleterious to health and the environment.

$BaO\text{-}B_2O_3\text{-}ZnO$ glass can act as a good replacement for PbO based glass. They have low firing voltage. All the other properties are comparable with that of Pb based glass.

There are several patents for the dielectric layer. Nippon Electric glass has patented glass with the composition

-Glass powder (60-80%)

-Ceramic powder (<10%)

-TP resin (5-30%)

-Plasticizer (<10%)

Protective layer

As is discussed earlier, in a AC PDP cell, electrodes are covered with a dielectric layer. During discharge ions are attracted toward cathode and when they fall on the deposited dielectric layer, it deteriorates. In order to protect this dielectric, a protective layer 500-1000 nm thick is deposited over the dielectric.

If the protective layer on bombardment of ions created in the discharge produces a large number of secondary electrons, the gas breakdown occurs at a lower voltage. Thus the secondary electron emission coefficient, which can be defined as the ratio of number of electrons emitted to the number of ions incident on the surface, should be as large as possible.

The protective layer should have a quick discharge response. In case of AC PDP, if the response time is large, it becomes necessary to use writing pulse of long duration or writing operation must be repeated several times. Thus writing of cell becomes very slow.

Accordingly MgO is the most widely used protective layer, which satisfies all these requirements for use in PDP.

The secondary electron emission coefficient of a layer is sensitive to its energy band structure. Therefore by modifying the energy band structure of the layer, secondary electron emission property can be modified. The addition of controlled amount of TiO_2 impacts the overall electrical properties of the panel, because TiO_2 has higher dielectric constant than MgO and that the ion radius of Ti is similar to that of Mg. When the $TiO_2/(MgO+TiO_2)$ ratio is between 0.1-0.15, the secondary electron emission yield improves by 50% compared to the conventional MgO protective layer[8]. The result is reduction in discharge voltage by 12%.

CVD diamond[9] can also be used as protective coating, as its γ is very high. But its deposition on a large area glass is a problem.

Phosphors

The full colour representation is made possible through photoluminescence of the three primary colours from three kinds of phosphors, coated on their respective discharge cells. Phosphors are excited by the UV radiations produced by the gas discharge in the display cells.

The typical combinations of tricolour phosphors reported for PDPs in the time order of their development is shown in table 1.1[10] given below

Table 1.1

Blue	*Green*	*Red*
$CaWO_4:Pb^{2+}$	$Zn_2SiO_4:Mn^{2+}$	$Y_2O_3:Eu^{3+}$
$Y_2SiO_5:Ce^{3+}$	$Zn_2SiO_4:Mn^{2+}$	$Y_2O_3:Eu^{3+}$
$YP_{0.85}V_{0.15}O_4$	$Zn_2SiO_4:Mn^{2+}$	$YP_{0.65}V_{0.35}O_4:Eu^{3+}$
$BaMgAl_{14}O_{23}:Eu^{2+}$	$Zn_2SiO_4:Mn^{2+}$	$YBO_3: Eu^{3+}$
$BaMgAl_{14}O_{23}:Eu^{2+}$	$Zn_2SiO_4:Mn^{2+}$	$Y_{0.65}Gd_{0.35}BO_3: Eu^{3+}$
$BaMgAl_{14}O_{23}:Eu^{2+}$	$BaAl_{12}O_{19}:Mn^{2+}$	$Y_{0.65}Gd_{0.35}BO_3: Eu^{3+}$

The last combination in the table 1.1 has been widely adopted for colour PDPs. The main advantages of this combination are

a) High conversion efficiency to visible luminescence from UV radiations.
b) Wide reproducible colour gamut.
c) White colour representation at equal discharge current.
d) No serious damage to other panel characteristics.

1.6Species Involved in Gas Discharge

Gas Discharge consists of electrons, positive ions and neutral species. Electrons and positive ions are formed by ionisation of neutral species. There are three type of neutral species; ground state, excited state and metastable state. The lowest energy state of the atom is the ground state. The other energy states where electrons are still bound to the particle are excited state and metastable state.

When an accelerated electron collides with the neutral atom it gives part of its energy to atom. If this energy imparted to an electron in the atom is high enough

to cross the ionisation barrier of the atom, it results in the formation of ions and electrons. For example in Ne-Xe mixture, ionisation results in formation of Xe^+, Ne^+, Xe_2^+, Ne_2^+ and $NeXe^+$ ions. But if this imparted energy is less than the ionisation barrier, it results in the excitation of the electron in the atom to a higher energy state. The electron is still bound to the atom. The lifetime of these states is generally short (10^{-8} -10^{-6} s). This state of atom is called excited state. For example in case of Ne-Xe mixture it results in formation of $Xe^*(^3P_1)$, Xe^{**}, Xe^{***}, $Xe_2^*(O_u^+)$, $Xe_2^*(^3\Sigma_u^+)$, $Xe_2^*(^1\Sigma_u^+)$ and Ne^* [7]. The transition of these states to ground state occurs spontaneously which result in emission of radiations.

But sometimes, electronic excitation or radiative de-excitation can cause the transition of an electron to an energy level from which, the transition rules forbid a spontaneous transition to a lower energy level. The lifetime of such a state is higher than that for excited atoms. This state of atom is called a metastable state. For example in Ne-Xe mixture, it results in formation of $Xe^*(^3P_2)$ [7]. Such states can be de-excited only by collisions with other particles or by absorption of radiative energy.

1.7Gas Discharge Reactions

There are various types of reactions involved in the gas discharge. They are categorised as ionisation, penning ionisation, excitation, dimer ion formation, electron ion recombination, charge exchange, neutral kinetics and spontaneous emission reactions.

Ionisation is the most vital reaction of a gas discharge used in plasma displays. When an electric field is applied across the gas, the electrons within the gas are accelerated and collide with neutral gas atoms. These collisions can cause an electron to be ejected from the neutral atom, thereby creating a positive ion and an extra free electron. This ionisation process can be direct or stepwise. In case of direct ionisation, electron collides with ground state atom and produces electron and positive ion. Consider, for example, the direct ionisation of Ne atom. The reaction is

$$e^- + Ne \rightarrow Ne^+ + 2e^-$$

In the case of stepwise ionisation, electron collides with excited or metastable atom and produce electron and positive ion. Stepwise ionisation of Ne metastable atom is shown below.

$$e^- + Ne^* \rightarrow Ne^+ + 2e^-$$

Penning ionisation is a process in which ions are produced, when atoms or molecules in a gas collide with metastable atoms. This help in reduction of firing voltage. For Ne-Xe mixture the penning reaction proceeds as

$$Ne^* + Xe \rightarrow Ne + Xe^+ + e^-$$

Excitation reactions are those reactions in which an accelerated electron collides with a ground state atom and impart part of its energy to the neutral atom. But this energy is not sufficient for electron in the atom to break free. So this results in the transition of the electron to a higher energy state, even though it is bound to the atom. This results in the formation of excited and metastable atoms. For Ne atom this reaction takes place according to.

$$e^- + Ne \rightarrow Ne^* + e^-$$

In dimmer ion formation reaction, positive ion reacts with neutral atom to form dimmer. For Neon atom this reaction is

$$Ne^+ + 2Ne \rightarrow Ne_2^+ + Ne$$

In electron ion recombination reaction, electron and positive ions recombine to form neutral atoms. For neon atom the reaction proceed as

$$Ne_2^+ + e^- \rightarrow Ne^* + Ne$$

In charge exchange reactions, exchange of charge takes place between positive ion and neutral atom. In these reactions, one positive ion collides with neutral atom and results in ionisation of that neutral atom. This is shown below for Ne-Xe mixture.

$$Ne_2^+ + Ne + Xe \rightarrow Xe^+ + 3Ne$$

Neutral kinetics involves reaction between neutral species as is given for Ne-Xe mixture.

$$Xe^{**} + Ne \rightarrow Xe^* + Ne$$

In spontaneous reactions, the excited atom spontaneously comes to ground state emitting radiations.

$$Xe^*(^3P_1) \rightarrow Xe + h\upsilon(147\,nm)$$

These UV radiations emitted, excite the phosphors deposited in three fundamental colours, red, blue and green.

1.8 Gas mixture used and reactions involved for that gas mixture

In this thesis Neon–10%Xenon gas mixture is used. Table (1.2) shows the various reactions that are involved during a gas discharge[7]. For the mixture used, there are various type of species involved in the discharge. In total there are electron, positive ions (Xe^+,Ne^+,Xe_2^+,Ne_2^+,$NeXe^+$), ground state particle (Xe, Ne), metastable particle ($Xe^*(^3P_2)$) and excited states ($Xe^*(^3P_1)$, Xe^{**}, Xe^{***}, $Xe^*_2(O^+_u)$, $Xe^*(^3\Sigma^+_u)$, $Xe^+_2(^1\Sigma^+_u)$ and Ne^*).

Table 1.2

Reaction	Energy (eV)	Rate Coefficient	Ref
Direct Ionization			
$e + Xe \rightarrow Xe^+ + 2e$	12.12		b
$e + Ne \rightarrow Ne^+ + 2e$	21.56		b
Stepwise Ionization			
$e + Xe^*(^3P_2) \rightarrow Xe^+ + 2e$	3.8		b
$e + Xe^*(^3P_1) \rightarrow Xe^+ + 2e$	3.68		b
$e + Xe^{**} \rightarrow Xe^+ + 2e$	2.54		b
$e + Ne^*(^3P_0 - ^3P_2) \rightarrow Ne^+ + 2e$	4.95		b
Penning Ionisation			
$Ne^* + Xe \rightarrow Ne + Xe^+ + e$		7.5×10^{-11} cm^3 s^{-1}	
$Ne^* + Xe \rightarrow NeXe^+ + e$		2.3×10^{-11} cm^3 s^{-1}	
Excitation			
$e + Xe \rightarrow Xe^*(^3P_2) + e$	8.32		b

$e + Xe \rightarrow Xe^{*}\left(^{3}P_{1}\right) + e$	8.44		b
$e + Xe \rightarrow Xe^{**} + e$	9.58		b
$e + Xe \rightarrow Xe^{***} + e$	11		b
$e + Ne \rightarrow Ne^{*}\left(^{3}P_{0} - {}^{3}P_{2}\right) + e$	16.61		b
Dimer Ion Formation			
$Ne^{+} + 2Ne \rightarrow Ne_{2}^{+} + Ne$		$4.4\text{x}10^{-32}$ cm^{6} s^{-1}	
$Ne^{+} + Xe + Ne \rightarrow NeXe^{+} + Ne$		$1.0\text{x}10^{-31}$ cm^{6} s^{-1}	
$Xe^{+} + 2Ne \rightarrow NeXe^{+} + Ne$		$1.0\text{x}10^{-31}$ cm^{6} s^{-1}	
$Xe^{+} + 2Xe \rightarrow Xe_{2}^{+} + Xe$		$2.5\text{x}10^{-31}$ cm^{6} s^{-1}	
$Xe^{+} + Xe + Ne \rightarrow Xe_{2}^{+} + Ne$		$1.5\text{x}10^{-31}$ cm^{6} s^{-1}	
Electron Ion Recombination			
$Ne_{2}^{+} + e \rightarrow Ne^{*} + Ne$		$3.7\text{x}10^{-8}$ Te$^{-0\,43}$ cm^{3} s^{-1}	
$Xe_{2}^{+} + e \rightarrow Xe^{**} + Xe$		$2\text{x}10^{-8}$ Te$^{-0\,5}$ cm^{3} s^{-1}	
$NeXe^{+} + e \rightarrow Xe^{**} + Ne$		$8\text{x}10^{-8}$ Te$^{-0\,5}$ cm^{3} s^{-1}	
Charge exchange			
$Ne_{2}^{+} + Xe + Ne \rightarrow Xe^{+} + 3Ne$		$4.0\text{x}10^{-30}$ cm^{6} s^{-1}	
$NeXe^{+} + Xe \rightarrow Xe_{2}^{+} + Ne$		$5.0\text{x}10^{-12}$ cm^{3} s^{-1}	
$NeXe^{+} + Xe \rightarrow Xe^{+} + Xe + Ne$		$5.0\text{x}10^{-10}$ cm^{3} s^{-1}	
Neutral Kinetics			
$Xe^{**} + Ne \rightarrow Xe^{*}\left(^{3}P_{2}, {}^{3}P_{1}\right) + Ne$		$2.0\text{x}10^{-12}$ cm^{3} s^{-1}	
$Xe^{**} + Xe \rightarrow Xe^{*}\left(^{3}P_{2}, {}^{3}P_{1}\right) + Xe$		$1.0\text{x}10^{-10}$ cm^{3} s^{-1}	
$Xe^{*}\left(^{3}P_{1}\right) + Ne \rightarrow Xe^{*}\left(^{3}P_{2}\right) + Ne$		$3.11\text{x}10^{-14}$ cm^{3} s^{-1}	
$Xe^{*}\left(^{3}P_{2}\right) + Ne \rightarrow Xe^{*}\left(^{3}P_{1}\right) + Ne$		$1.62\text{x}10^{-16}$ cm^{3} s^{-1}	
$Xe^{*}\left(^{3}P_{1}\right) + Xe \rightarrow Xe^{*}\left(^{3}P_{2}\right) + Xe$		$2.18\text{x}10^{-14}$ cm^{3} s^{-1}	
$Xe^{*}\left(^{3}P_{2}\right) + Xe \rightarrow Xe^{*}\left(^{3}P_{1}\right) + Xe$		$1.26\text{x}10^{-16}$ cm^{3} s^{-1}	
$Xe^{*}\left(^{3}P_{1}\right) + 2Xe \rightarrow Xe_{2}^{*}\left(O_{u}^{+}\right) + Xe$		$1.55\text{x}10^{-31}$ cm^{6} s^{-1}	
$Xe^{*}\left(^{3}P_{2}\right) + 2Xe \rightarrow Xe_{2}^{*}\left(^{3}\Sigma_{u}^{+}\right) + Ne$		$8.53\text{x}10^{-32}$ cm^{6} s^{-1}	

$Xe^*(^3P_1) + Xe + Ne \rightarrow Xe_2^*(O_u^+) + Ne$	4.07×10^{-32} cm^6 s^{-1}
$Xe^*(^3P_2) + Xe + Ne \rightarrow Xe_2^*(^3\Sigma_u^+) + Ne$	1.35×10^{-32} cm^6 s^{-1}
$Xe_2^*(O_u^+) + Xe \rightarrow Xe_2^*(^1\Sigma_u^+) + Xe$	2.6×10^{-10} cm^3 s^{-1}
Spontaneous emission	
$Xe^{**} \rightarrow Xe(^3P_2, ^3P_1) + h\upsilon$	3×10^7 s^{-1}
$Xe^*(^3P_1) \rightarrow Xe + h\upsilon$ (147 nm)	2.7×10^6 s^{-1}
$Xe_2^*(^1\Sigma_u^+) \rightarrow 2Xe + h\upsilon$ (173 nm)	5×10^8 s^{-1}
$Xe_2^*(^3\Sigma_u^+) \rightarrow 2Xe + h\upsilon$ (173 nm)	1.66×10^8 s^{-1}
$Xe_2^*(O_u^+) \rightarrow 2Xe + h\upsilon$ (150 nm)	9×10^6 s^{-1}

b Calculated as a function of E/N, with a Boltzmann code

Chapter 2

Literature Review

2.1Introduction

The technology for plasma displays has been around for almost three and half decades. Indeed large area plasma display panel has been commercially available since 1970. Extensive research, in order to understand the physics and working of a PDP, has lead to improvement in the efficiency of a PDP cell.

Last decade saw some extensive work been done in this field. During this period large size colour monitors using PDP were manufactured on commercial scale. Some of the major producers of monitors using PDP are LG Electronics, Fujitsu Limited, Sony Electronics and Thomson Electronics.

Apart from the different gas mixtures used, the work done by various researchers differs in the modelling approach adopted. There are mainly two modelling approaches i.e. fluid approach and particle approach.

In the fluid approach, plasma particle species are represented by macroscopic properties such as particle number density, flux etc. The space and time variation of these quantities are expressed by fluid equation. Boundary condition of the fluid equation describes the processes occurring at the surface. But in these fluid equations and boundary conditions, many assumptions are made which restricts their use to a limited range of discharge conditions. None the less, they are computationally efficient, implying a short simulation time.

The second type of approach is particle approach, also known as Monte Carlo method. In this method individual particle are considered. Since it is impossible to calculate the path of all the particles, only a small number of particles, which represent the whole sample, are studied. As no assumptions are made, this approach can be used for a wide range of discharge conditions. But this method takes a long computational time. This restricts its use for complex geometries.

In order to take advantages of both the approaches, these two methods are combined in a hybrid model. In hybrid model one part of the particles, ions, neutral and slow electrons, are described by fluid equation and other part, fast secondary electrons, are treated with Monte Carlo simulation.

2.2Work done in last decade

Meunier et al[7] provided a one-dimensional model for discharge in a Neon-10%Xenon gas mixture. A fluid model consisting of continuity equation and momentum transfer equation, with the local field approximation, was used. These equations are coupled with poisson's equation for electric field and with a set of kinetic equations characterizing the evolution of excited species leading to UV emission. In order to descritize the continuity equation, Sharfetter-Gummel method was used. The method of integration of continuity and field equation was explicit in time. In their work, the effect of stepwise ionisation and penning ionization was found to be negligible.

Veerasingam et al[11][12] also investigated the one dimension simulation for single gas, Helium, as well as gas mixture filled ac plasma display cell. Helium was used, because data for the cross section for ionization and excitation for the various atomic states of Helium were well known. The model used includes, continuity equation, poisson's equation and circuit equation. The circuit equation couples panel to the power supply. They have reported the work for the simulation of 100% He, 100%Xe and 2%Xe in He gas mixture. Work was carried out for both single pulse and multipulse. In case of Xe2%-Ne mixture, the rate of ionization of ground state of Xenon was much higher then the ionization of same in pure Xenon. This can be attributed to the change in electron velocity distribution function in the mixture. This in turn lowers the firing voltage. The secondary electron emission is important to initiate the process and without secondary electrons the process is halted. The secondary electron enhances the ionization and excitation in the discharge and a large value of secondary electron emission coefficient reduces the firing voltage.

The work of Meunier et al and Veerasingam et al, differ in equation solving technique and the method adopted for descritizing. Meunier et al have used explicit method of solving the equation. This method is very easy to implement, but with the limitation of time step for integration. Smaller time steps might lead to instability. The time step chosen, was of the order of 10^{-12} seconds. Whereas Veerasingam et al have used implicit method. In case of implicit method, there is no constraint of the time step, but then this method is computationally intense and

may be unstable. The method of descritization used by them is also different. Meunier et al uses Scharfetter-Gummel method of descritization, whereas, Veerasingam et al have used central difference scheme. But it is seen that the use of any other scheme, apart from Scharfetter-Gummel method, might lead to instability. Thus for one dimensional simulation, implicit method with Scharfetter-Gummel descritization scheme can be used.

In a time dependent two dimensional model by Veerasingam et al for matrix geometry[13], continuity equations for charged particle and excited neutral species were coupled with the Poisson's equation, a radiation transport equation, a surface charge equation and an external L-C-R circuit equation. These equations were solved using fully implicit numerical method. Single gas, Helium, was used in the panel for discharge. In order to match the multipulse data, secondary electron emission coefficient was roughly a factor of two larger than that required for single pulse data, for the same reaction rate. This could be attributed to the fact that the dependence of emission from the MgO surface is a function of its history. They have also studied the plasma flow and charge spreading across barrier pixels, for the same case but with a gas mixture of 2% xenon in neon[14]. Simulation of adjacent pixels separated by a barrier height equalling 80% of the gap height revealed that there is plasma transport through the gap to the adjacent pixel, which is in the sustained off state. For low resolution displays, the plasma overflow does not cause a gas discharge in the adjacent off pixel, while for a higher resolution display a 20% gap in the barrier height could result in the breakdown in the adjacent off pixel. A higher picture resolution implies smaller pixel pitch or width. This requires, higher firing voltage and sustain voltage, in order to increase the electric field and hence the ionization source, to compensate for increased particle losses, as a result of the reduced particle transit times to the side barrier. The plasma overflows through the gap to the adjacent pixel, in order of 10^{18} m^{-3}, which is sufficient to cause local ionization in the pixel thereby turning it ON.

Punset et al[15] worked on the two dimensional simulation of an alternating current matrix plasma display cell with Ne-10%Xe gas mixture. The coupling between the electrical model and excited species kinetics is weak under the

operating conditions of a plasma display panel, so the excited species kinetics was not included in the simulation work. The descritization was based on Scharfetter-Gummel finite difference scheme. The electrical model consists of moment equations for electron and ion transport coupled with Poisson's equation for the electric field. These equations were integrated using semi implicit method. The simulation of a single pulse with no memory charge and with an applied voltage across the electrodes equal to twice the sustaining voltage gives a good representation of the main properties of the discharge pulses in the ON state. For their geometry, barrier ribs did not induce charged particle losses to the walls but when the barrier ribs were absent, overlap of discharges in the adjacent cells occurred and this made it impossible to control them separately. The height of ribs was an important factor. If the height of rib to total gap length ratio was decreased from ¾ to ½, strong electrical interactions were found. Most of the ionization in the discharge was due to electron impact ionization from the ground state of the Xenon and Neon atoms.

The approach of Veerasingam et al and Punset et al, for two dimensional simulation of matrix plasma display, is different in many respects. Veerasingam et al have considered the excited species kinetics, which is neglected by Punset et al. For voltage margin studies and I-V characteristics, one need only treat ions and electrons. But if detailed spectral information is required, excited kinetics must also be included. Veerasingam et al have used finite difference method for descritization of equations and have fully implicitly solved these equations, whereas Punset et al makes use of Scharfetter-Gummel method for descritization and have solved it explicitly. In order to make use of the advantages of both the approaches, semi implicit method with Scharfetter-Gummel descritization scheme can be used. In case of semi implicit integration of equations, for solving transport equations at any time t+1, electric field is taken at time t+1 and not at time t, as is the case of explicit integration. The semi implicit technique is stable for time step much larger than to what it is in case of explicit technique.

In a related work, Punset et al[16] investigated the addressing and sustaining of an alternating current coplanar plasma display cell. The discharge model used was same as used by Punset et al[15] for matrix geometry. Semi implicit method for

simulation of Neon-5%Xenon gas mixture was used. Various terminologies used for coplanar PDP working were explained, along with different driving methods. The excited species model was decoupled from the electric model of the discharge because in a typical PDP condition the energy density dissipated by electrons in the cell at each discharge pulse was low. The density of excited species in the discharge was not found to be large enough for stepwise excitation or ionization process to strongly influence the time evolution of the plasma density and electric field in the discharge.

Hagelaar[17] used Ne-5% Xe gas mixture for simulation in coplanar geometry, using fluid model with the continuity and momentum transfer equation. However, the manner in which the reaction rates and transport properties dependence on reduced local electric field were handled was different for positive ions and electrons. For positive ions, local field approximation was used, while for electrons, these properties were calculated as a function of the electron mean energy. The boundary equations used were also different from the usually used boundary equations. Apart from the flux due to local particles at the wall, an extra factor for the flux due to random motion of particles within a certain mean path from the wall was also included. Electrons were treated in two groups, electron coming from bulk and electrons emitted by the surface. Both groups were treated equally and indistinguishably with the drift diffusion equation, but have different boundary equations. The usually used boundary condition implies that all the electrons in front of surface contribute to the diffusion flux to the wall, including the electrons emitted by secondary emission. Whereas it has been demonstrated by several studies that in reality, virtually no emitted electrons are scattered back to surface if a high enough electric field (>100 V cm^{-1} $Torr^{-1}$) is present, as is typically the case in front of cathode surfaces. Thus in order to avoid overaccounting of the backscattering of emitted electrons, they were treated in two groups. It was seen that the largest part of electrical energy was transferred to ions and subsequently to the gas and the surface. The electrical energy transferred to electrons was mostly used for ionization and excitation. The part used for xenon excitation largely ends up in UV radiation. The efficiency of discharge in

generating UV photons increases with increasing secondary electron emission coefficient. It also increases with increasing sustain voltage.

In the work of Punset et al, explained above for coplanar geometry, local field approximation was used, for positive ions as well as for electrons. This might lead to unsatisfactory results, because of poor energy transfer in electron-neutral collisions, due to huge mass difference. This problem can be removed by using different scheme for electrons, as is done by Hagelaar et al. Also in the work of Hagelaar et al, the problem of overaccounting of the backscattering of emitted electrons is eliminated. Thus we can say that the approach of Hagelaar et al might lead to better simulation results.

Rauf and Kushner[18][19] developed a two dimensional hybrid plasma display panel model for dc pulsed coplanar electrode geometry, using a three gas mixture of He/Ne/Xe = 70/26/4. The basic purpose of using Xe in the mixture was that Xe gas mixture generates UV photons, which are converted into visible light through phosphors. The model used, implicitly integrates the coupled set of Poisson's equation and continuity equation for charged particles. The density of neutral species was calculated using explicit time integration. The model had a Monte Carlo simulation for fast secondary electrons. The electron temperature was calculated by solving the electron energy conservation law.

Byoung-Kuk Min et al [20] used zero dimensional simulation to calculate the densities of different species and electron temperature for He-Ne-Xe-Ar mixture. The work includes finding of the optimum mixing condition of the mixture. The effect of argon mixing ratio ranging from 0% to 10% on the electron temperature and various densities was studied. The electron temperature decreases as the Ar mixing ratio increases and the density of Xe^* increases with argon mixing ratio from 0.1% to 0.5%, when compared with the three component gas He-Ne-4% Xe. This shows that the luminance of the four-component gas He-Ne-Xe-Ar with Ar gas mixing ratio of around 0.5% will be higher than that of the three component gas He-Ne-Xe.

The work of Byoung et al clearly shows that by adding fourth gas in the mixture, luminance of gas mixture can be increased.

Chapter 3

Model of Microdischarge

3.1Introduction

Modelling has become a very important and useful tool in the research of complex phenomena that involves many aspects of physics at the same time. Models are used to theoretically interpret and predict experimental observations. As is discussed in chapter 2, there are mainly two modelling approaches i.e. fluid approach and particle approach.

In this chapter we describe the physical equations and data that define the fluid model. In section 3.2 simple model of PDP discharge cell is discussed. Before outlining the basic system of equations in section 3.4, in section 3.3 various assumptions made are stated. After that, in section 3.5, boundary conditions for the basic equations are explained. In the end, in section 3.6, sources of various input data are discussed.

3.2 Model of PDP discharge cell

A complete model of a PDP discharge is schematically shown in figure 3.1.

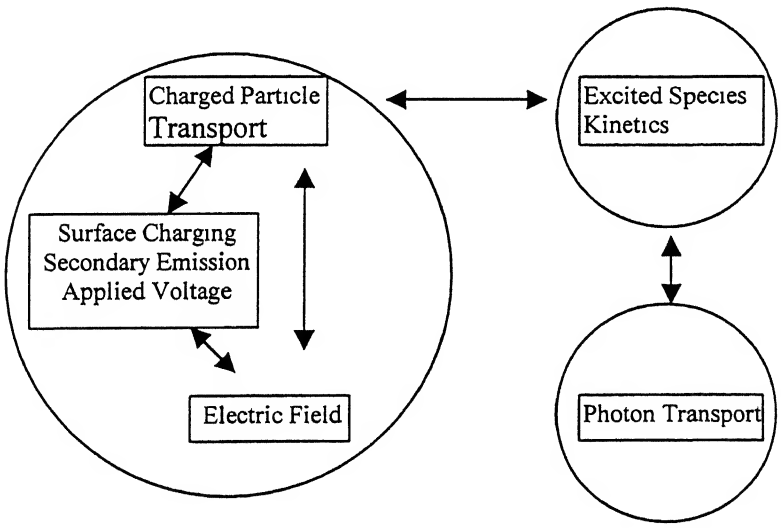

Fig. 3.1[21]: Schematic of discharge model

The central part of the model is related to the description of the electron and ion transport in the electric field, taking into account the voltage waveform and

charging of the dielectric surface. This part of model is usually termed as "electric model". The energy deposition by electrons leads to ionisation and excitation of the gas mixture. The reactions between excited species, charged particles and neutral atoms lead to the production of photons. This is discussed in second part of model. The photon transport is described in third part of the model. These three parts of models are coupled together.

3.3 Assumptions

Fluid model is used in this thesis. In fluid model continuity and momentum equation is used. However in these equations there are certain quantities, like ionisation frequency and electron mobility, which cannot be expressed as a function of charged particle density or velocity. These quantities are averaged over the electron energy distribution function that is not known, since Boltzmann equation is not solved. So in order to take care of this, Local Field Approximation is used.

LFA assumes that the electron distribution function, at a given location and time, is same as that corresponding to a uniform electric field, for the value of the electric field that exists at this location and time in the discharge. This assumption is equivalent to assuming that the energy gain due to electric field at a particular location and time is exactly balanced by the energy losses due to collisions at that location and time. Thus no energy equation is needed. In that case the frequencies and other transport parameters are pre-tabulated as a function of reduced electric field (E/N or E/p, where E is the electric field, N is the gas density and p is the gas pressure) and the value for a particular E/N or E/p is taken from this pre-tabulated table directly.

Apart from LFA, we have made additional assumptions in our simulation work.

(a) Since the degree of ionisation is small, the temperature of gas particle is assumed to be constant.

(b) The ion temperature is assumed to be equal to gas temperature.

(c) The electron temperature is also assumed constant such that $kT_e = 1eV$, where k is Boltzmann constant and T_e is electron temperature.

(d) The mobility of charged particle is assumed to be a function of E/p or E/N.

(e) Secondary electron emission coefficient is assumed to be constant with respect to E/N or E/p.

(f) It is assumed that the charged particle transport coefficient satisfy the Einstein relation $D = kT\mu/q$, where D is diffusion coefficient of particle, k is Boltzmann constant, T is the temperature of charged particle, μ is the mobility of charged particle and q is the charge of particle.

(g) Diffusion coefficient of neutral species is assumed to be equal to that of corresponding positive ion.

3.4 System of fluid equations

Figure 3.2 shows a simple PDP cell, with all the nomenclature as used in the remaining part of the thesis.

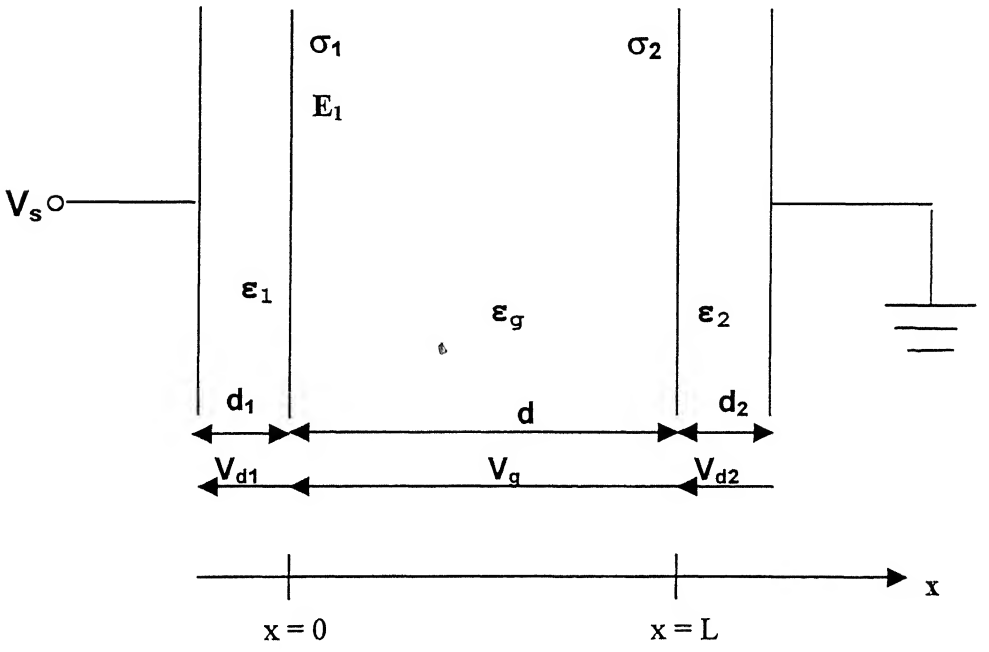

Fig 3.2: Simple PDP cell

In the figure 3.2

V_s is the applied voltage

σ_1 and σ_2 are the charge density on the left and right electrodes, respectively.

ε_1, ε_2 and ε_g are the dielectric of left dielectric, right dielectric and gas gap, respectively.

d_1, d_2 and d are the thickness of left dielectric, right dielectric and gas gap, respectively.

V_{d1} and V_{d2} are the voltage drops across the left and right dielectric, respectively.

V_g is the voltage drop across the gas gap.

Simulation domain, considered in this thesis work, is $0 < x < L$. This implies that all the fluid equations considered, are solved in this domain only.

In this thesis fluid approach is used and the behaviour of plasma particle is described by the continuity equation and the momentum transfer equation. These equations are coupled with the Poisson's equation for the electric field.

Poisson's Equation

Poisson's equation is written as

$$\nabla \cdot \mathbf{E} = \frac{\rho}{\varepsilon} \tag{3.1}$$

$$\mathbf{E} = -\nabla \cdot V \tag{3.2}$$

where,

ε is the permittivity of the region

ρ is the space charge density

V is the electrostatic potential

The space charge density ρ can be calculated using density of charged particle as

$$\rho = \sum q_p n_p \tag{3.3}$$

where,

q_p is the charge of particle

The Poisson's equation is solved everywhere in the region, i.e., in the gas gap as well as the dielectric region.

For given distribution of ρ and values σ_1 and σ_2, such that $\sigma_1 + \sigma_2 = -\int_0^L \rho dx$ (for charge neutrality), solution of the Poisson's equation is available (Appendix 1) and is given by

$$\mathbf{E}(x) = \frac{1}{\varepsilon_g}\int \rho dx + \mathbf{E}_1 \tag{3.4}$$

where, E_1 is the electric field on the left electrode, as shown in figure 3.2.

The analytical solution for E_1 is also given in Appendix 1 and it can be written as

$$\mathbf{E}_1 = \frac{V_s - A + \frac{\sigma_1}{\varepsilon_1}d_1 + \frac{\sigma_1}{\varepsilon_2}d_2}{\frac{\varepsilon_g}{\varepsilon_1}d_1 + \frac{\varepsilon_g}{\varepsilon_2}d_2 + d} \tag{3.5}$$

where, $A = \int_0^d \left(\frac{1}{\varepsilon_g}\int_0^x \rho dx \right) dx$

Fluid Equations

The continuity equation, for a particle of type p, is given by

$$\frac{\partial n_p}{\partial t} + \nabla \cdot \mathbf{J}_p = S_p \tag{3.6}$$

where,

n_p gives the density of plasma particle of type p

S_p indicates the net source term of the particle p.

$\mathbf{J}_p$ is the flux of particle

p = e, for electrons

= i, for ions

= n , for neutral species

Flux

The flux **J** is given by momentum transfer equation. This flux consists of two terms, drift term due to electric field and diffusion term due to concentration gradient. Thus this flux for charged particle, p, can be written as

$$\mathbf{J}_p = \mathrm{sgn}(q_p)\mu_p \mathbf{E} n_p - D_p \nabla n_p \qquad (3.7)$$

where,

E is the electric field.

$\mathrm{sgn}(q_p)$ is the sign of particle charge, negative for electron, positive for ions and zero for neutral species.

μ_p is the mobility of particle.

D_p is the diffusion coefficient of particle.

Source Term

The source term, S_p, included in the continuity equation, is the net source term for particles of type p. The net source of the particle implies, a positive contribution from the reactions in which particle p is created and a negative contribution from those reactions in which particle p is lost.

S_p can be written as

$$S_p = \sum c_{p,r} R_r \qquad (3.8)$$

The index r refers to a reaction.

$c_{p,r}$ is the net number of particle p created in the reaction r. This could be negative or positive, depending upon whether the particle is lost or generated in that reaction r.

The term R is the reaction rate of the reaction.

Consider reactions which do not involve electrons, for example

$$Ne^+ + Xe + Ne \rightarrow NeXe^+ + Ne$$

This reaction can be treated as a source for $NeXe^+$ ion and sink for Ne^+ ion.

Hence for Ne^+ ion, $c_{p,r}$ is 1 and

$$R = k_r n_{Ne^+} n_{Xe} n_{Ne}$$

where, k_r is the rate of reaction r

So, the contribution of this reaction in S_p for Ne^+ is given by

$$R = k_r n_{Ne^+} n_{Xe} n_{Ne}$$

where, k_r is the rate of reaction r

So, the contribution of this reaction in S_p for Ne^+ is given by

$$S_p = -k_r n_{Ne^+} n_{Xe} n_{Ne}$$

Similarly for $NeXe^+$,

$$S_p = k_r n_{Ne^+} n_{Xe} n_{Ne}$$

For those reactions, which involve electrons, there are two ways of writing the source term. The reaction could be

$$e + Xe \rightarrow Xe^+ + 2e$$

In the first method, ionization coefficient is used. Ionization coefficient is the number of ionization events per unit distance traveled by an electron, in the drift direction. This is equal to the ionization frequency divided by the drift velocity.

In this case source term is given by,

S_p = (ionization coefficient) (electron flux) (3.9)

In the second method, the ionization rate coefficient is used. The ionization rate coefficient is the number of ionization events per unit time. This is equal to the ionization frequency divided by the density of the particle involved in that reaction, with the electron.

In this case source term is given by

S_p = (ionization rate coefficient) n_e n_{Xe} (3.10)

3.5 Boundary Conditions

The boundary conditions are the essential part of the modelling process. The boundary condition for positive ion flux to the wall is given by

$$\mathbf{J_i}.\mathbf{n} = a\,\mu_i\,\mathbf{E}.\mathbf{n}\,n_i + 0.25\,v_{th}\,n_i \quad (3.11)$$

Where

$\mathbf{J_i}$ is the positive ion flux

$\mathbf{n}$ is the normal vector pointing towards the wall

$a = 1$ if $\mathbf{E}.\mathbf{n} > 0$

$= 0$ if $\mathbf{E}.\mathbf{n} \leq 0$

n_i is density of positive ions

μ_i is mobility of positive ions

v_{th} is thermal velocity of particle

As can be seen, this boundary condition consists of two parts: one due to drift of charge particle and other due to motion of particle because of thermal velocity.

The basic assumption in the drift flux is that, every particle that strikes the wall, sticks to it. The particle motion is defined by the electric field direction. If the electric field is directed towards the wall, determined by **E.n**, the positive ions move in the direction of it. Therefore, for **E.n** > 0, a is taken as 1, otherwise zero.

The thermal motion of the gas in the cell leads to an isotropic flux of atoms impinging on the wall. Thus the second part of boundary flux, consists of flux due to thermal velocity, with a factor of 0.25[26].

Similarly, the boundary condition for electron flux to the wall is given by

$$\mathbf{J_e}.\mathbf{n} = -a\,\mu_e\,\mathbf{E}.\mathbf{n}\,n_e + 0.25\,v_{th}\,n_e - \Sigma\,\gamma_i\,\mathbf{J_i}.\mathbf{n} \qquad (3.12)$$

Where

$\mathbf{J_e}$ is the electron flux

n_e is density of electrons

n is the normal vector pointing towards the wall

a = 0 if **E.n** > 0

= 1 if **E.n** ≤ 0

μ_e is mobility of electrons

γ_i is the secondary electron emission coefficient of ion i

In the boundary condition for electrons, an additional flux source is added due to the secondary electron emission by positive ions striking the wall, apart from the two factors discussed above. When a positive ions strike the wall, γ electrons are ejected from the wall. So depending on the flux of positive ions, secondary electrons are generated. But the direction of it is away from wall so the flux due to secondary electrons, is treated as negative.

3.6 Input Data for Simulation

In this thesis Neon–10%Xenon gas mixture is used. The reactions which are involved are given in table 1.1. There are various data which are taken from different sources. These are discussed in subsequent sections.

3.6.1 Data for Reaction Rate

As shown in the table 1.1, there are various reactions occurring in the gas mixture, used in this thesis. These reactions can be divided in two parts, reactions involving electrons and reactions without electrons.

For the reactions without electrons, the reaction rates are constant and are taken directly from references, as shown in the table 1.1.

But for the reactions involving electrons, marked as **b** in table 1.1, the reaction rate is dependent on the electric field. As is discussed earlier, LFA is used in this thesis. So for these reactions Boltzmann equation is solved for a constant value of electric field and then the collision frequency or collision coefficient is tabulated as a function of reduced electric field.

The Boltzmann solver used in this thesis work is BOLSIG[27], which gives collision frequency and collision coefficient, as a function of reduced electric field. At a particular reduced electric field, BOLSIG code gives collision frequency or collision coefficient for different reactions, which are differentiated by means of mean energy given in the table 1.1. If at a particular reduced electric field, collision frequency or collision coefficient is required for a particular reaction, the value corresponding to mean energy for that reaction is taken.

For example, consider reaction

$$e + Xe \rightarrow Xe^{+} + 2e$$

The mean electron energy lost in the reaction is 12.12 eV[17]. If the collision frequency of this reaction is required, at a particular value of E/p, for e.g. at 40 V/cm/torr, file rates.out is used. In this file, attached in appendix 2, output is arranged for different value of E/p. For a particular value of E/p and reaction, decided by the energy value, collision frequency value is taken. For example, in the case mentioned above, the value of collision frequency is 0.244×10^{8} $s^{-1}torr^{-1}$.

If instead of collision frequency, collision coefficient values are needed, to calculate the source term, then the file swarm.out is used. In the end of this output file, attached in the appendix 3, the values of collision coefficient are given for different values of E/p and reactions. In this file the output is in different manner. In the starting, all the E/p values are given. Then for each reaction, values corresponding to these E/p values are given. The reaction type can be identified by

again looking back to the file rates.out. We can note the position of the reaction required, as it occurs in the file, on the basis of the energy values. Corresponding to this we can find the value, for the reaction required. For the case taken in the example above, the reaction occurs last in the file rates.out. Thus the collision coefficient value is 0.9138 cm-1.torr-1. Based on the method used for calculating source term, either of the two values, collision frequency and collision coefficient, can be used.

3.6.2 Data for Mobility and Diffusion coefficient

The electron mobility as a function of reduced electric field is obtained from the Boltzmann equation solving code BOLSIG. In this code the mobility of electron is given as a function of reduced electric field, in the starting of the output file swarm.out. This mobility is tabulated and the value required for particular value of reduced electric field is taken. For example for E/p = 40.0 V/cm/torr, mobility of electron is 0.6683×10^{6} torr.cm2/V/s.

Since the mixture contains 90% Neon, the mobility of neon atomic ions in the neon–xenon gas mixture, is supposed to be same as that in pure neon[7] and are taken from Beaty and Patterson[22]. But there is printing error in that paper. The formula given for the atomic neon mobility is different in abstract and in the paper. We tried to find the correct formula using trial and error method. This was cross checked with the plot given there and the correct formula obtained is

$$K(Ne^{+})=4.07[1 + 8.0e10^{-3} (E/p_o)^2 + 2.0e\text{-}6 (E/p_o)^4]^{-1/8}$$

Where,

K is the mobility at a standard gas density of 2.69×10^{19} atoms/cm^3, which corresponds to 760 torr pressure.

$K= \mu \times p_o/760$

μ is the mobility at given gas pressure p and gas temperature T

E is the electric field

$p_o = p \times 273/T$

In order to calculate the mobility of atomic xenon ion in neon-xenon mixture, Blanc's law is used. According to Blanc's law mobility of A^+ ion in a mixture A-B containing fraction X of A and (1-X) of B is given by

$$[\mu_{A/AB}]^{-1} = X [\mu_{A/A}]^{-1} +(1-X)[\mu_{A/B}]^{-1}$$

where, $\mu_{A/AB}$ is the mobility of A in AB mixture, $\mu_{A/A}$ is the mobility of A in A and $\mu_{A/B}$ is the mobility of A in B.

The mobility of atomic xenon ions in pure xenon is taken from Larsen and Elford[23] for fields below 180 Td (1 Td = 10^{-17} V-cm^2). In this reference, the mobility values are given as a function of E/N, as shown in Appendix 4.

For E/N > 180 Td, the mobility of atomic xenon in pure xenon is taken from analytical formula of Ward[24], which is

$$\mu = \frac{u_+}{p}\left(1 - \frac{CE}{p}\right) \qquad \text{for } E/p \le W_1$$

$$\mu = \frac{k_+}{(Ep)^{\frac{1}{2}}}\left(1 - \frac{D}{(Ep)^{\frac{3}{2}}}\right) \qquad \text{for } E/p \le W_1$$

where,

μ is the mobility of ion

E is the electric field

p is the pressure of gas

$u_+ = 4.0\times10^2$ cm^2 torr volt^{-1} sec^{-1}

$k_+ = 4.0\times10^3$ cm$^{3/2}$ torr$^{1/2}$ volt$^{-1/2}$ sec^{-1}

$C = 2.25\times10^{-3}$ torr cm volt^{-1}

$D = 225$ volt$^{-1/2}$ cm$^{-1/2}$ torr$^{-1/2}$

$W_1 = 100$ volt cm^{-1} torr^{-1}

The mobility of atomic xenon ion in pure neon is taken from Ellis et al[25], and given in appendix 5. But in the table given there, the mobility values are given for E/N in the range of 15 to 140 Td. For E/N less than 15 Td, the mobility value is assumed to be same as that at 15 Td. For E/N greater than 140 Td, the mobility is assumed to be linear, with the starting value equal to value of 140 Td. The final value, i.e. mobility value at E/N=1000 Td, is taken from the plot of mobility given in reference 7.

The plot of mobility of ions and electron is given in figure 3.3.

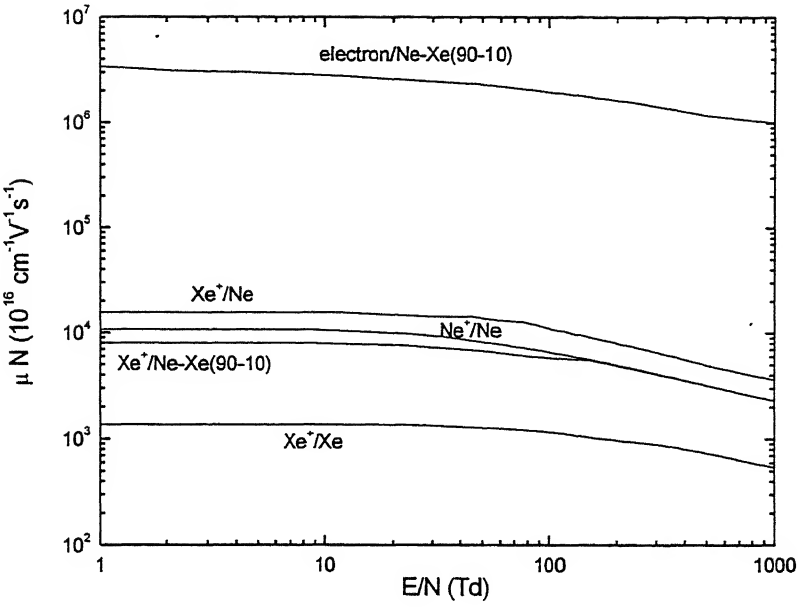

Fig 3.3 Mobility of ions and electrons as a function of reduced electric field

The diffusion coefficient of positive ions and electrons is calculated by using the formula

$$\frac{D_p}{\mu_p} = \frac{kT_p}{q}$$

where,

D_p is the diffusion coefficient of particle

μ_p is the mobility of the particle

p = e for electrons and i for ions

k is Boltzmann constant

T_p is the particle temperature, which is assumed to be same as gas Temperature for ions and T_e, for electrons

q is the charge of particle which is equal to electron charge, e, in our case.

For electron, $kT_e = 1eV$.

3.6.3 Data for secondary electron emission coefficient

The secondary electron emission coefficient is assumed to be a constant and not a function of electric field. A secondary electron emission coefficient of 0.5 is taken for neon atomic ion and 0.05 for xenon atomic ion[7].

Chapter 4

Numerical solution of Fluid Equation

4.1 Introduction

The system of fluid equations presented in the previous chapter, is solved numerically using different techniques, for one-dimensional case. To start with, the momentum transfer equation is solved, using Scharfetter-Gummel method for charged particle, in section 4.2. This solution is used in the continuity equation, which is then integrated in time using Crank Nicholson method of descritization, as shown in section 4.3. Section 4.4 explains the procedure for solving these equations and in section 4.5, different parameters used in this thesis work are discussed.

4.2 Solution of momentum transfer equation

For charged particle

The momentum transfer equation for charged particle, equation 3.7, is solved using Scharfetter-Gummel method.

Consider any internal point, **i**, in a one-dimensional mesh, as shown below

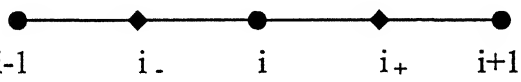

Points i , i-1 and i+1 are the main node points of the mesh. Whereas points i_- and i_+ are the mid points between i-1, i and i, i+1 node points, respectively.

The momentum transfer equation for any charged particle p, is given by equation 3.7, which is

$$\mathbf{J_p} = \mathrm{sgn}(q_p)\mu_p \mathbf{E} n_p - D_p \nabla n_p$$

For one-dimensional case it is written as

$$\mathbf{J_p} = \mathrm{sgn}(q_p)\mu_p \mathbf{E} n_p - D_p \frac{\partial (n_p)}{\partial x} \qquad (4.1)$$

In Scharfetter-Gummel approach, between any two node points, $\mathbf{J_p}$, μ_p, $\mathbf{E}$ and D_p are assumed to be constant. Or in other way, we can say that the distance between two node points is chosen in such a way that between them, $\mathbf{J_p}$, μ_p, $\mathbf{E}$ and D_p are constant.

For electrons

For region between i-1 and i, for electrons, equation 4.1 can be written as

$$\mathbf{J}_{i\_} = -n\mu_{i\_}E_{i\_} - D_{i\_}\frac{\partial n}{\partial x} \qquad (4.2)$$

This could be written as

$$\frac{\partial n}{\partial x} + \left(\frac{\mu_{i\_}E_{i\_}}{D_{1\_}}\right)n = -\frac{\mathbf{J}_{i\_}}{D_{i\_}}$$

Multiplying both sides by $e^{\frac{\mu_{1\_}E_{1\_}}{D_{1\_}}x}$,

$$\frac{\partial}{\partial x}\left(ne^{\frac{\mu_{1\_}E_{1\_}}{D_{1\_}}x}\right) = -\frac{\mathbf{J}_{i\_}}{D_{1\_}}e^{\frac{\mu_{1\_}E_{i\_}}{D_{1\_}}x}$$

Integrating both sides,

$$ne^{\frac{\mu_{1\_}E_{1\_}}{D_{1\_}}x} = -\frac{\mathbf{J}_{i\_}}{D_{i\_}}\left(\frac{e^{\frac{\mu_{i\_}E_{1\_}}{D_{1\_}}x}}{\frac{\mu_{1\_}E_{1\_}}{D_{1\_}}}\right) + C$$

where, C is the constant of integration.

This could be written as

$$ne^{\frac{\mu_{1\_}E_{1\_}}{D_{1\_}}x} = -\frac{\mathbf{J}_{i\_}}{\mu_{i\_}\mathbf{E}_{i\_}}\left(e^{\frac{\mu_{1\_}E_{1\_}}{D_{1\_}}x}\right) + C$$

This is equivalent to

$$n = -\frac{J_{i\_}}{\mu_{i\_} E_{1\_}} + Ce^{\frac{\mu_{1\_} E_{1\_}}{D_{1\_}} x} \qquad (4.3)$$

Let x_i be the position of the node point i and let n_i be the density at point i.

Similarly, for point i-1 the position and density is given by x_{i-1} and n_{i-1}, respectively.

For x_i and x_{i-1}, the equation 4.3 can be written as

$$n_i = -\frac{J_{i\_}}{\mu_{1\_} E_{1\_}} + Ce^{\frac{\mu_{1\_} E_{1\_}}{D_{1\_}} x_i} \qquad (4.4)$$

and

$$n_{i-1} = -\frac{J_{i\_}}{\mu_{1\_} E_{i\_}} + Ce^{\frac{\mu_{i\_} E_{1\_}}{D_{1\_}} x_{i-1}} \qquad (4.5)$$

Subtracting equation (4.5) from equation (4.4),

$$n_i - n_{i-1} = C\left(e^{\frac{\mu_{1\_} E_{1\_}}{D_{1\_}} x_i} - e^{\frac{\mu_{1\_} E_{1\_}}{D_{1\_}} x_{i-1}} \right)$$

From this we get value of C as

$$C = \frac{n_i - n_{i-1}}{\left(e^{\frac{\mu_{1\_} E_{1\_}}{D_{1\_}} x_i} - e^{\frac{\mu_{1\_} E_{1\_}}{D_{1\_}} x_{i-1}} \right)} \qquad (4.6)$$

Substituting value of C in equation (4.4),

$$n_1 = -\frac{J_{1\_}}{\mu_{i\_}E_{1\_}} + \frac{n_i - n_{1-1}}{\left(e^{\frac{\mu_{1\_}E_{1\_}}{D_{1\_}}x_1} - e^{\frac{\mu_{1\_}E_{1\_}}{D_{1\_}}x_{1-1}}\right)} e^{\frac{\mu_{1\_}E_{1\_}}{D_{1\_}}x_1} \qquad (4.7)$$

This equation could be written as

$$-\frac{J_{1\_}}{\mu_{i_1}E_{1\_}} = n_1\left(1 - \frac{e^{\frac{\mu_{1_1}E_{1\_}}{D_{1\_}}x_1}}{e^{\frac{\mu_{1\_}E_{1\_}}{D_{1\_}}x_1} - e^{\frac{\mu_{1\_}E_{1\_}}{D_{1\_}}x_{1-1}}}\right) + n_{1-1}\left(\frac{e^{\frac{\mu_{1_1}E_{1\_}}{D_{1\_}}x_1}}{e^{\frac{\mu_{1\_}E_{1\_}}{D_{1\_}}x_i} - e^{\frac{\mu_{1\_}E_{i\_}}{D_{1\_}}x_{i-1}}}\right)$$

Rearranging different coefficients,

$$J_{i\_} = \left(-\frac{\mu_{i\_}E_{i\_}}{1 - e^{\frac{\mu_{1\_}E_{1\_}}{D_{1\_}}[x_1 - x_{1-1}]}}\right)n_i + \left(-\frac{\mu_{1\_}E_{i\_}}{1 - e^{\frac{\mu_{1\_}E_{1\_}}{D_{1\_}}[x_i - x_{1-1}]}}\right)n_{i-1} \qquad (4.8)$$

Similarly,

$$J_{i_+} = \left(-\frac{\mu_{1_+}E_{1_+}}{1 - e^{\frac{\mu_{1+}E_{1+}}{D_{1+}}[x_{1+1} - x_1]}}\right)n_{1+1} + \left(-\frac{\mu_{1_+}E_{1_+}}{1 - e^{\frac{\mu_{1+}E_{1+}}{D_{1+}}[x_{1+1} - x_1]}}\right)n_i \qquad (4.9)$$

Let,

$$P_{1\_} = \left(-\frac{\mu_{i\_}E_{1\_}}{1 - e^{\frac{\mu_{1\_}E_{1\_}}{D_{1\_}}[x_1 - x_{1-1}]}}\right) \qquad (4.10)$$

$$Q_{i_-} = \left(-\frac{\mu_{i_-} \mathbf{E}_{i_-}}{1 - e^{\frac{\mu_{i_-} E_{i_-}}{D_{i_-}}[x_i - x_{i-1}]}} \right) \tag{4.11}$$

$$Q_{i_+} = \left(-\frac{\mu_{i_+} \mathbf{E}_{i_+}}{1 - e^{\frac{\mu_{i_+} E_{i_+}}{D_{i_+}}[x_{i+1} - x_i]}} \right) \tag{4.12}$$

$$P_{i_+} = \left(-\frac{\mu_{i_+} \mathbf{E}_{i_+}}{1 - e^{\frac{\mu_{i_+} E_{i_+}}{D_{i_+}}[x_{i+1} - x_i]}} \right) \tag{4.13}$$

Thus equation (4.8) and (4.9) can be written as

$$\mathbf{J}_{i_-} = P_{i_-} n_i + Q_{i_-} n_{i-1} \tag{4.14}$$

$$\mathbf{J}_{i_+} = P_{i_+} n_i + Q_{i_+} n_{i+1} \tag{4.15}$$

For positive ions

For region between i-1 and i, for positive ions, equation 4.1 can be written as

$$\mathbf{J}_{i_-} = n\mu_{i_-} \mathbf{E}_{i_-} - D_{i_-} \frac{\partial n}{\partial x} \tag{4.16}$$

This could be written as

$$\frac{\partial n}{\partial x} - \left(\frac{\mu_{i_-} \mathbf{E}_{i_-}}{D_{i_-}} \right) n = -\frac{\mathbf{J}_{i_-}}{D_{i_-}}$$

Multiplying both sides by $e^{\frac{\mu_{i_-} E_{i_-}}{D_{i_-}} x}$,

$$\frac{\partial}{\partial x}\left(ne^{-\frac{\mu_{i\_} E_{i\_}}{D_{i\_}}x} \right) = -\frac{J_{i\_}}{D_{i\_}} e^{-\frac{\mu_{i\_} E_{i\_}}{D_{i\_}}x}$$

Integrating both sides,

$$ne^{-\frac{\mu_{i\_} E_{i\_}}{D_{i\_}}x} = -\frac{J_{i\_}}{D_{i\_}}\left(\frac{e^{-\frac{\mu_{i\_} E_{i\_}}{D_{i\_}}x}}{-\frac{\mu_{i\_} E_{i\_}}{D_{i\_}}} \right) + C$$

where, C is the constant of integration.

This could be written as

$$ne^{-\frac{\mu_{i\_} E_{i\_}}{D_{i\_}}x} = \frac{J_{i\_}}{\mu_{i\_} E_{i\_}}\left(e^{-\frac{\mu_{i\_} E_{i\_}}{D_{i\_}}x} \right) + C$$

This is equivalent to

$$n = \frac{J_{i\_}}{\mu_{i\_} E_{i\_}} + Ce^{\frac{\mu_{i\_} E_{i\_}}{D_{i\_}}x} \qquad (4.17)$$

Let x_i be the position of the node point i and let n_i be the density at point i.

Similarly, for point i-1 the position and density is given by x_{i-1} and n_{i-1}, respectively.

For x_i and x_{i-1}, the equation 4.17 can be written as

$$n_i = \frac{J_{i\_}}{\mu_{i\_} E_{i\_}} + Ce^{\frac{\mu_{i\_} E_{i\_}}{D_{i\_}}x_i} \qquad (4.18)$$

and

$$n_{i-1} = \frac{J_{i\_}}{\mu_{i\_} E_{i\_}} + Ce^{\frac{\mu_{i\_} E_{i\_}}{D_{i\_}}x_{i-1}} \qquad (4.19)$$

Subtracting equation (4.19) from equation (4.18),

$$n_i - n_{i-1} = C\left(e^{\frac{\mu_{1\_}E_{1\_}}{D_{1\_}}x_1} - e^{\frac{\mu_{1\_}E_{1\_}}{D_{1\_}}x_{1-1}} \right)$$

From this we get value of C as

$$C = \frac{n_i - n_{i-1}}{\left(e^{\frac{\mu_{1\_}E_{1\_}}{D_{1\_}}x_1} - e^{\frac{\mu_{1\_}E_{1\_}}{D_{1\_}}x_{1-1}} \right)} \tag{4.20}$$

Substituting value of C in equation (4.18),

$$n_i = \frac{J_{i\_}}{\mu_{i\_}E_{1\_}} + \frac{n_i - n_{i-1}}{\left(e^{\frac{\mu_{1\_}E_{1\_}}{D_{1\_}}x_1} - e^{\frac{\mu_{1\_}E_{1\_}}{D_{1\_}}x_{1-1}} \right)} e^{\frac{\mu_{i\_}E_{1\_}}{D_{1\_}}x_1} \tag{4.21}$$

This equation could be written as

$$\frac{J_{1\_}}{\mu_{i_1}E_{1\_}} = n_i\left(1 - \frac{e^{\frac{\mu_{1_1}E_{1\_}}{D_{1\_}}x_1}}{e^{\frac{\mu_{1\_}E_{i\_}}{D_{1\_}}x_1} - e^{\frac{\mu_{1\_}E_{1\_}}{D_{1\_}}x_{1-1}}} \right) + n_{i-1}\left(\frac{e^{\frac{\mu_{1_1}E_{1\_}}{D_{1\_}}x_1}}{e^{\frac{\mu_{1\_}E_{1\_}}{D_{1\_}}x_1} - e^{\frac{\mu_{1\_}E_{1\_}}{D_{1\_}}x_{1-1}}} \right)$$

Rearranging different coefficients,

$$J_{i\_} = \left(\frac{\mu_{1\_}E_{1\_}}{1 - e^{\frac{\mu_{1\_}E_{1\_}}{D_{1\_}}[x_1 - x_{1-1}]}} \right) n_i + \left(\frac{\mu_{1\_}E_{1\_}}{1 - e^{\frac{\mu_{1\_}E_{1\_}}{D_{1\_}}[x_1 - x_{1-1}]}} \right) n_{i-1} \tag{4.22}$$

Similarly,

$$\mathbf{J}_{i_+} = \left(\frac{\mu_{i_+} \mathbf{E}_{i_+}}{1 - e^{-\frac{\mu_{i_+} E_{i_+}}{D_{i_+}}[x_{i+1} - x_i]}} \right) n_{i+1} + \left(\frac{\mu_{i_+} \mathbf{E}_{i_+}}{1 - e^{-\frac{\mu_{i_+} E_{i_+}}{D_{i_+}}[x_{i+1} - x_i]}} \right) n_i \qquad (4.23)$$

Let,

$$P_{i_-} = \left(\frac{\mu_{i_-} \mathbf{E}_{i_-}}{1 - e^{-\frac{\mu_{i_-} E_{i_-}}{D_{i_-}}[x_i - x_{i-1}]}} \right) \qquad (4.24)$$

$$Q_{i_-} = \left(\frac{\mu_{i_-} \mathbf{E}_{i_-}}{1 - e^{-\frac{\mu_{i_-} E_{i_-}}{D_{i_-}}[x_i - x_{i-1}]}} \right) \qquad (4.25)$$

$$Q_{i_+} = \left(\frac{\mu_{i_+} \mathbf{E}_{i_+}}{1 - e^{-\frac{\mu_{i_+} E_{i_+}}{D_{i_+}}[x_{i+1} - x_i]}} \right) \qquad (4.26)$$

$$P_{i_+} = \left(\frac{\mu_{i_+} \mathbf{E}_{i_+}}{1 - e^{-\frac{\mu_{i_+} E_{i_+}}{D_{i_+}}[x_{i+1} - x_i]}} \right) \qquad (4.27)$$

Thus equation (4.22) and (4.23) can be written as

$$\mathbf{J}_{i_-} = P_{i_-} n_i + Q_{i_-} n_{i-1} \qquad (4.28)$$

$$\mathbf{J}_{i_+} = P_{i_+} n_i + Q_{i_+} n_{i+1} \qquad (4.29)$$

For neutral particle

The momentum transfer equation for neutral particle is given by equation 3.7. For one dimensional case, it can be written as

$$\mathbf{J}_p = -D_p \frac{\partial n_p}{\partial x} \tag{4.30}$$

The solution of this equation is

$$\mathbf{J}_{i_+} = -D_{i_+}\left(\frac{n_{i+1} - n_i}{x_{i+1} - x_i}\right) \tag{4.31}$$

and

$$\mathbf{J}_{i_-} = -D_{i_-}\left(\frac{n_i - n_{i-1}}{x_i - x_{i-1}}\right) \tag{4.32}$$

4.3 Descritization Scheme for Continuity Equation

For one-dimensional case, the continuity equation, given in equation (3.6), can be written as

$$\frac{\partial n_p}{\partial t} + \frac{\partial \mathbf{J}_P}{\partial x} = S_p \tag{4.33}$$

There are two ways of discretizing this equation, one is implicit method and other is explicit method. In explicit method $\mathbf{J}_p$ and S_p are taken from the previous time step, i.e. they are already known. In implicit method $\mathbf{J}_p$ and S_p are taken from the current time at which the equation is solved, i.e. they are not known. Both the methods have certain advantages and disadvantages. Explicit method is simple to implement, but the time step that could be chosen in this method is very small. In case of implicit method, there is no constraint of the time step, but then this method is computationally intense and may be unstable.

Thus in order to utilize the merits of both, in this thesis, S_p is taken as explicit and J_P is descritized using Crank Nicholson method with α as factor of implicity. For any point i, equation 4.33 can be descritized as

$$\frac{n_i^{t+1}-n_i^t}{\Delta t}+\frac{(1-\alpha)}{(x_{i_+}-x_{i_-})}\left[J_{i_+}-J_{i_-}\right]^t+\frac{\alpha}{(x_{i_+}-x_{i_-})}\left[J_{i_+}-J_{i_-}\right]^{t+1}=S_p^t \quad (4.34)$$

In this equation, the superscript 't' implies that the quantity is at time 't' and superscript 't+1' implies that the quantity is at time 't+1'

4.3.1 Descritization of Continuity equation for electrons

Consider a one-dimensional mesh as shown below

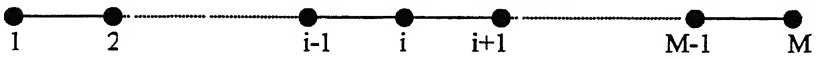

M is the total node points in the mesh.

The continuity equation is solved in three parts, for i = 1, for internal mesh points i.e. 2< i < M and for i = M.

i = 1

Consider node point i=1, as shown below

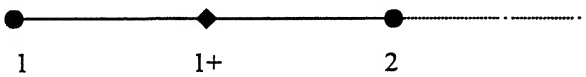

Continuity equation for i=1 can be written as

$$\frac{n_1^{t+1}-n_1^t}{\Delta t}+\frac{(1-\alpha)}{(x_{1_+}-x_1)}\left[J_{1_+}-J_1\right]^t+\frac{\alpha}{(x_{1_+}-x_1)}\left[J_{1_+}-J_1\right]^{t+1}=S_1^t \quad (4.35)$$

The value of J_{1_+} is taken from equation 4.15 for i=1. The value of J_1 is taken from the boundary equation. Boundary equation at i=1, for electrons, can be simplified as

$$J_1=-an_1\mu_1E_1-0.25n_1V_{th}-\left|\sum\gamma J_1^+\right| \quad (4.36)$$

where,

γ is the secondary electron emission coefficient of positive species

$\mathbf{J}_1^+$ is the flux of positive ions

a = 1, if $\mathbf{E}_1 > 0$

a = 0, if $\mathbf{E}_1 \leq 0$

The subscript 1 implies that all these values are at i=1

V_{th} is the thermal velocity of the particle, which is calculated by formula

$$V_{th} = \sqrt{\frac{8kT_e}{\pi m}}$$

k = Boltzmann constant

T_e = Temperature of electron

m = mass of electron.

Equation 4.35 can be rewritten as

$$\frac{n_1^{t+1}}{\Delta t} + \frac{\alpha}{(x_{1_+} - x_1)}\left[\mathbf{J}_{1_+} - \mathbf{J}_1\right]^{t+1} = S_1^t - \frac{(1-\alpha)}{(x_{1_+} - x_1)}\left[\mathbf{J}_{1_+} - \mathbf{J}_1\right]^t + \frac{n_1^t}{\Delta t} \qquad (4.37)$$

The right hand side of the equation is a constant and can be replaced by R_1^e, which is a known constant.

Equation 4.37can be written as

$$\frac{n_1^{t+1}}{\Delta t} + \frac{\alpha}{(x_{1_+} - x_1)}\left[\mathbf{J}_{1_+} - \mathbf{J}_1\right]^{t+1} = R_1^e \qquad (4.38)$$

$$R_1^e = S_1^t - \frac{(1-\alpha)}{(x_{1_+} - x_1)}\left[\mathbf{J}_{1_+} - \mathbf{J}_1\right]^t + \frac{n_1^t}{\Delta t}$$

Dropping out superscript, equation 4.38 can be written as

$$\frac{n_1}{\Delta t} + \frac{\alpha}{(x_{1_+} - x_1)}\left[\mathbf{J}_{1_+} - \mathbf{J}_1\right] = R_1^e \qquad (4.39)$$

Substituting value of $\mathbf{J}_1$ and $\mathbf{J}_{1_+}$ from equations 4.36 and 4.15, respectively, in equation 4.39,

$$\frac{n_1}{\Delta t}+\frac{\alpha}{(x_{1_+}-x_1)}\left[P_{1_+}n_1+Q_{1_+}n_2+an_1\mu_1E_1+0.25n_1V_{th}+\left[\sum\gamma J_1^+\right]\right]=R_1^e$$

The value of 'a' and V_{th} is same as described above.

P_{1_+} and Q_{1_+} is taken from equation 4.12 and 4.13 for i=1.

Rearranging different coefficients in this equation we get

$$\left[\frac{1}{\Delta t}+\frac{\alpha}{(x_{1_+}-x_1)}\left(P_{1_+}-an_1\mu_1E_1+0.25V_{th}\right)\right]n_1+\left[\frac{\alpha}{(x_{1_+}-x_1)}Q_{1_+}\right]n_2=R_1^e-\left[\frac{\alpha\left[\sum\gamma J_1^+\right]}{(x_{1_+}-x_1)}\right]^{t+1} \quad \text{..... (4.40)}$$

2 < i <M-1

Consider any node point 'i' as shown below

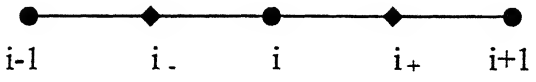

Continuity equation for any point i such that 2 < i <M-1 is

$$\frac{n_1^{t+1}-n_1^t}{\Delta t}+\frac{(1-\alpha)}{(x_{1_+}-x_{1_-})}\left[J_{1_+}-J_{i_-}\right]^t+\frac{\alpha}{(x_{1_+}-x_{1_-})}\left[J_{i_+}-J_{i_-}\right]^{t+1}=S_p^t \quad (4.41)$$

as given in equation 4.34.

The value of J_{i_+} and J_{i_-} is taken from equation 4.14 and 4.15.

Equation 4.41 can be written as

$$\frac{n_1^{t+1}}{\Delta t}+\frac{\alpha}{(x_{1_+}-x_{1_-})}\left[J_{i_+}-J_{i_-}\right]^{t+1}=S_p^t-\frac{(1-\alpha)}{(x_{1_+}-x_{1_-})}\left[J_{i_+}-J_{i_-}\right]^t+\frac{n_1^t}{\Delta t}$$

Right hand side being a constant, can be replaced by constant R_i^e

$$\frac{n_1^{t+1}}{\Delta t}+\frac{\alpha}{(x_{1_+}-x_{1_-})}\left[J_{1_+}-J_{i_-}\right]^{t+1}=R_1^e$$

Substituting value of J_{1_+} and J_{1_-}.

$$\frac{n_i^{t+1}}{\Delta t}+\frac{\alpha}{(x_{i_+}-x_{i_-})}\left[P_{i_+}n_i+Q_{i_+}n_{i+1}-P_{i_-}n_i-Q_{i_-}n_{i-1}\right]^{t+1}=R_i^e$$

Values of $P_{i_+}, Q_{i_+}, P_{i_-}$ & Q_{i_-} are calculated using equation 4.10, 4.11, 4.12 and 4.13, respectively.

Rearranging different coefficients, we get

$$\left[-\frac{\alpha}{x_{i_+}-x_{i_-}}Q_{i_-}\right]n_{i-1}+\left[\frac{1}{\Delta t}+\frac{\alpha}{x_{i_+}-x_{i_-}}\left(P_{i_+}-P_{i_-}\right)\right]n_i+\left[\frac{\alpha}{x_{i_+}-x_{i_-}}Q_{i_+}\right]n_{i+1}=R_i^e$$

.....(4.42)

i=M

Consider node point i=M, as shown below

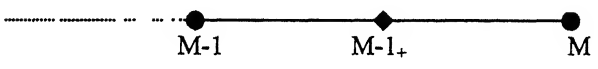

Continuity equation for i=M can be written as

$$\frac{n_M^{t+1}-n_M^t}{\Delta t}+\frac{(1-\alpha)}{(x_M-x_{M\text{-}1_+})}\left[J_{M_+}-J_{M\text{-}1_+}\right]^t+\frac{\alpha}{(x_M-x_{M\text{-}1_+})}\left[J_M-J_{M\text{-}1_+}\right]^{t+1}=S_M^t \quad (4.43)$$

The value of $J_{M\text{-}1_+}$ is taken from equation 4.15 for i=M-1. The value of J_M is taken from the boundary equation. Boundary equation at i=M for positive ions can be simplified as

$$J_M=-an_M\mu_M E_M+0.25n_M V_{th}-\left[\sum\gamma J_M^+\right] \quad (4.44)$$

where

γ is the secondary electron emission coefficient

J_M^+ is the flux of positive ions

$a = 0$, if $E_I \geq 0$

$a = 0$, if $E_1 < 0$

V_{th} is same as calculated by

$$V_{th} = \sqrt{\frac{8kT_e}{\pi m}}$$

Equation 4.43 can be written as

$$\frac{n_M^{t+1}}{\Delta t} + \frac{\alpha}{(x_M - x_{M\text{-}1_+})}\left[J_M - J_{M\text{-}1_+}\right]^{t+1} = S_M^t - \frac{(1-\alpha)}{(x_M - x_{M\text{-}1_+})}\left[J_M - J_{M\text{-}1_+}\right]^t + \frac{n_M^t}{\Delta t}$$

The right hand side of the equation is a constant. Thus right hand side can be replaced by R_M^e, which is a known constant.

Thus we get

$$\frac{n_M^{t+1}}{\Delta t} + \frac{\alpha}{(x_M - x_{M\text{-}1+})}\left[J_M - J_{M\text{-}1_+}\right]^{t+1} = R_M^e \qquad (4.45)$$

$$R_M^e = S_M^t - \frac{(1-\alpha)}{(x_M - x_{M\text{-}1_+})}\left[J_M - J_{M\text{-}1_+}\right]^t + \frac{n_M^t}{\Delta t}$$

Now dropping out superscript, equation 4.45 can be written as

$$\frac{n_M}{\Delta t} + \frac{\alpha}{(x_M - x_{M\text{-}1_+})}\left[J_M - J_{M\text{-}1_+}\right] = R_M^e \qquad (4.46)$$

Substituting value of J_M and $J_{M\text{-}1_+}$ from equations 4.44 and 4.15, respectively, in equation 4.46,

$$\frac{n_M}{\Delta t} + \frac{\alpha}{(x_M - x_{M\text{-}1_+})}\left[-an_M\mu_M E_M + 0.25n_M V_{th} - \left[\sum \gamma J_M^+\right] - Q_{M\text{-}1_+} n_M - P_{M\text{-}1_+} n_{M\text{-}1}\right] = R_M^e$$

Rearranging different coefficients

$$\left[-\frac{\alpha}{x_M - x_{M\text{-}1_+}} P_{M\text{-}1_+}\right] n_{M\text{-}1} + \left[\frac{1}{\Delta t} + \frac{\alpha}{x_M - x_{M\text{-}1_+}}\left[-a\mu_M E_M + 0.25V_{th} - Q_{M\text{-}1_+}\right]\right] n_M = R_M^e + \left[\sum \gamma J_M^+\right]^{t+1}$$

..... (4.47)

4.3.2 Descritization of Continuity equation for positive ions

Consider a one-dimensional mesh as shown below

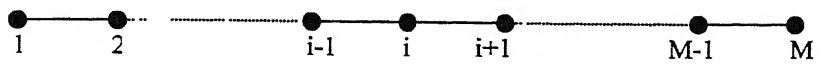

M is the total node points in the mesh.

The continuity equation is solved in three parts, for i = 1, for internal mesh points i.e. 2< i < M and for i = M.

i = 1

Consider node point i=1, as shown below

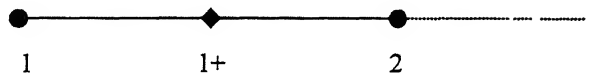

Continuity equation for i=1 can be written as

$$\frac{n_1^{t+1}-n_1^t}{\Delta t}+\frac{(1-\alpha)}{(x_{1_+}-x_1)}\left[J_{1_+}-J_1\right]^t+\frac{\alpha}{(x_{1_+}-x_1)}\left[J_{1_+}-J_1\right]^{t+1}=S_1^t \quad (4.48)$$

The value of J_{1_+} is taken from equation 4.29 for i=1. The value of J_1 is taken from the boundary equation. Boundary equation at i=1, for positive ions, can be simplified as

$$J_1 = an_1\mu_1 E_1 - 0.25n_1 V_{th} \quad (4.49)$$

where,

a = 1, if $E_1 < 0$

a = 0, if $E_1 \geq 0$

The subscript 1 implies that all these values are at i=1

V_{th} is the thermal velocity of the particle, which is calculated by formula

$$V_{th} = \sqrt{\frac{8kT}{\pi m}} \qquad (4.50)$$

k = Boltzmann constant

T = Temperature of particle

m = mass of the particle

Equation 4.48 can be rewritten as

$$\frac{n_1^{t+1}}{\Delta t} + \frac{\alpha}{(x_{1_+} - x_1)}\left[\mathbf{J}_{1_+} - \mathbf{J}_1\right]^{t+1} = S_1^t - \frac{(1-\alpha)}{(x_{1_+} - x_1)}\left[\mathbf{J}_{1_+} - \mathbf{J}_1\right]^t + \frac{n_1^t}{\Delta t} \qquad (4.51)$$

The right hand side of the equation is a constant, as all the parameters in that are already known from previous time step.

Thus, the right hand side can be replaced by, R_1^+, which is a known constant.

Equation 4.51 can be written as

$$\frac{n_1^{t+1}}{\Delta t} + \frac{\alpha}{(x_{1_+} - x_1)}\left[\mathbf{J}_{1_+} - \mathbf{J}_1\right]^{t+1} = R_1^+ \qquad (4.52)$$

$$R_1^+ = S_1^t - \frac{(1-\alpha)}{(x_{1_+} - x_1)}\left[\mathbf{J}_{1_+} - \mathbf{J}_1\right]^t + \frac{n_1^t}{\Delta t}$$

Now, dropping out superscript, equation 4.52 can be written as

$$\frac{n_1}{\Delta t} + \frac{\alpha}{(x_{1_+} - x_1)}\left[\mathbf{J}_{1_+} - \mathbf{J}_1\right] = R_1^+ \qquad (4.53)$$

Substituting value of $\mathbf{J_1}$ and $\mathbf{J}_{1_+}$ from equations 4.49 and 4.29, respectively, in equation 4.53, we get

$$\frac{n_1}{\Delta t} + \frac{\alpha}{(x_{1_+} - x_1)}\left[P_{1_+} n_1 + Q_{1_+} n_2 - a n_1 \mu_1 \mathbf{E_1} + 0.25 n_1 V_{th}\right] = R_1^+$$

The value of 'a' and V_{th} is same as described above.

P_{1_+} and Q_{1_+} are taken from equation 4.26 and 4.27, for i=1.

Rearranging different coefficients in this equation we get

$$\left[\frac{1}{\Delta t}+\frac{\alpha}{(x_{1_+}-x_1)}\left(P_{1_+}-an_1\mu_1E_1+0.25V_{th}\right)\right]n_1+\left[\frac{\alpha}{(x_{1_+}-x_1)}Q_{1_+}\right]n_2=R_1^+ \quad (4.54)$$

2 < i <M-1

Consider any node point 'i' as shown below

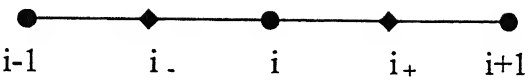

Continuity equation for any point I, such that 2 < i <M-1, is

$$\frac{n_1^{t+1}-n_1^t}{\Delta t}+\frac{(1-\alpha)}{(x_{1_+}-x_{1_-})}\left[J_{i_+}-J_{i_-}\right]^t+\frac{\alpha}{(x_{1_+}-x_{1_-})}\left[J_{i_+}-J_{i_-}\right]^{t+1}=S_p^t \quad (4.55)$$

The values of J_{i_+} and J_{i_-} are taken from equation 4.28 and 4.29.

Equation 4.55 can be written as

$$\frac{n_1^{t+1}}{\Delta t}+\frac{\alpha}{(x_{1_+}-x_{1_-})}\left[J_{1_+}-J_{i_-}\right]^{t+1}=S_p^t-\frac{(1-\alpha)}{(x_{1_+}-x_{1_-})}\left[J_{i_+}-J_{i_-}\right]^t+\frac{n_1^t}{\Delta t}$$

Right hand side, being a constant, can be replaced by constant R_1^+.

$$\frac{n_1^{t+1}}{\Delta t}+\frac{\alpha}{(x_{1_+}-x_{1_-})}\left[J_{i_+}-J_{i_-}\right]^{t+1}=R_1^+$$

Substituting value of J_{1_+} and J_{1_-}.

$$\frac{n_1^{t+1}}{\Delta t}+\frac{\alpha}{(x_{1_+}-x_{1_-})}\left[P_{1_+}n_1+Q_{1_+}n_{1+1}-P_{1_-}n_1-Q_{1_-}n_{1-1}\right]^{t+1}=R_1^+$$

Values of $P_{1_+}, Q_{1_+}, P_{1_-}$ & Q_{1_-} are calculated using equation 4.24, 4.25, 4.26 and 4.27, respectively.

Rearranging different coefficients,

$$\left[-\frac{\alpha}{x_{i_+}-x_{i_-}}Q_{i_-}\right]n_{i-1}+\left[\frac{1}{\Delta t}+\frac{\alpha}{x_{i_+}-x_{i_-}}\left(P_{i_+}-P_{i_-}\right)\right]n_i+\left[\frac{\alpha}{x_{i_+}-x_{i_-}}Q_{i_+}\right]n_{i+1}=R_i^+$$

.....(4.56)

i=M

Consider node point i=M, as shown below

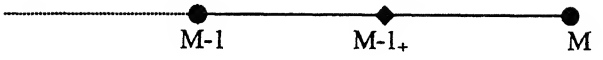

Continuity equation for i=M can be written as

$$\frac{n_M^{t+1}-n_M^t}{\Delta t}+\frac{(1-\alpha)}{(x_M-x_{M\text{-}1_+})}\left[J_{M_+}-J_{M\text{-}1_+}\right]^t+\frac{\alpha}{(x_M-x_{M\text{-}1_+})}\left[J_M-J_{M\text{-}1_+}\right]^{t+1}=S_M^t \quad (4.57)$$

The value of $J_{M\text{-}1_+}$ is taken from equation 4.29, for i=M-1. The value of J_M is taken from the boundary equation. Boundary equation at i=M for positive ions can be simplified as

$$J_M = an_M\mu_M E_M + 0.25n_M V_{th} \quad (4.58)$$

where,

$a = 1$, if $E_1 > 0$

$a = 0$, if $E_1 \le 0$

V_{th} is same as given in equation 4.50.

Equation 4.57 can be written as

$$\frac{n_M^{t+1}}{\Delta t}+\frac{\alpha}{(x_M-x_{M\text{-}1_+})}\left[J_M-J_{M\text{-}1_+}\right]^{t+1}=S_M^t-\frac{(1-\alpha)}{(x_M-x_{M\text{-}1_+})}\left[J_M-J_{M\text{-}1_+}\right]^t+\frac{n_M^t}{\Delta t}$$

The right hand side of the equation is a constant and can be replaced by, R_M^+, which is a known constant.

Thus we get

$$\frac{n_M^{t+1}}{\Delta t} + \frac{\alpha}{(x_M - x_{M\text{-}1_+})}\left[J_M - J_{M\text{-}1_+}\right]^{t+1} = R_M^+ \qquad (4.59)$$

$$R_M^+ = S_M^t - \frac{(1-\alpha)}{(x_M - x_{M\text{-}1_+})}\left[J_M - J_{M\text{-}1_+}\right]^t + \frac{n_M^t}{\Delta t}$$

Now dropping out superscript, equation 4.59 can be written as

$$\frac{n_M}{\Delta t} + \frac{\alpha}{(x_M - x_{M\text{-}1_+})}\left[J_M - J_{M\text{-}1_+}\right] = R_M^+ \qquad (4.60)$$

Substituting value of J_M and $J_{M\text{-}1_+}$ from equations 4.58 and 4.29, respectively, in equation 4.60,

$$\frac{n_M}{\Delta t} + \frac{\alpha}{(x_M - x_{M\text{-}1_+})}\left[an_M\mu_M E_M + 0.25n_M V_{th} - Q_{M\text{-}1_+}n_M - P_{M\text{-}1_+}n_{M\text{-}1}\right] = R_M^+$$

Rearranging different coefficients,

$$\left[-\frac{\alpha}{x_M - x_{M\text{-}1_+}}P_{M\text{-}1_+}\right]n_{M\text{-}1} + \left[\frac{1}{\Delta t} + \frac{\alpha}{x_M - x_{M\text{-}1_+}}\left[a\mu_M E_M + 0.25V_{th} - Q_{M\text{-}1_+}\right]\right]n_M = R_M^+$$

..... (4.61)

4.3.3 Solution of Continuity equation for neutral species

Consider a one-dimensional mesh as shown below

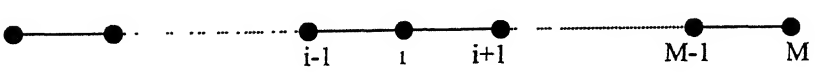

M is the total node points in the mesh.

Thus continuity equation is solved in three parts, for i = 1, for internal mesh points, i.e. 2< i < M and for i = M.

i = 1

Consider node point i=1, as shown below

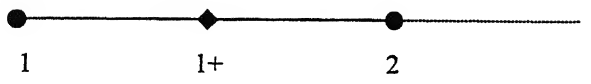

Continuity equation for i=1 can be written as

$$\frac{n_1^{t+1}-n_1^t}{\Delta t}+\frac{(1-\alpha)}{(x_{1_+}-x_1)}\left[J_{1_+}-J_1\right]^t+\frac{\alpha}{(x_{1_+}-x_1)}\left[J_{1_+}-J_1\right]^{t+1}=S_1^t \qquad (4.62)$$

The value of J_{1_+} is taken from equation 4.31 for i=1. The value of J_1 is taken from the boundary equation. Boundary equation at i=1 for neutral species can be simplified as

$$J_1=-0.25n_1V_{th} \qquad (4.63)$$

The subscript 1 implies that all these values are at i=1.

V_{th} is calculated as given in equation 4.50.

Equation 4.62 can be rewritten as

$$\frac{n_1^{t+1}}{\Delta t}+\frac{\alpha}{(x_{1_+}-x_1)}\left[J_{1_+}-J_1\right]^{t+1}=S_1^t-\frac{(1-\alpha)}{(x_{1_+}-x_1)}\left[J_{1_+}-J_1\right]^t+\frac{n_1^t}{\Delta t} \qquad (4.64)$$

The right hand side of the equation is a constant, as all the parameters in that are already known, from previous time step.

Thus right hand side can be replaced by, R_1^n, which is a known constant.

Thus equation 4.64 can be written as

$$\frac{n_1^{t+1}}{\Delta t}+\frac{\alpha}{(x_{1_+}-x_1)}\left[J_{1_+}-J_1\right]^{t+1}=R_1^n \qquad (4.65)$$

$$R_1^n=S_1^t-\frac{(1-\alpha)}{(x_{1_+}-x_1)}\left[J_{1_+}-J_1\right]^t+\frac{n_1^t}{\Delta t}$$

Now dropping out superscript equation 4.65 can be written as

$$\frac{n_1}{\Delta t}+\frac{\alpha}{(x_{1_+}-x_1)}\left[\mathbf{J}_{1_+}-\mathbf{J}_1\right]=R_1^n \qquad (4.66)$$

Substituting, value of $\mathbf{J}_1$ and $\mathbf{J}_{1_+}$ from equations 4.63 and 4.31, respectively, in equation 4.66,

$$\frac{n_1}{\Delta t}+\frac{\alpha}{(x_{1_+}-x_1)}\left[-\frac{D_{1_+}(n_2-n_1)}{(x_2-x_1)}+0.25n_1V_{th}\right]=R_1^n$$

Rearranging different coefficients in this equation,

$$\left[\frac{1}{\Delta t}+\frac{\alpha}{(x_{1_+}-x_1)}\left(-\frac{D_{1_+}}{(x_2-x_1)}+0.25V_{th}\right)\right]n_1+\left[-\frac{\alpha D_{1_+}}{(x_{1_+}-x_1)(x_2-x_1)}\right]n_2=R_1^n \quad (4.67)$$

2 < i <M-1

Consider any node point 'i' as shown below

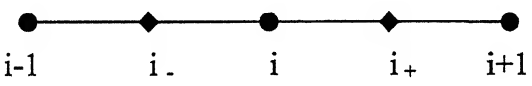

Continuity equation for any point i such that 2 < i <M-1 is

$$\frac{n_i^{t+1}-n_i^t}{\Delta t}+\frac{(1-\alpha)}{(x_{i_+}-x_{i_-})}\left[\mathbf{J}_{i_+}-\mathbf{J}_{i_-}\right]^t+\frac{\alpha}{(x_{i_+}-x_{i_-})}\left[\mathbf{J}_{i_+}-\mathbf{J}_{i_-}\right]^{t+1}=S_p^t \quad (4.68)$$

The value of $\mathbf{J}_{i_+}$ and $\mathbf{J}_{i_-}$ is taken from equation 4.31 and 4.32.

Equation 4.68 can be written as

$$\frac{n_i^{t+1}}{\Delta t}+\frac{\alpha}{(x_{i_+}-x_{i_-})}\left[\mathbf{J}_{i_+}-\mathbf{J}_{i_-}\right]^{t+1}=S_p^t-\frac{(1-\alpha)}{(x_{i_+}-x_{i_-})}\left[\mathbf{J}_{i_+}-\mathbf{J}_{i_-}\right]^t+\frac{n_i^t}{\Delta t}$$

Right hand side, being a constant, can be replaced by constant R_i^n

Substituting value of $\mathbf{J}_{i_+}$ and $\mathbf{J}_{i_-}$.

$$\frac{n_i^{t+1}}{\Delta t}+\frac{\alpha}{(x_{i_+}-x_{i_-})}\left[-\frac{D_{i_+}(n_{i+1}-n_i)}{(x_{i+1}-x_i)}+\frac{D_{i_-}(n_i-n_{i-1})}{(x_i-x_{i-1})}\right]^{t+1}=R_i^n$$

Rearranging different coefficients,

$$\left[-\frac{\alpha D_{i_-}}{(x_{i_+}-x_{i_-})(x_i-x_{i-1})}\right]n_{i-1}+\left[\frac{1}{\Delta t}+\frac{\alpha D_{i_+}}{(x_{i+1}-x_i)(x_{i_+}-x_{i_-})}+\frac{\alpha D_{i_-}}{(x_i-x_{i-1})(x_{i_+}-x_{i_-})}\right]n_i$$
$$+\left[-\frac{D_{i_+}}{(x_{i+1}-x_i)(x_{i_+}-x_{i_-})}\right]n_{i+1}=R_i^n$$

.....(4.69)

i=M

Consider node point i=M, as shown below

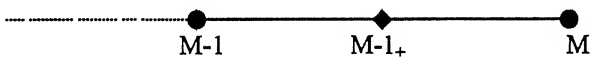

Continuity equation for i=M can be written as

$$\frac{n_M^{t+1}-n_M^t}{\Delta t}+\frac{(1-\alpha)}{(x_M-x_{M\text{-}1_+})}\left[\mathbf{J}_{M_+}-\mathbf{J}_{M\text{-}1_+}\right]^t+\frac{\alpha}{(x_M-x_{M\text{-}1_+})}\left[\mathbf{J}_M-\mathbf{J}_{M\text{-}1_+}\right]^{t+1}=S_M^t \quad (4.70)$$

The value of $J_{M\text{-}1_+}$ is taken from equation 4.31 for i=M-1. The value of J_M is taken from the boundary equation. Boundary equation at i=M for neutral species can be simplified as

$$\mathbf{J}_M=0.25n_M V_{th} \quad (4.71)$$

V_{th} is same as given in equation 4.50.

Equation 4.70 can be written as

$$\frac{n_M^{t+1}}{\Delta t}+\frac{\alpha}{(x_M-x_{M\text{-}1_+})}\left[J_M-J_{M\text{-}1_+}\right]^{t+1}=S_M^t-\frac{(1-\alpha)}{(x_M-x_{M\text{-}1_+})}\left[J_M-J_{M\text{-}1_+}\right]^t+\frac{n_M^t}{\Delta t}$$

The right hand side of the equation is a constant. Thus, right hand side can be replaced by R_M^n, which is a known constant.

$$\frac{n_M^{t+1}}{\Delta t}+\frac{\alpha}{(x_M-x_{M\text{-}1_+})}\left[J_M-J_{M\text{-}1_+}\right]^{t+1}=R_M^n \qquad (4.72)$$

$$R_M^n=S_M^t-\frac{(1-\alpha)}{(x_M-x_{M\text{-}1_+})}\left[J_M-J_{M\text{-}1_+}\right]^t+\frac{n_M^t}{\Delta t}$$

Dropping out superscript, equation 4.72 can be written as

$$\frac{n_M}{\Delta t}+\frac{\alpha}{(x_M-x_{M\text{-}1_+})}\left[J_M-J_{M\text{-}1_+}\right]=R_M^n \qquad (4.73)$$

Substituting value of J_M and $J_{M\text{-}1_+}$ from equations 4.71 and 4.31, respectively, in equation 4.73, we get

$$\frac{n_M}{\Delta t}+\frac{\alpha}{(x_M-x_{M\text{-}1_+})}\left[0.25n_M V_{th}+\frac{D_{M\text{-}1_+}(n_M-n_{M\text{-}1})}{(x_M-x_{M\text{-}1})}\right]=R_M^n$$

Rearranging different coefficients

$$\left[-\frac{\alpha D_{M\text{-}1_+}}{(x_M-x_{M\text{-}1_+})(x_M-x_{M\text{-}1})}\right]n_{M\text{-}1}+\left[\frac{1}{\Delta t}+\frac{\alpha}{(x_M-x_{M\text{-}1_+})}\left[0.25V_{th}+\frac{D_{M\text{-}1_+}}{(x_M-x_{M\text{-}1})}\right]\right]n_M=R_M^n$$

..... (4.74)

4.4 Procedure for Solving Equations

The method for solving continuity equations, of positive ions, electrons and neutral species, and Poisson's equation, used in this thesis, is explicit in time.

To start with, it is assumed that there is charge in the gas gap, even before application of the voltage, distributed uniformly across the gap. This could be attributed to cosmic rays, radioactive impurities or background radiations. Thus

the electric field across the gas gap is constant and is calculated first, from the value of capacitance known. Using this value of electric field transport parameters are calculated, which are then used in the continuity equations.

Firstly, continuity equation for neutral species is solved. As can be seen from equation 4.67, 4.69 and 4.74, we get a tridigonal system of equations, which are solved using an equation solver.

Then continuity equation for positive ions is solved. In this case also, equation 4.54, 4.56 and 4.61 yields tridigonal set of equations, which are solved in the same manner.

Similarly while solving equations for electron, equation 4.40, 4.42 and 4.47 yields tridigonal set, which is solved using solver.

Then electric field is calculated using these new densities and method discussed in chapter 3.

Then current density is calculates, as is explained in Appendix 6.

Then these new calculated electric field is used to calculate transport parameters and this process is repeated.

4.5 Parameters used for starting of simulation

The geometry used in this thesis is same as shown in figure 1.3. The gas mixture used is Neon-10% Xenon. The gas gap length is 100μm, the pressure is 560 torr and the capacity of the dielectric layer above each electrode is 460 pF/cm^2. The gas temperature is taken to be constant and is equal to 300 K. The dielectric layer thickness is 25μm.

Based on this the gas density is calculated using formula

$$\text{Gas density} = \frac{P}{KT}$$

Where P is the pressure, K is the Boltzmann constant and T is the gas temperature.

Just before voltage is applied it is assumed that because of cosmic rays, radioactive impurities or background radiations there is some charge present in

the gas gap. We assume an initial density of charged particles (positive ions and electrons) of 3×10^{6} cm^{-3}, distributed uniformly. In this thesis only two reactions, corresponding to the direct ionization, are considered. Thus the density of each positive ion is equal to half of the initial ion density.

We have assumed that there is no memory charge on the dielectric surface at t=0. But even then the voltage drop across the dielectric is not zero. This is because the equivalent capacitance C_D across the dielectric is in series with the capacitor formed by the gas gap, C_G Thus voltage drop across the dielectric is

$$V_D(t=0) = -\frac{C_G}{C_G + C_D} V_s$$

Chapter 5

Results and Discussions

5.1 Effect of Source Term

As is discussed earlier there are two ways in which, the source term can be handled, for reactions involving electrons.

1. Making use of ionization coefficient, equation 3.9.
2. Using ionization rate constant, equation 3.10.

Both the methods were tried in this thesis work.

When equation 3.10 was used to calculate the source term, the density of electron became negative after 1 ns of simulation. Whereas, use of equation 3.9 leads to satisfactory results.

From this we can conclude that use of equation 3.10 for calculating source term leads to instability. So, in this thesis work, equation 3.9 is used to calculate the source term.

5.2 Mesh Sensitivity

In order to check the mesh sensitivity, the program was made to run for same parameters and operating conditions, but with different number of mesh points. The result is shown in the Figure 5.1, as a plot of variation of voltage across the gas gap (V_g), with time of simulation.

From the figure it is clear that as the number of mesh points is increased from 50 to 100, the curve shifts to the right. But on further increasing the number of mesh points to 125, no shift is seen. This implies that the curve is stabilized for mesh points equal to or greater then 100. Thus in this thesis all the calculations are made for 100 mesh points.

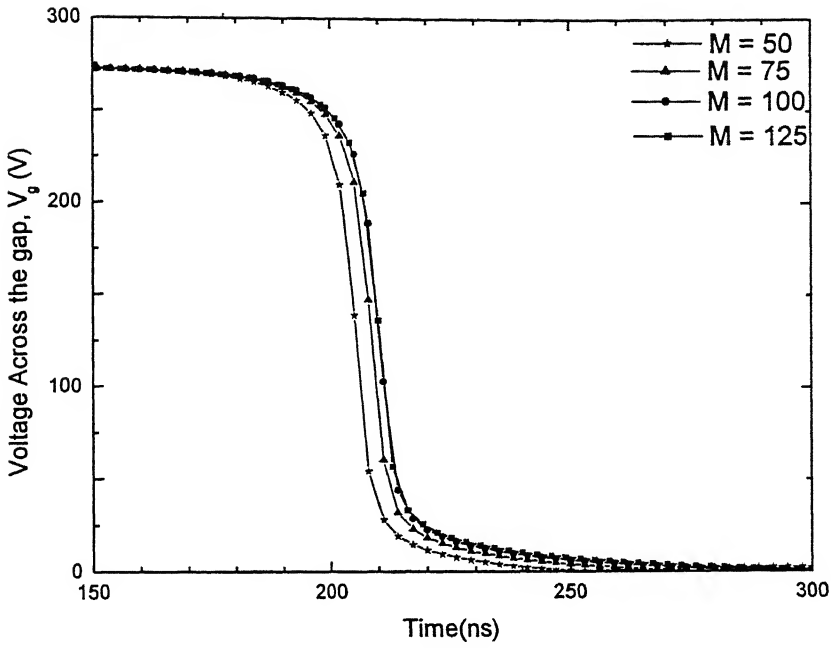

Fig 5.1: Effect of mesh points on the plot of voltage across the cell as a function of time.

5.3 Effect of neutral density

As is discussed earlier, in this thesis only two reactions are considered. Thus we have five species to consider; two neutral species (Xe, Ne), two positive ions (Xe^+, Ne^+) and an electron. In one case, we allowed neutral density to be unknown of the calculations. In the other, neutral densities are treated as constant, as a input parameter. The results with the two approaches are compared in figure 5.2, for the time evolution of the gap voltage and current density.

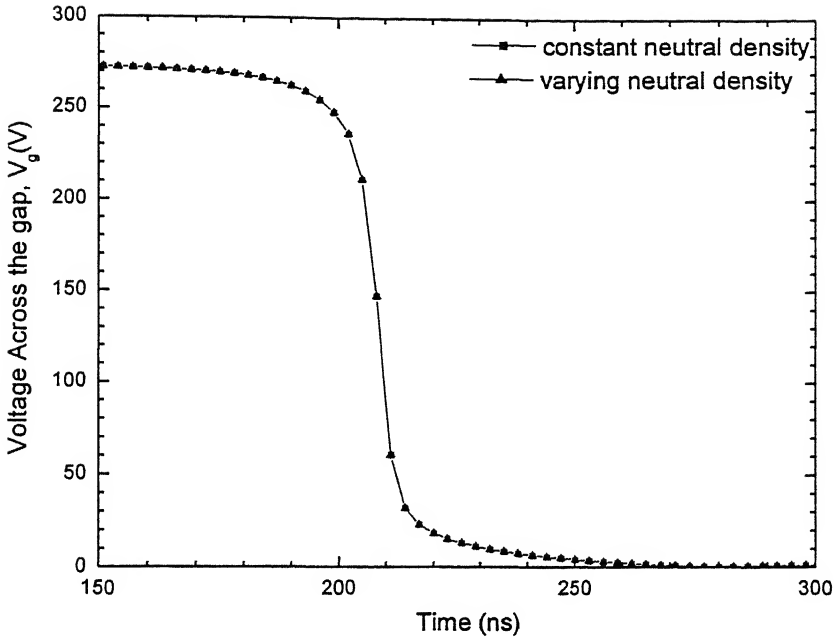

Fig 5.2(a): Effect of neutral density on time evolution of voltage across the cell

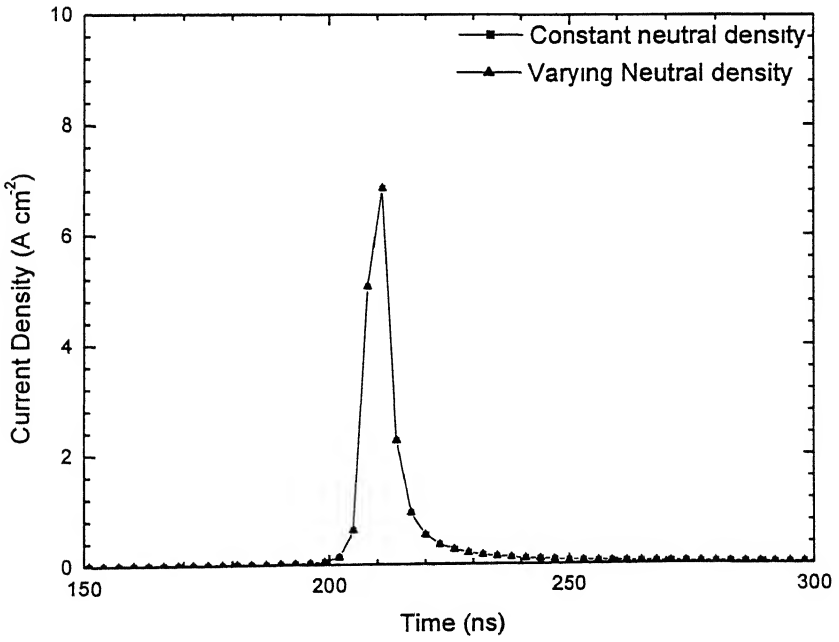

Fig 5.2(b): Effect of neutral density on time evolution of discharge current density

From the figure it is clear that considering neutral density as varying or constant does not makes any difference.

The above obtained results can also be explained theoretically. The neutral densities considered are of the order of 10^{19} cm^{-3}. But the maximum density of Xe^+ and Ne^+ ion are of the order of 10^{14} cm^{-3}. For each Xe^+ ion formed, one Xe is lost. Similarly for each Ne^+ ion formed, one Ne is lost. This implies that in the typical condition of PDP, Xe and Ne of the order of 10^{14} are lost, which is negligible as compared to the total initial density of Xe and Ne taken. Thus, effectively, there is not much change in the Xe and Ne density. So, considering Xe and Ne as constant or varying will not affect the simulation work. Thus in the further calculations, neutral density is treated as a constant.

5.4 Comparison of results for two reaction simulation and 36 reaction simulation

In this thesis work only two reactions, direct ionization, are considered. So, to check the validity of this, the results of two reaction simulation and all reaction simulation are compared. But because of unavailability of data, source term, the reactions named stepwise ionization in table 1.2, are not considered. In figure 5.3 the voltage across the gap and current density as a function of time for these two cases are compared.

Figure 5.3 clearly shows that considering two reactions or 36 reactions does not make any difference in the results, studied in this thesis.

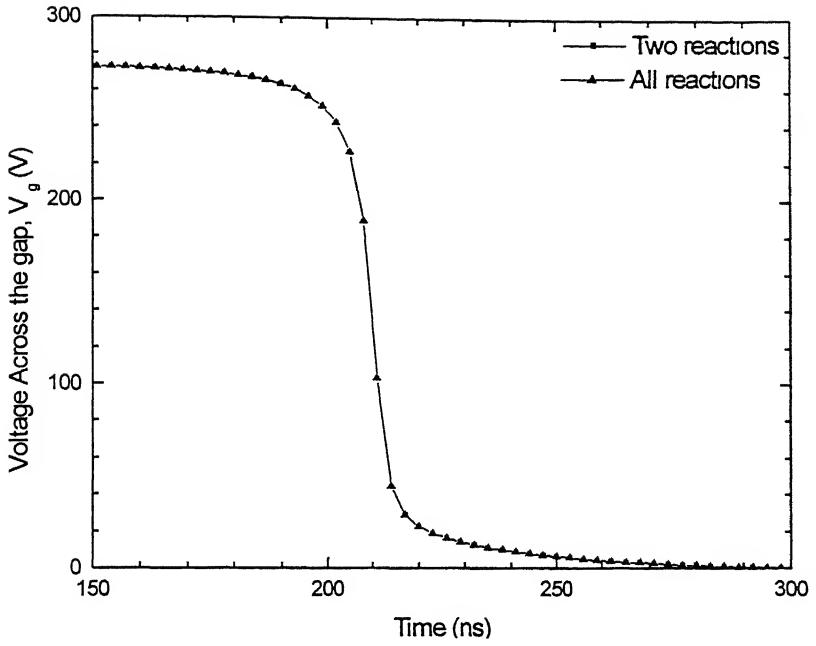

Fig 5.3(a): Effect of number of reactions considered on time evolution of voltage across the cell

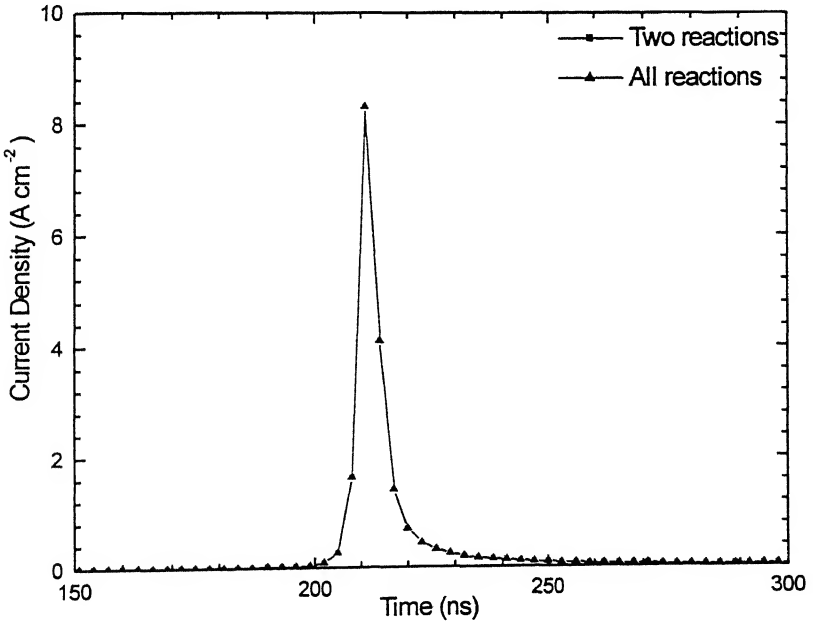

Fig 5.3(b): Effect of number of reactions considered on time evolution of current density.

5.5 Comparison of results with the Published literature

In order to check the validity of the simulation work, the results obtained are compared with the results given in the reference (7), for the same input parameters and conditions. They are shown in figure 5.4.

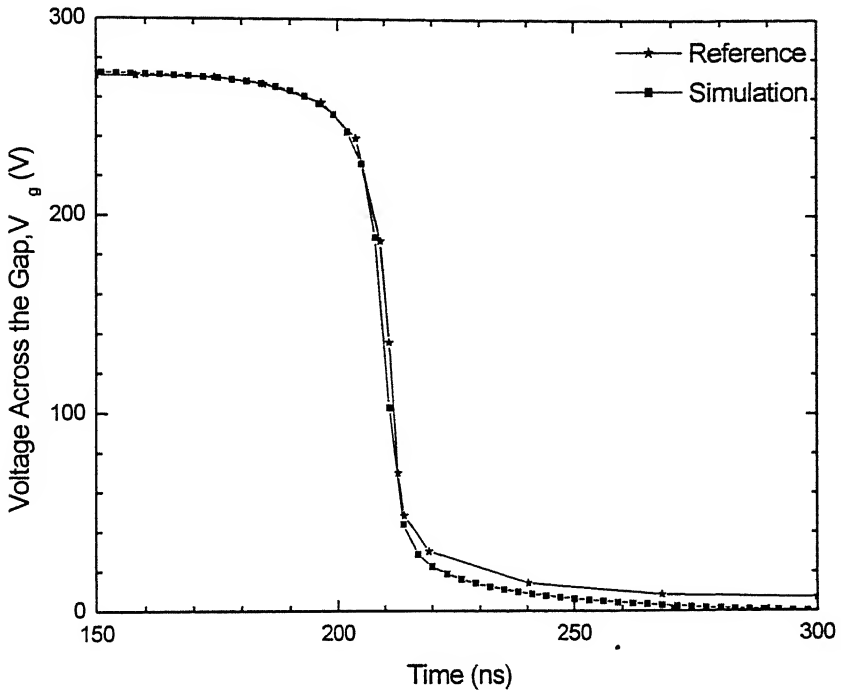

Fig 5.4(a): Voltage across the cell as a function of time

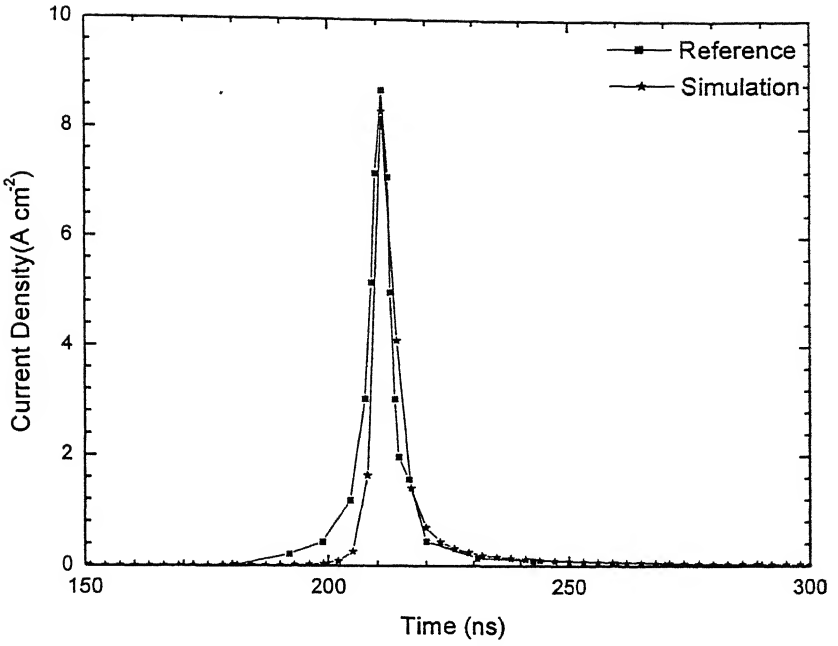

Fig 5.4(b): Current density as a function of time

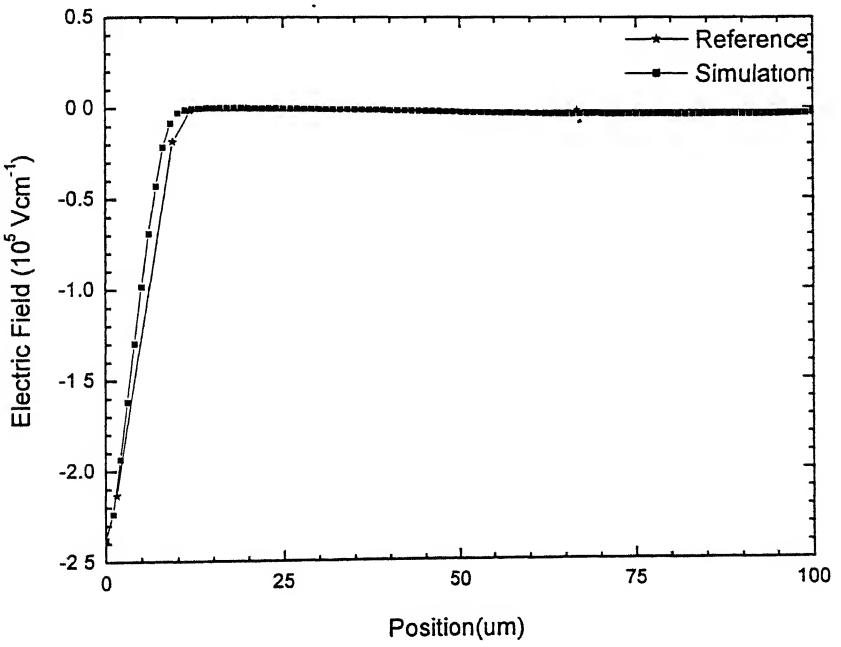

Fig 5.4(c): Spatial distribution of the electric field in the gap at 211 ns

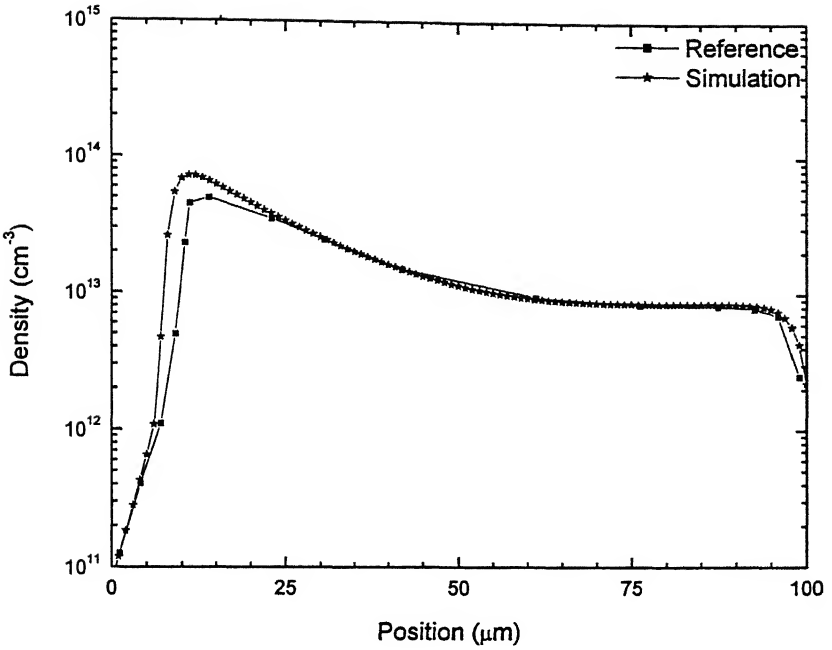

Fig 5.4(d): Spacial distribution of the density of electron at 211 ns

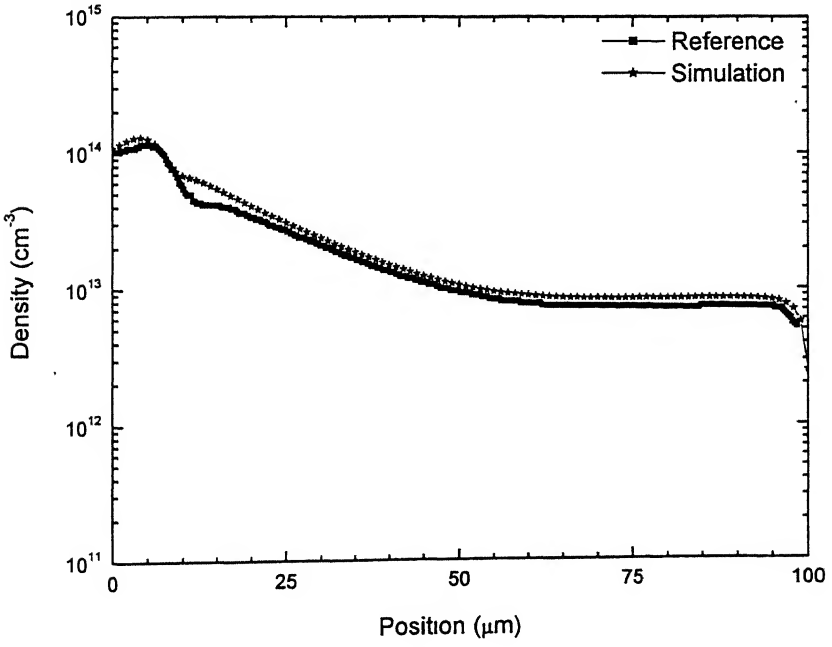

Fig 5.4(e): Spatial distribution of the density of Xe^+ ion at 211 ns

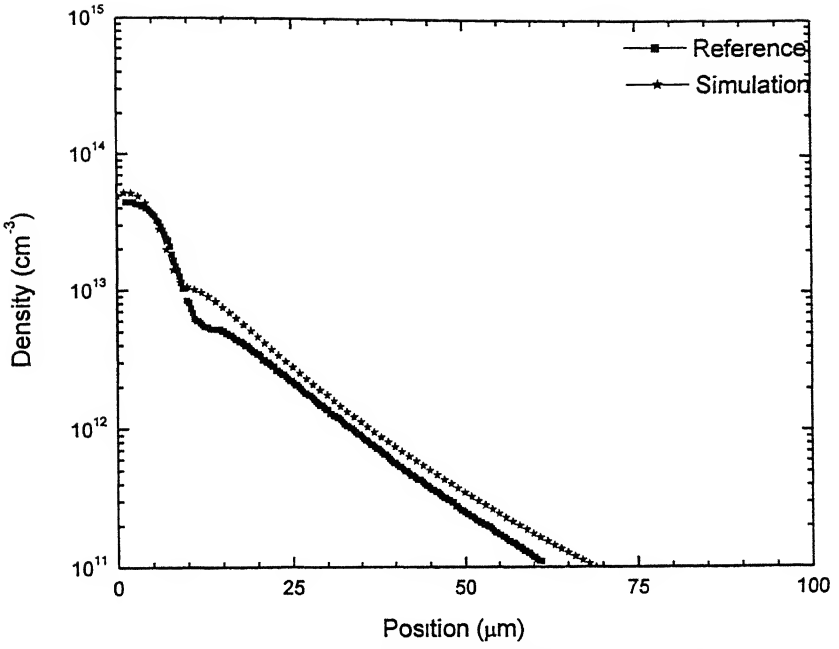

Fig 5.4(f): Spatial distribution of the density of Ne^{+} ion at 211 ns

The results clearly show that the simulation results are similar to that given in reference (7).

5.6 Discussion of results obtained

Before discussing the various results obtained, first let us consider the discharge formation. Initially there are small electrons and ions present in the discharge. Because of the applied electric field the electrons move towards the anode and ions towards the cathode. During the motion of electrons, ionization of gas takes place, which produce more electrons and positive ions. They also move towards anode and cathode, causing further ionization. The positive ions reaching cathode produces secondary electrons, which in turn produces further avalanches. This results in the breakdown of gas. The formation of discharge can be defined as substantial after a approximately 10% decrease in the voltage across the gap. As more and more electrons and positive ions reach anode and cathode, respectively, sheath is formed over them, restricting further charging of dielectric. The charge deposited over the electrodes induces an electric field, which opposes the applied electric field, and discharge is extinguished.

5.6.1 Voltage across the cell

Figure 5.5(a) shows the Voltage (V_g) across the cell as a function of time.

It can be clearly seen from the figure 5.5(a) that for 205 ns, before discharge, there is not much decrease in the voltage across the cell. Once discharge is started large number of positive ions and electrons are created in the discharge volume, which move towards the wall. This results in the charging up of the dielectric, which in turn induces a voltage that opposes the applied voltage. Thus in next 20 ns the voltage across the cell reduces to value close to zero. Even after the V_g is dropped to a value close to zero, the dielectric layer continues to charge and it takes 100 ns for V_g to drop to zero.

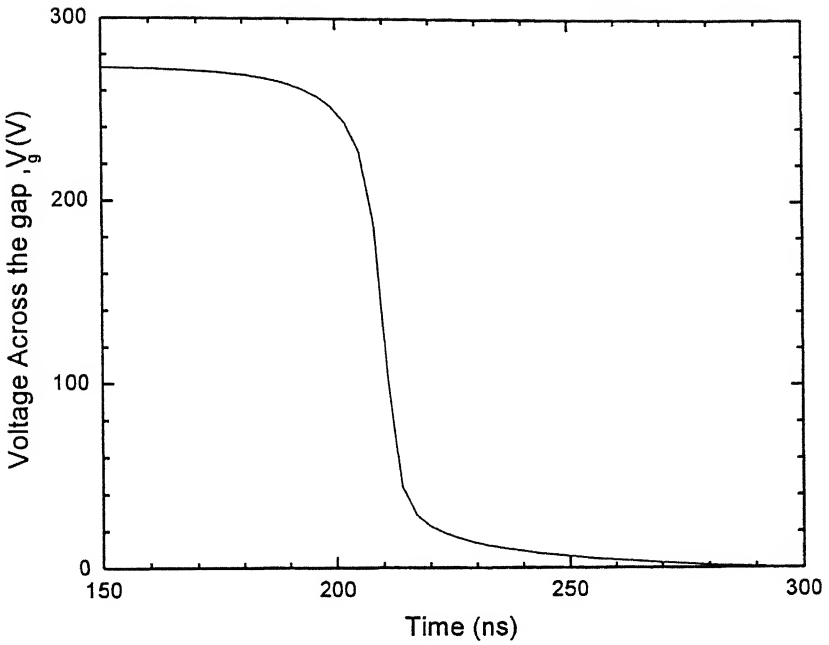

Fig 5.5(a): Voltage across the cell (V_g) as a function of time

5.6.2 Current density in the cell

Figure 5.5(b) shows the current density in the cell, as a function of time.

From the figure we can see that a discharge is initiated in the gap after a time delay of about 200ns. The discharge current density increases abruptly after t=200 ns and reaches a peak of 8.3 A/cm^2 in 10 ns. The current then decreases rapidly and reaches a value close to zero in less then 10 ns. The decrease of current density is due to the charging of the dielectric layers by electrons and ions, which are generated in the discharge volume. As is discussed above, this results in reduction of voltage across the gap. The decrease of the current density after time t=220 ns is much slower. And a small current density, on the order of 0.5 A/cm^2 continues to flow through the cell and to charge the dielectric for about 100 ns.

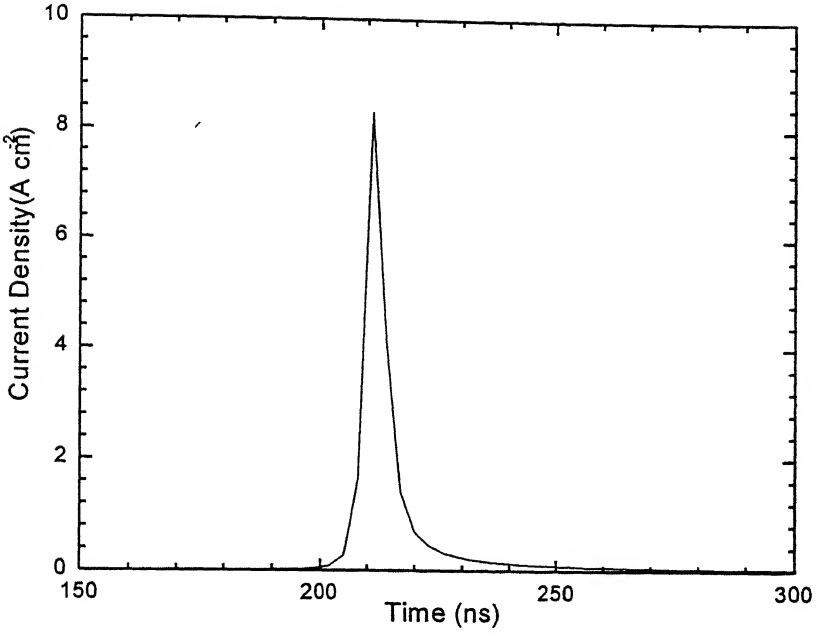

Fig 5.5(b): Discharge current density as a function of time

5.6.3 Electric Field

Figure 5.5(c) gives the spatial distribution of electric field in the gap at five different times.

At time t=160 ns the field is almost uniform in the gap. This means that the charged particle densities are still too small to distort the applied field.

As the ions density increases in the gap, the ion space charge is no longer negligible in the poisons equation and the field starts to decrease on the anode side of the discharge. The distortion of the electric field induces a fast increase in the electron multiplication corresponding to the discharge current increase. This results in the expansion of plasma region towards the cathode. At 205 ns the discharge current is substantial and the plasma occupies more then 50% of the gas gap. There is strong distortion of the electric field near the cathode, as can be seen

in the figure 5.5(c). One can clearly distinguish the formation of sheath near the cathode and the plasma.

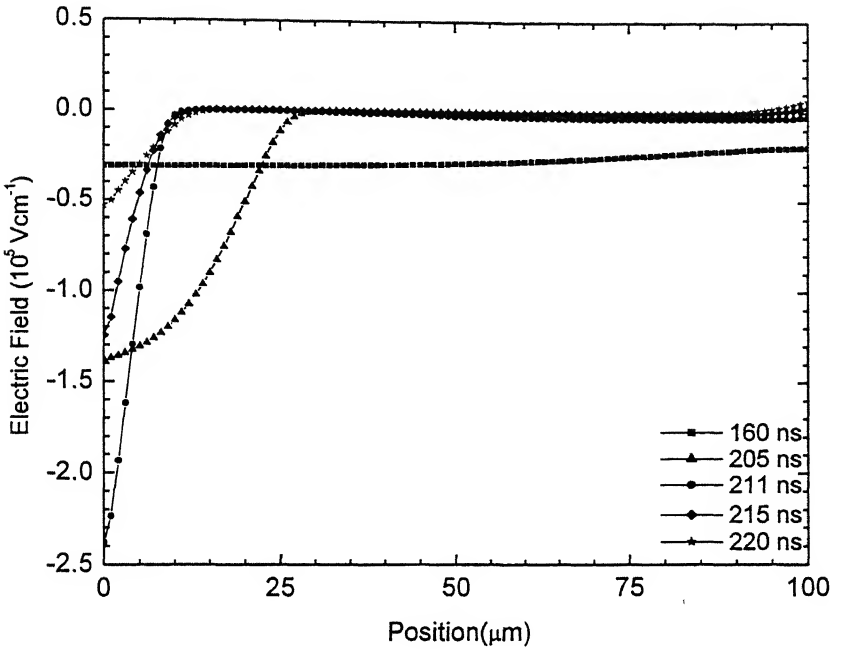

Fig 5.5(c): Spatial distribution of the electric field in the gap

Between t=205 ns and t=211 ns the plasma continues to expand toward the cathode side and the sheath contracts.

At t=211 ns, the sheath electric field is maximum, corresponding to the maximum current density. After that time, the electric field at the sheath further decreases and plasma moves towards the sheath.

At time t = 215 ns the electric field at the sheath is of the order of 1.4×10^5 Vcm^{-1}.

It decrease further to 0.5×10^5 Vcm^{-1} at t=220 ns.

5.6.4 Particle density

Figure 5.5(d) and 5.5(e) shows the density of Xe^+, Ne^+ and electron at t=211 ns and t =220 ns.

As is discussed above, the plasma first forms at the anode and moves towards the cathode. Thus a boundary between the plasma and sheath, over cathode, is formed. The electron density reaches a maximum of 8×10^{13} cm^{-3} coincident with the maximum in the current density and is situated at the sheath plasma boundary at that time, Fig 5.5(d). In the sheath region the density is very less as compared to that in the plasma.

At t=220 ns, at the end of current pulse, the maximum electron density is decreased, but is still high.

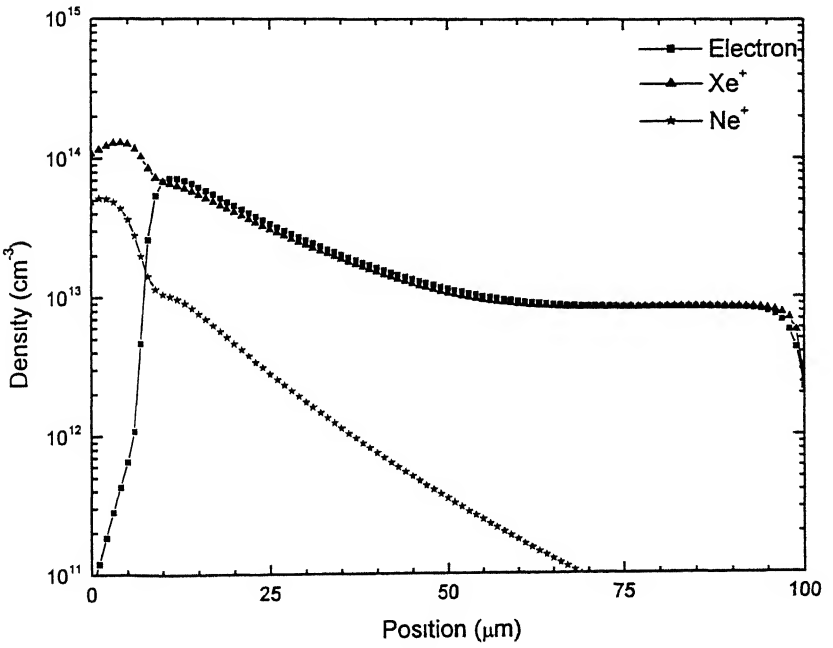

Fig 5.5(d): Spatial distribution of density of electrons and ions at t=211 s

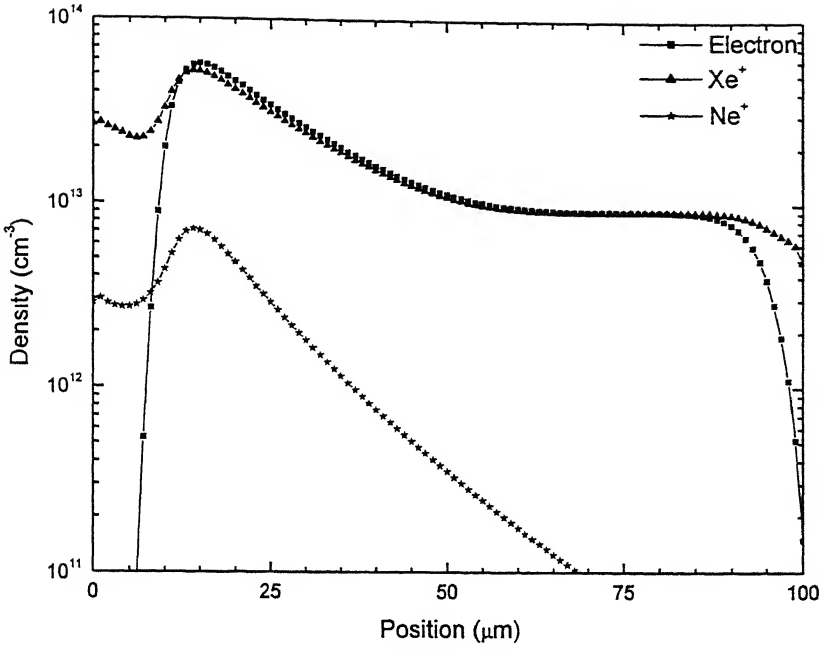

Fig 5.5(d): Spatial distribution of density of electrons and ions at t=211 s

From the figure it is clear that the dominant ion in the discharge is Xe^+. At t=211 ns, the density of Xe^+ ion is about three times larger than the density of Ne^+ ion in the cathode sheath, and much larger in the plasma region.

At t=220ns, at the end of current pulse, Fig 5.5(e), the concentration of Xe^+ ion is much larger than the concentration of Ne^+ ion.

5.7 Voltage transfer curve

We have considered a discharge cell before breakdown occurs. Let V_a be the voltage applied across cell. During the discharge pulse, the dielectric layers collect positive and negative charge and the voltage induced by these surface charges tend to decrease the cell voltage, until the charge is extinguished. Let ΔV_w be the change in wall voltage during the discharge. The curve defined by

$$\Delta V_w = f(V_a)$$

is called the voltage transfer curve and is used to defined the range of bistability, as is discussed in section 1.4.

Before breakdown, there is negligible charge on the dielectric. So the change in wall voltage, during discharge, is equal to that voltage which is induced due to charging of the dielectric layer. If

Q_w is the charge stored on the dielectric

C_d is the equivalent capacitance of the dielectric layer

C_g is the gas gap capacitance

V_w is the voltage induced due to charge stored

Then,

$$\Delta V_w = V_w = -\frac{Q_w}{K(C_d + C_g)} \quad (7)$$

where, $K = \frac{C_d}{C_d + C_g}$

Figure 5.6 shows the voltage transfer curve, $\Delta V_w = f(V_a)$

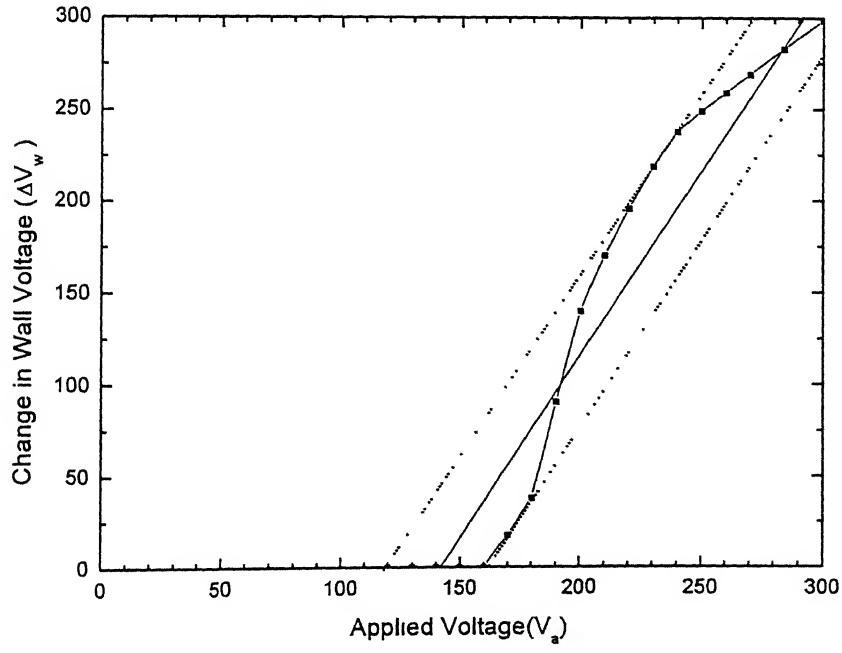

Fig 5.6: Voltage transfer curve, $\Delta V_w = f(V_a)$

As is discussed in section 1.4, the dashed lines, which are tangent to the voltage transfer curve, define the range of bistability for the sustaining voltage of 142 V. From the figure we are getting a bistability margin of 120 V to 160 V. This implies that for any V_s less than 120 volts the cell will never be switched ON, whatever the writing voltage is, and for V_s greater than 160, the cell can never be switched OFF. Thus for stability the sustaining voltage should be kept in between 120 V and 160 V.

The slope one line drawn at V_s =142 V, gives the location of equilibrium points. Comparing this plot with that of figure 1.11, we get stable equilibrium point as 284V.

5.8 Comparison of discharge in the cell for different value of firing voltage and same sustain voltage

In order to study the discharge, one writing pulse and then series of sustain pulses were simulated. To reduce the time of simulation, 76 node points were used. As can be seen from the Fig. 5.1, the results with 76 node points are close to those used 100 node points.

Fig 5.7 shows the voltage applied (V_s), voltage across the gas gap (V_g), voltage across the left dielectric (V_{d1}), voltage across the right dielectric (V_{d2}), charge density on the left dielectric (σ_1) and charge density on the right dielectric (σ_2), for same value of the sustain voltage (130 V) and different firing voltage. Similar results are plotted in figure 5.8 for sustain voltage equal to 150V.

The various results obtained are

1. The charge density on the two dielectrics is same in magnitude and different in sign. This is in accordance to what is discussed in section 1.4, that in each half cycle the discharge is identical except for sign

2. For all firing voltages, voltage drop across the dielectric, V_{d1} and V_{d2}, are same. As the charge density over two dielectrics is same, the voltage drop across them is same.
3. No breakdown of gas occurs for firing voltage less than or equal to 180V. From this we can conclude that the breakdown voltage of the gas is above 180V.
4. It can be seen from the figure 5.7 and 5.8 that from second pulse onwards, all the properties , V_g, V_{d1}, V_{d2}, σ_1 and σ_2, are same , for different firing voltages and same sustain voltages. Thus, we can say that these properties are a function of sustain voltage and are independent of firing voltage. For same firing voltage and different voltage, we found that the V_g is higher for the higher sustain voltage. Thus, we can use lower firing voltage and higher sustain voltage, in order to optimize the working of PDP cell.

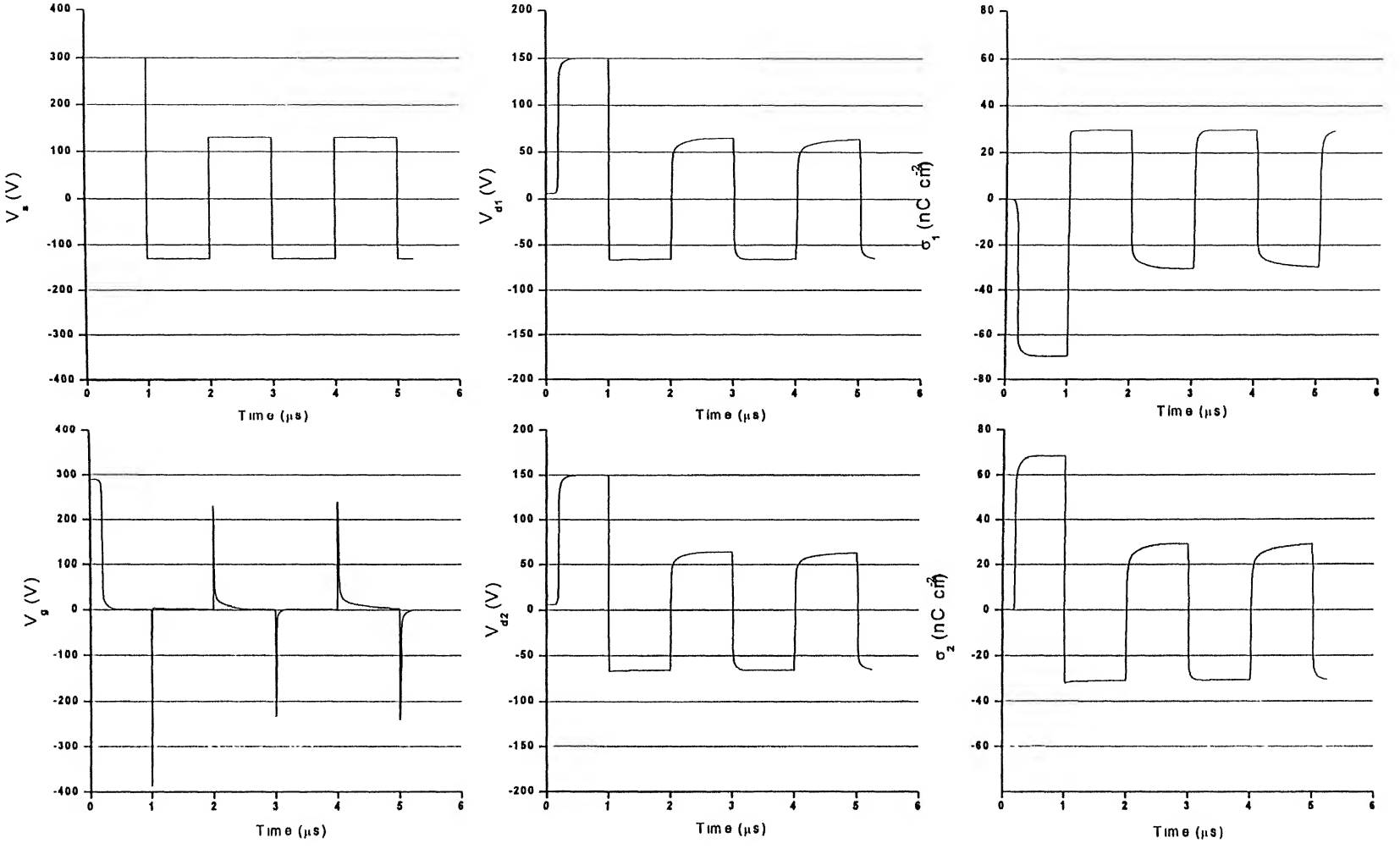

Fig 5.7(a): Various properties of PDP cell for V_a= 300 V and V_s = 130 V

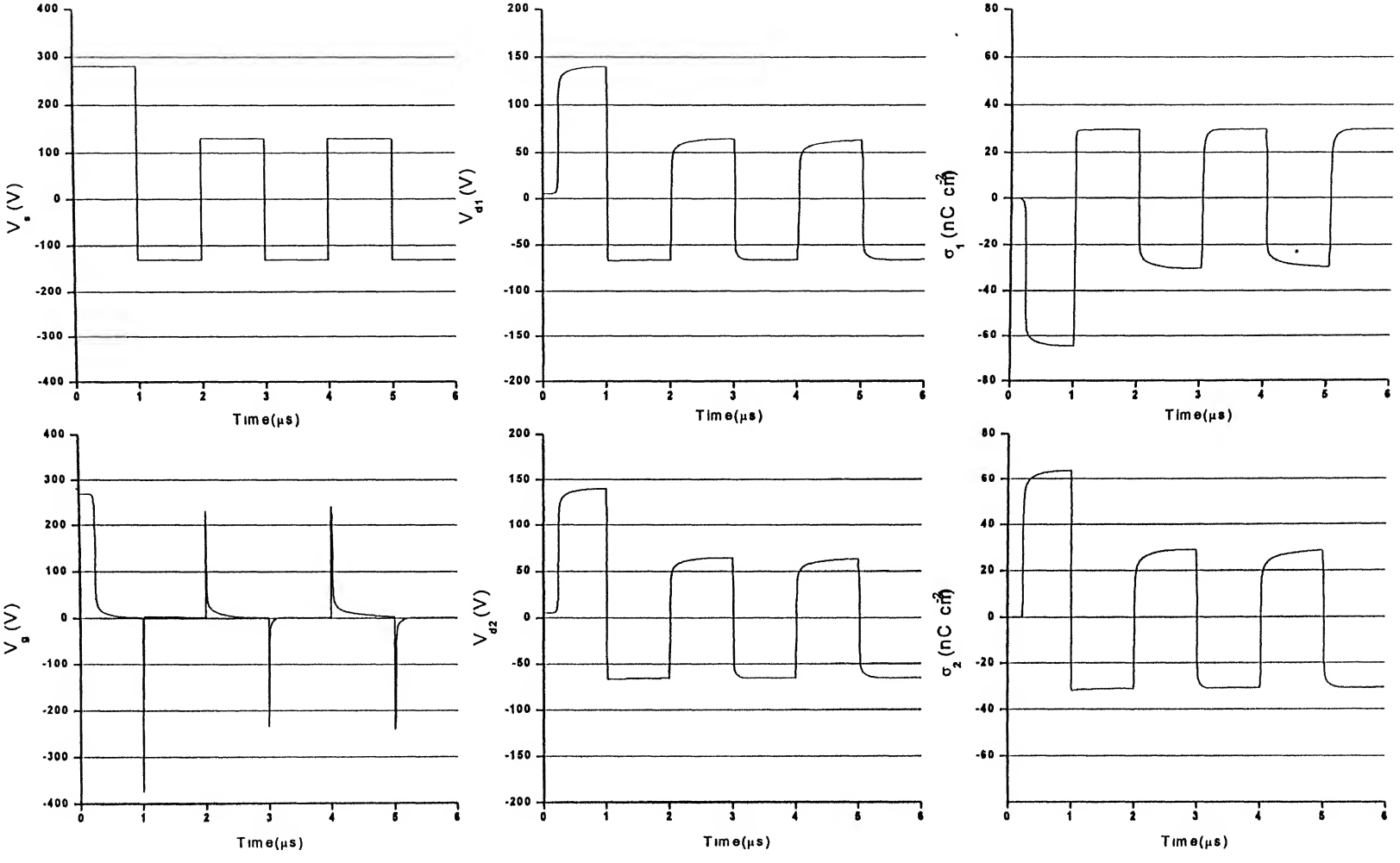

Fig 5.7(b): Various properties of PDP cell for V_a= 280 V and V_s = 130 V

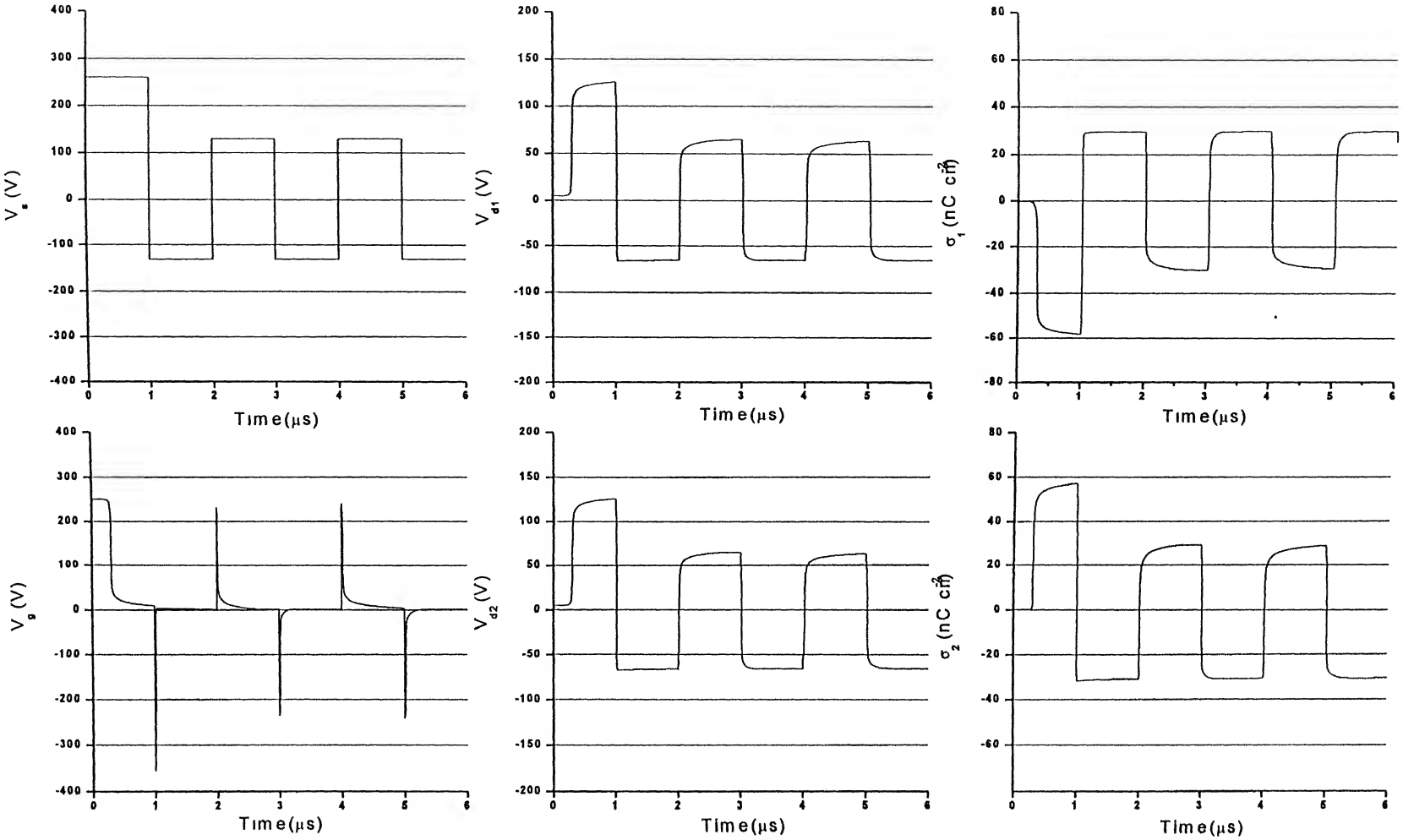

Fig 5.7(c): Various properties of PDP cell for V_a= 260 V and V_s = 130 V

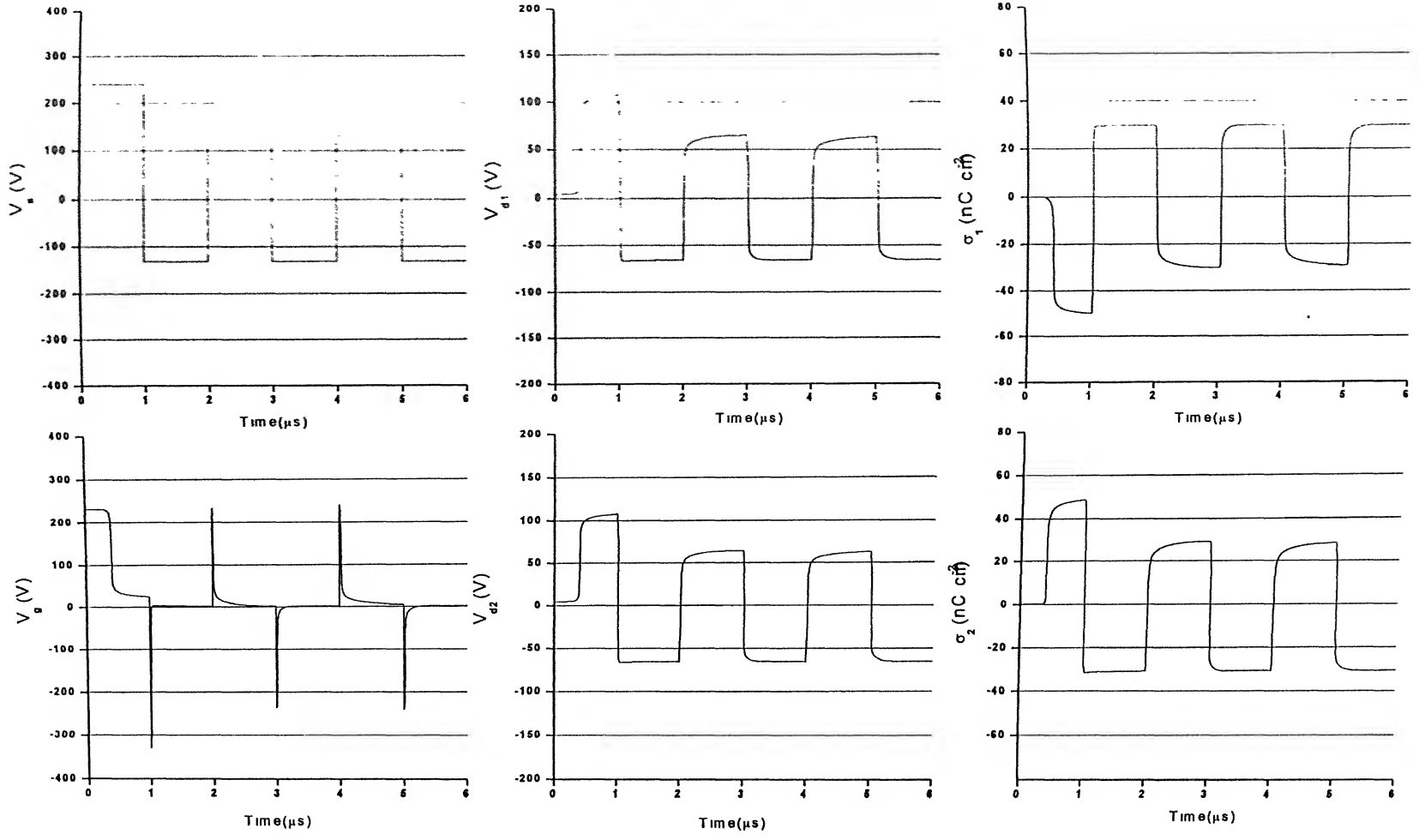

Fig 5.7(d): Various properties of PDP cell for V_a= 240 V and V_s = 130 V

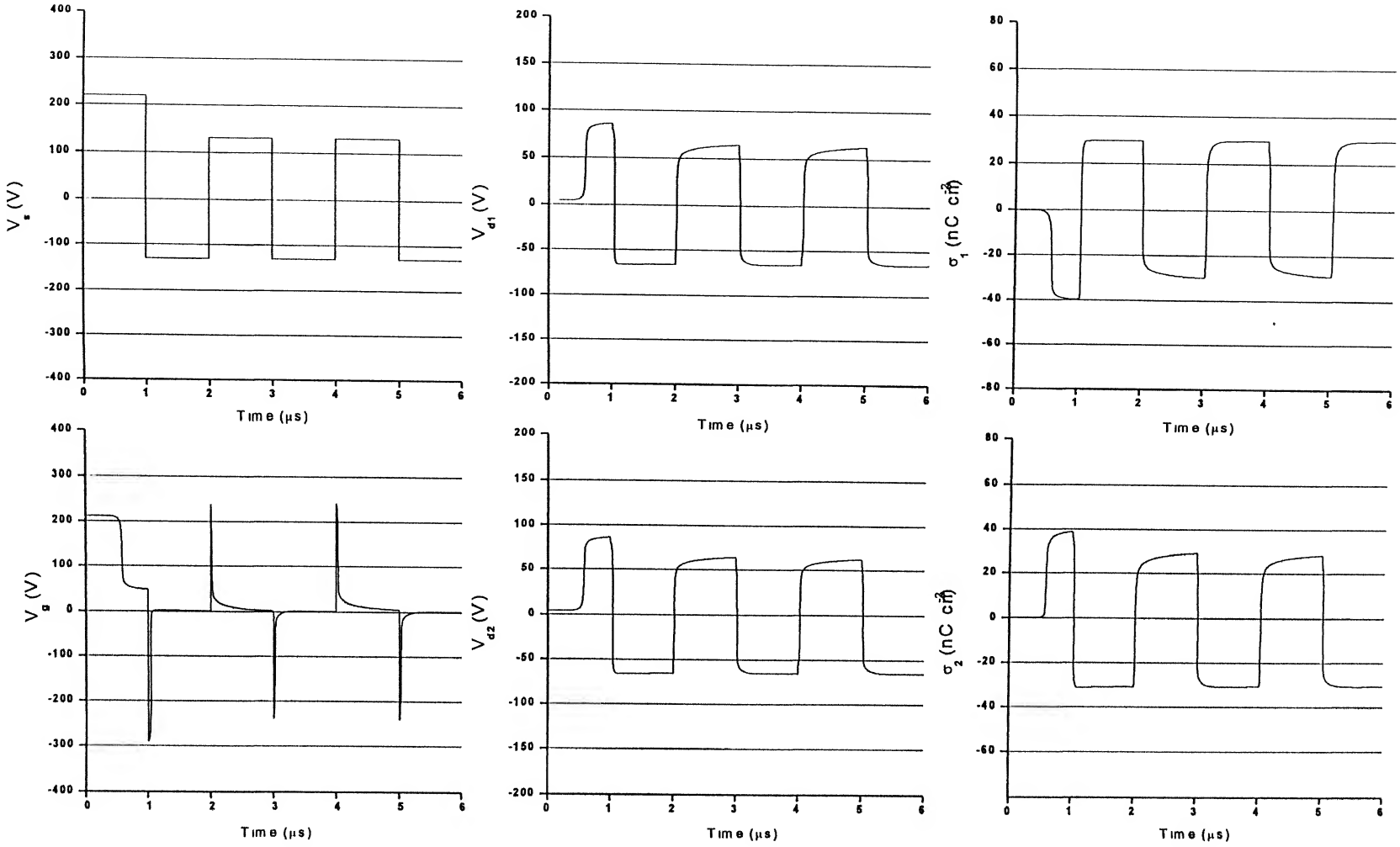

Fig 5.7(e): Various properties of PDP cell for V_a= 220 V and V_s = 130 V

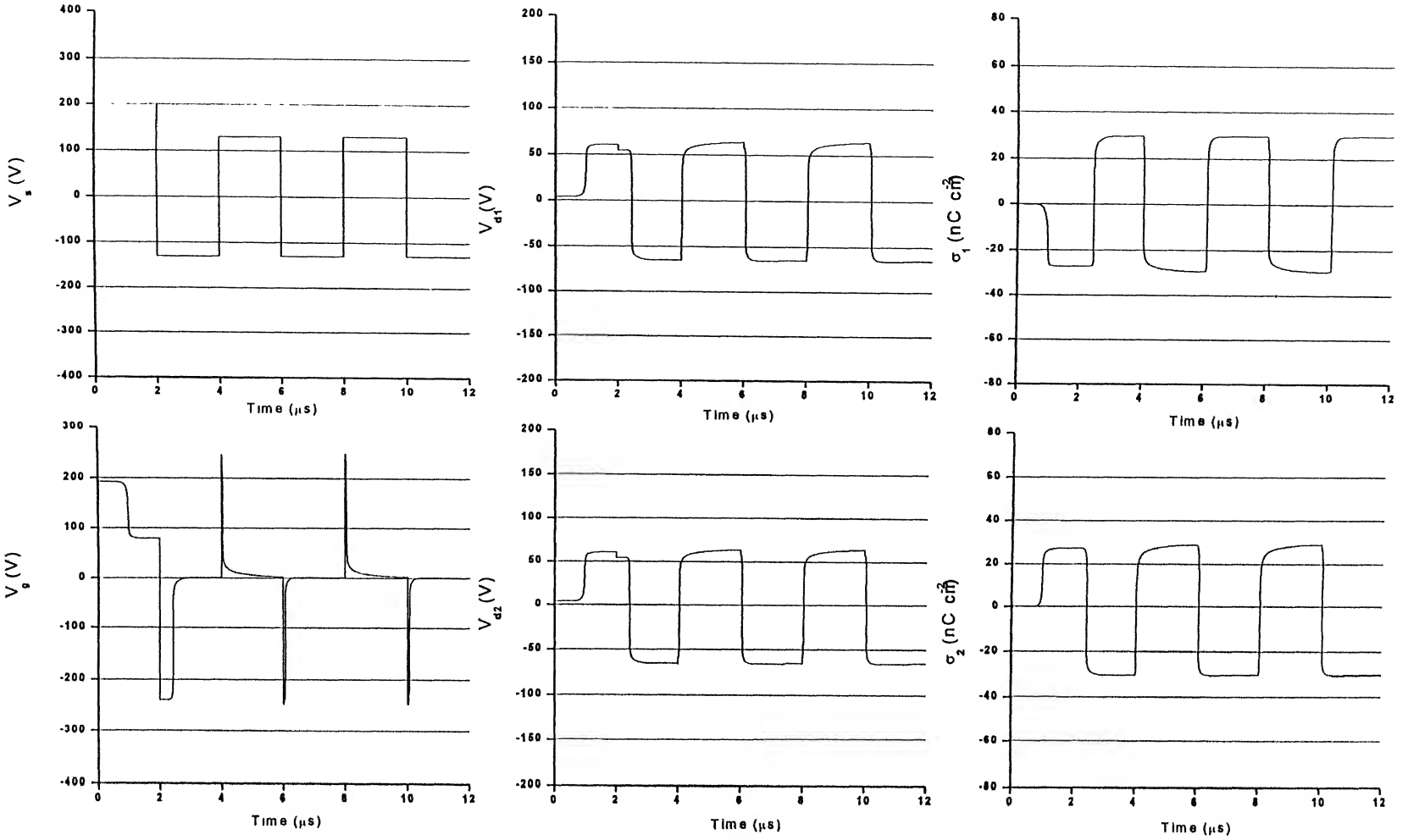

Fig 5.7(f): Various properties of PDP cell for V_a= 200 V and V_s = 130 V

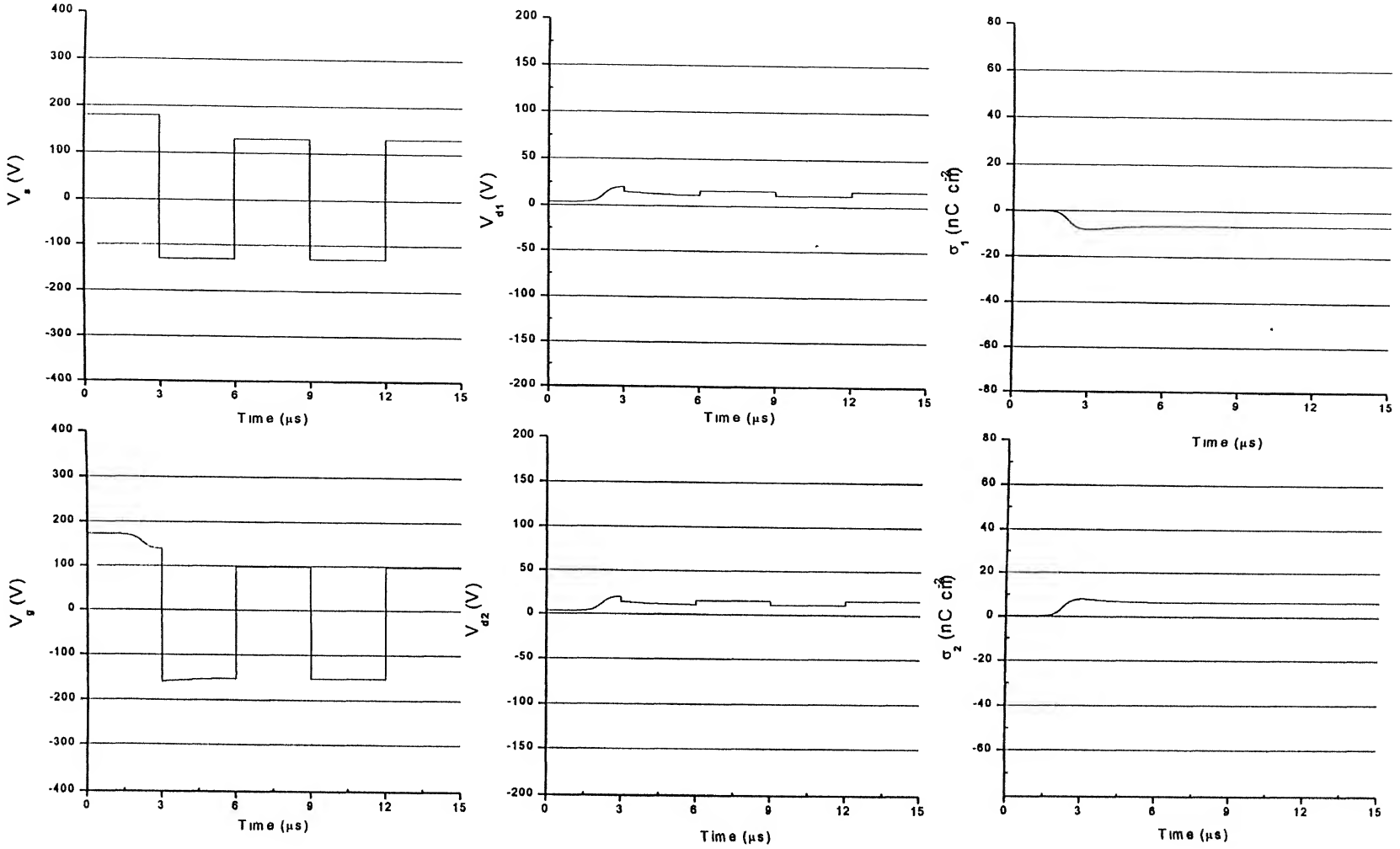

Fig 5.7(g): Various properties of PDP cell for V_a= 180 V and V_s = 130 V

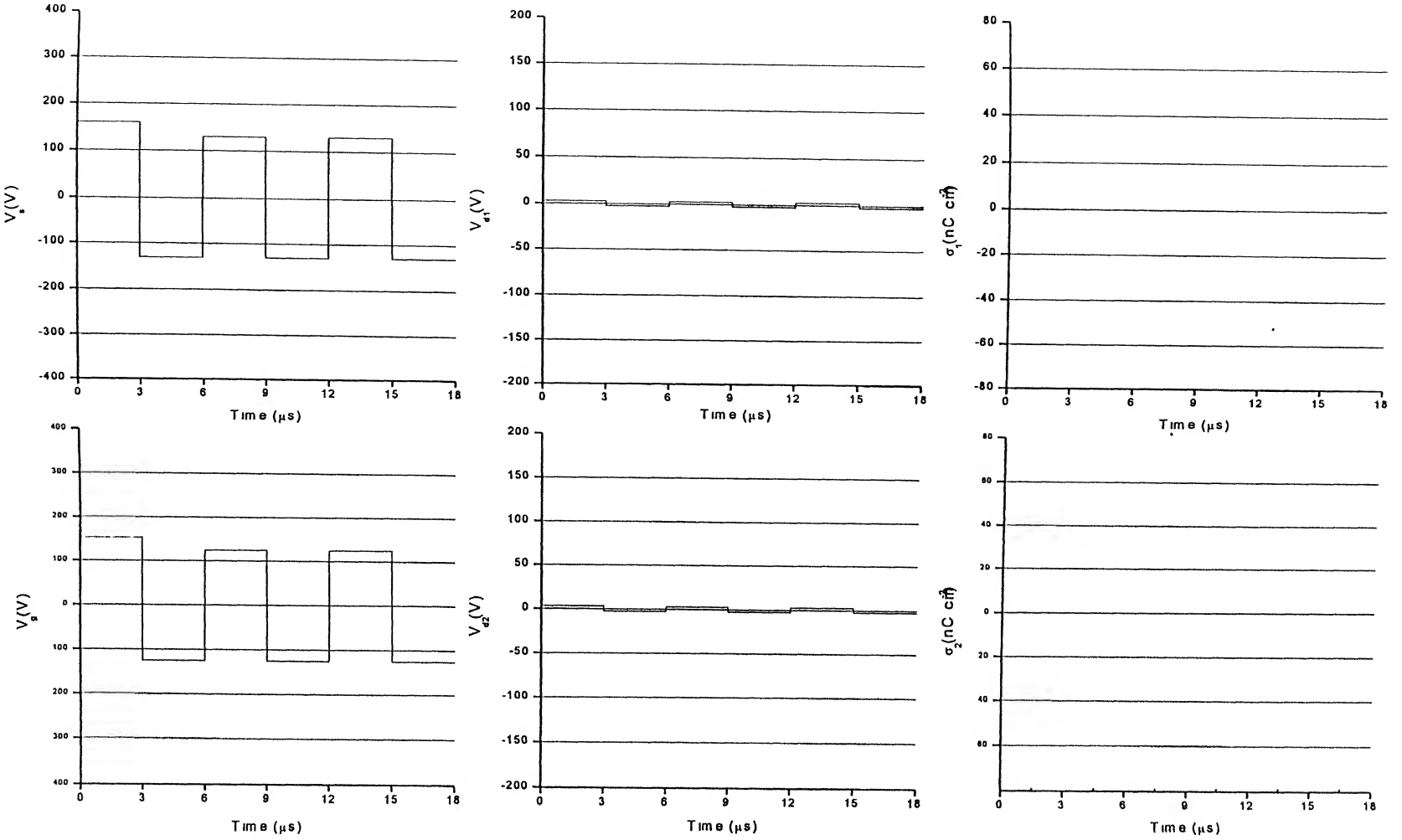

Fig 5.7(h): Various properties of PDP cell for V_a= 160 V and V_s = 130 V

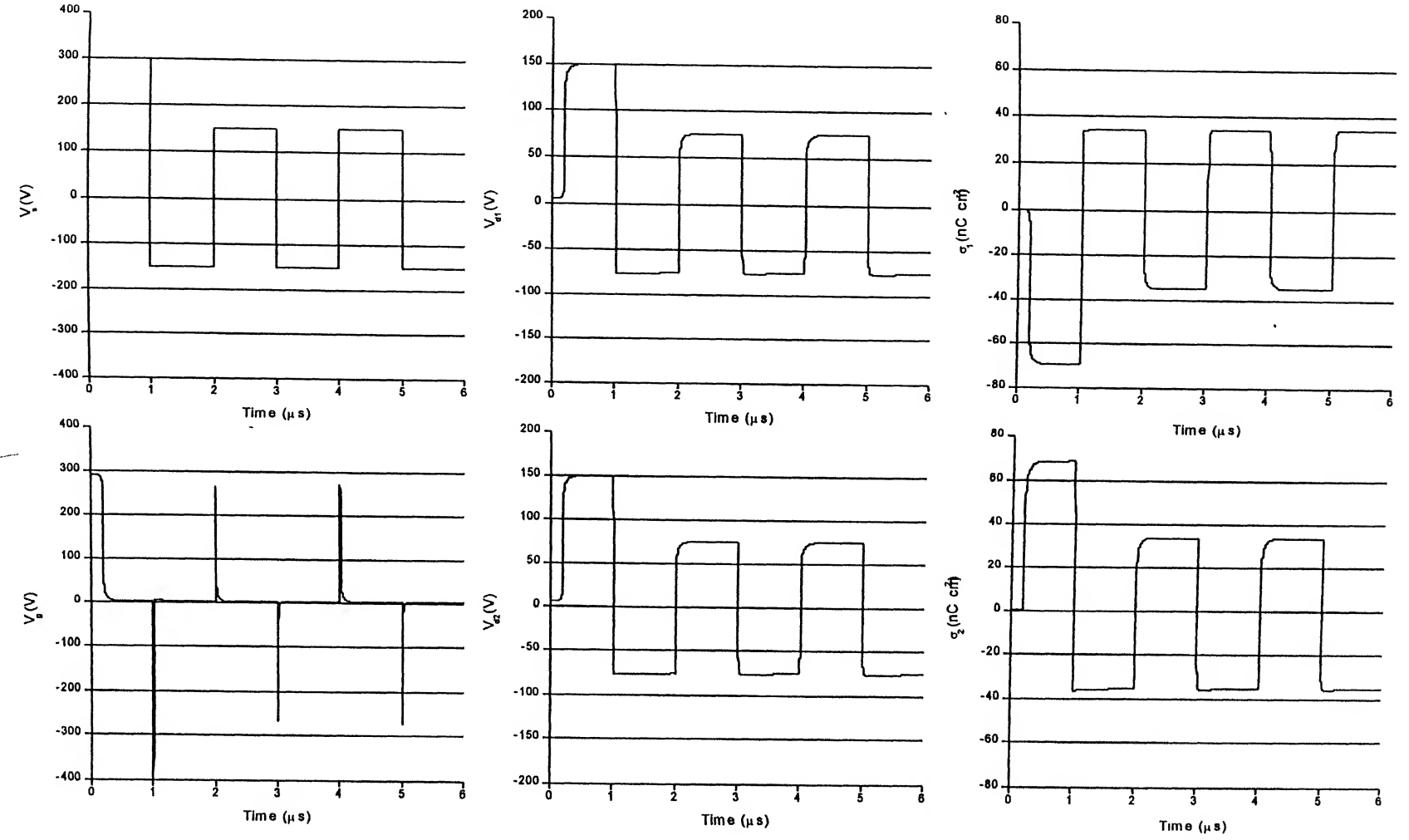

Fig 5.8(a): Various properties of PDP cell for V_a= 300 V and V_s = 150 V

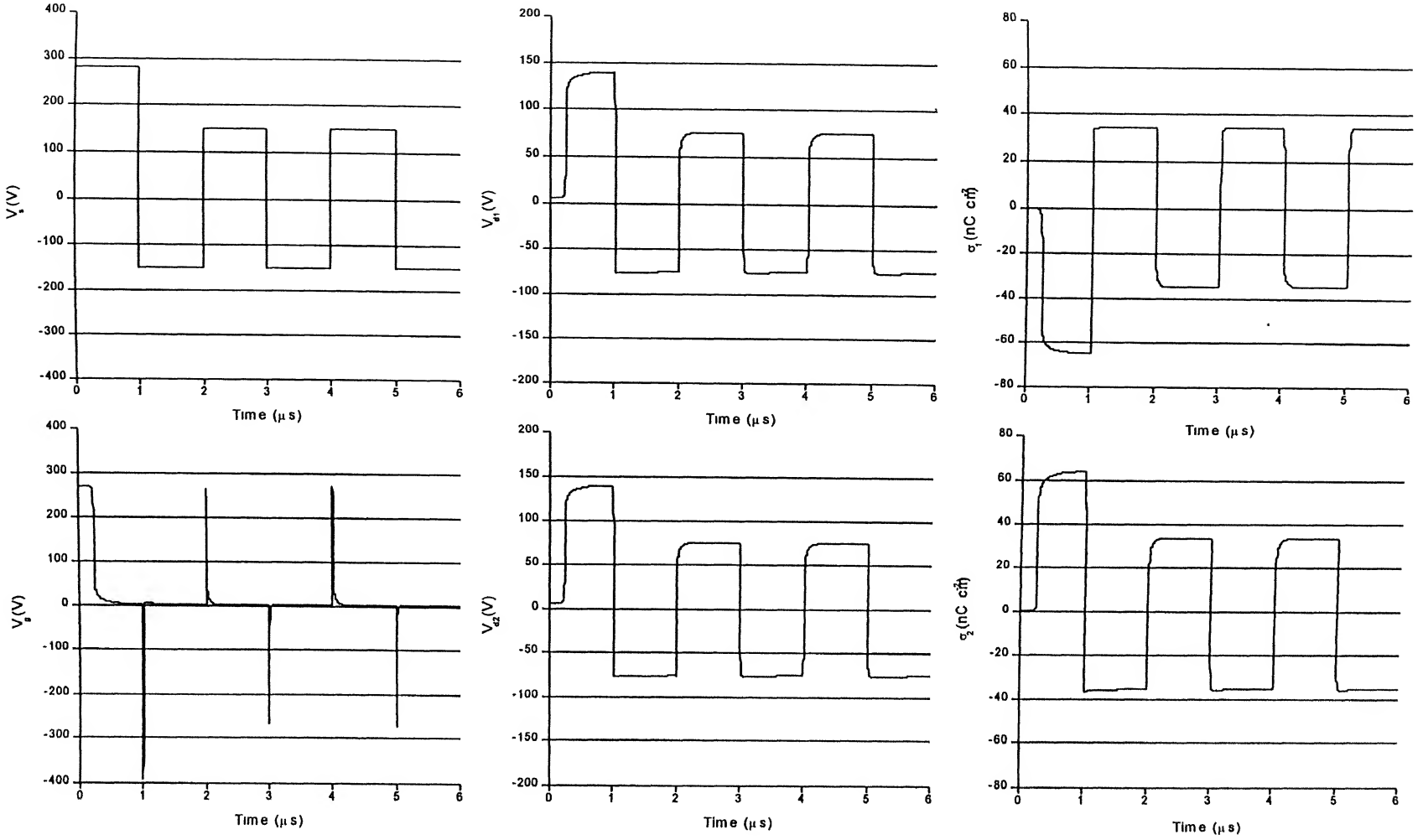

Fig 5.8(b): Various properties of PDP cell for V_a= 280 V and V_s = 150 V

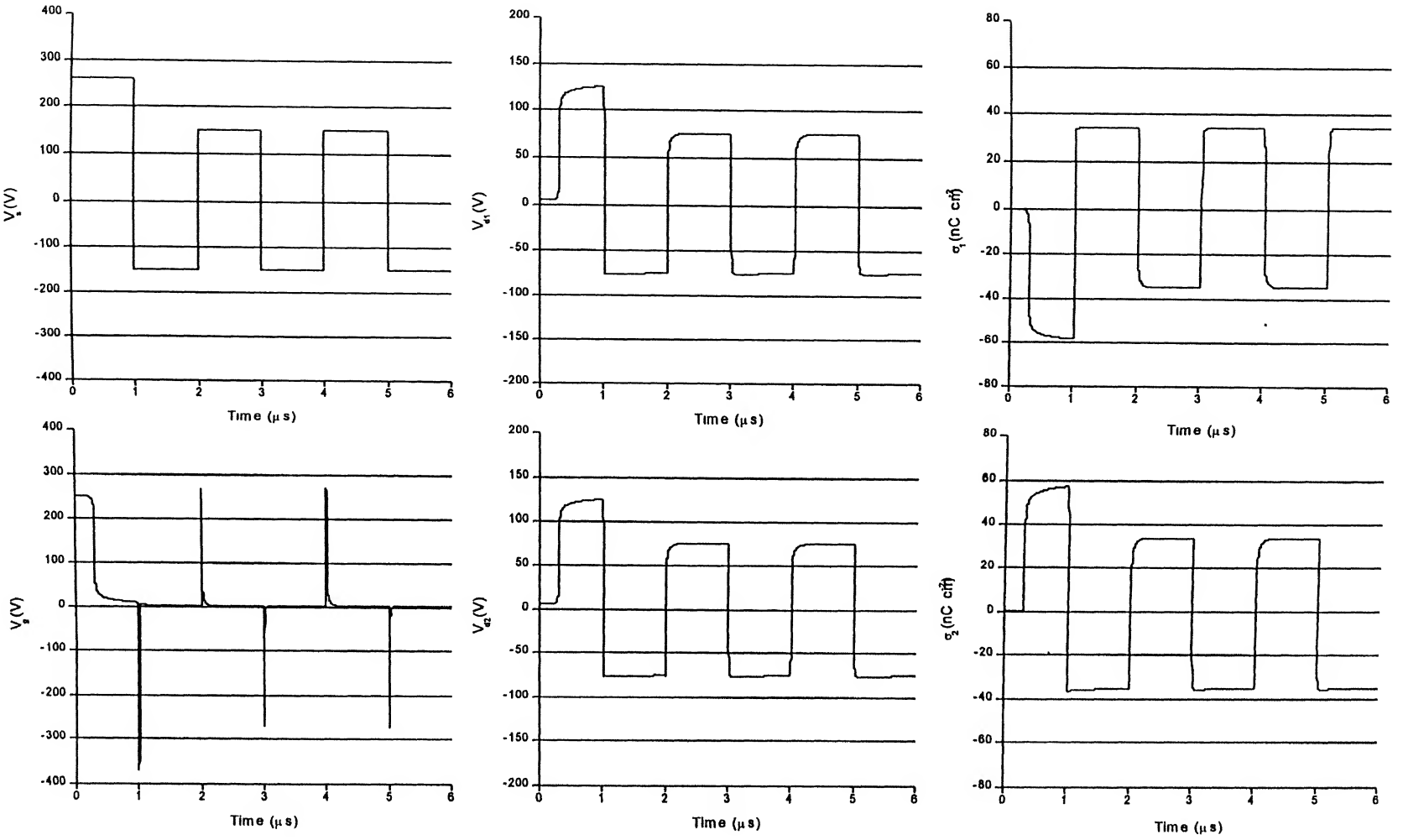

Fig 5.8(c): Various properties of PDP cell for V_a= 260 V and V_s = 150 V

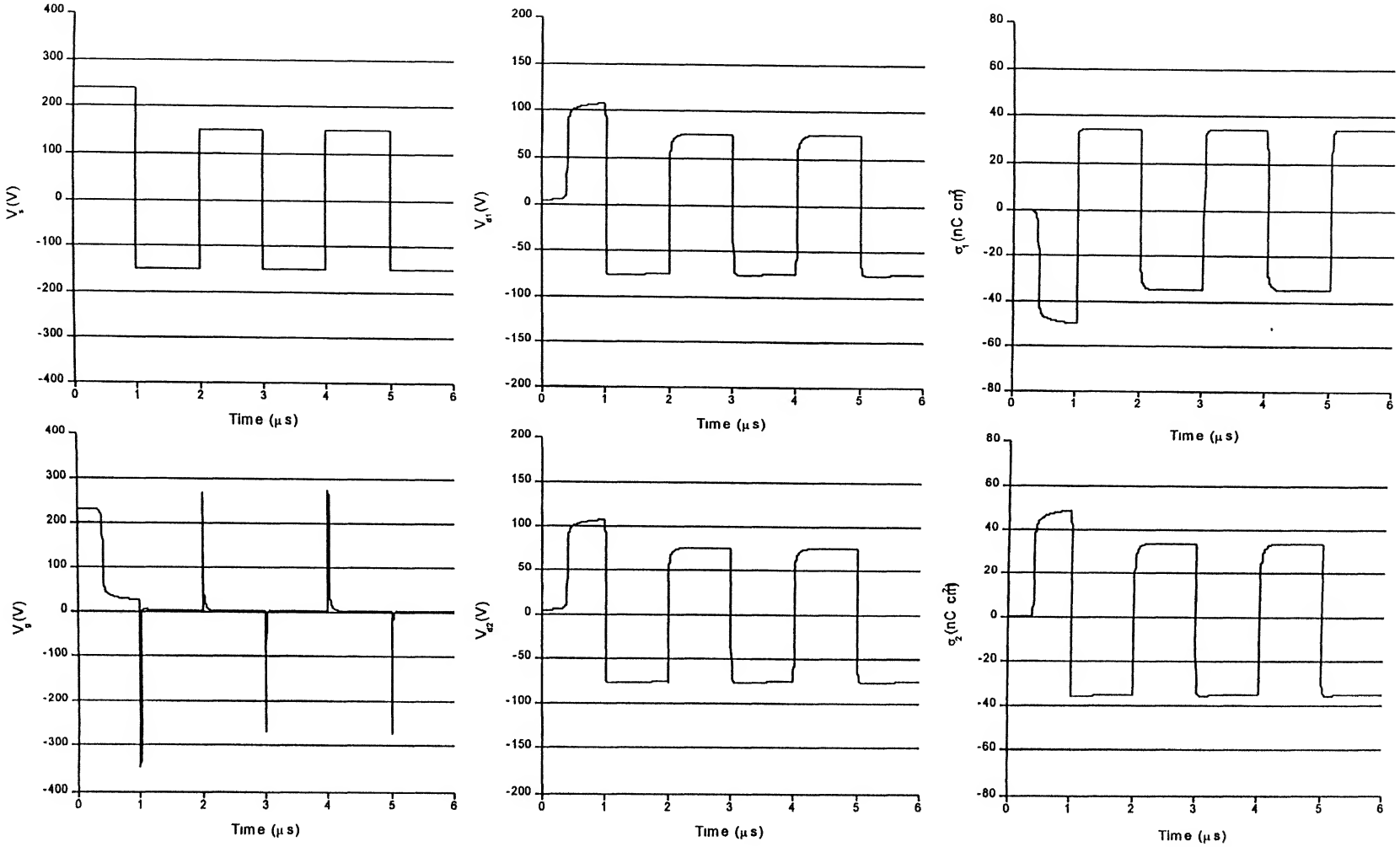

Fig 5.8(d): Various properties of PDP cell for V_a= 240 V and V_s = 150 V

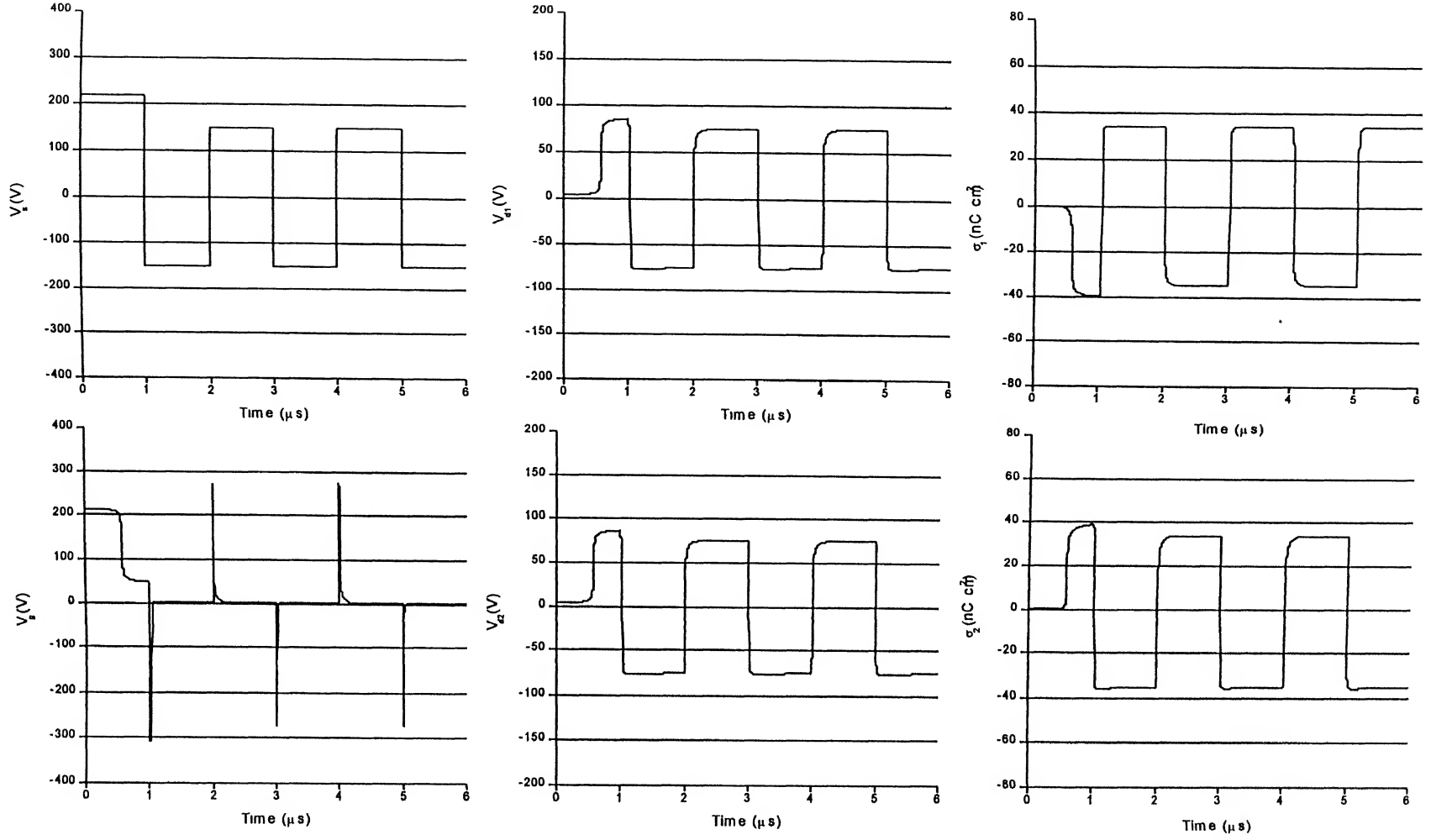

Fig 5.8(c): Various properties of PDP cell for V_a= 220 V and V_s = 150 V

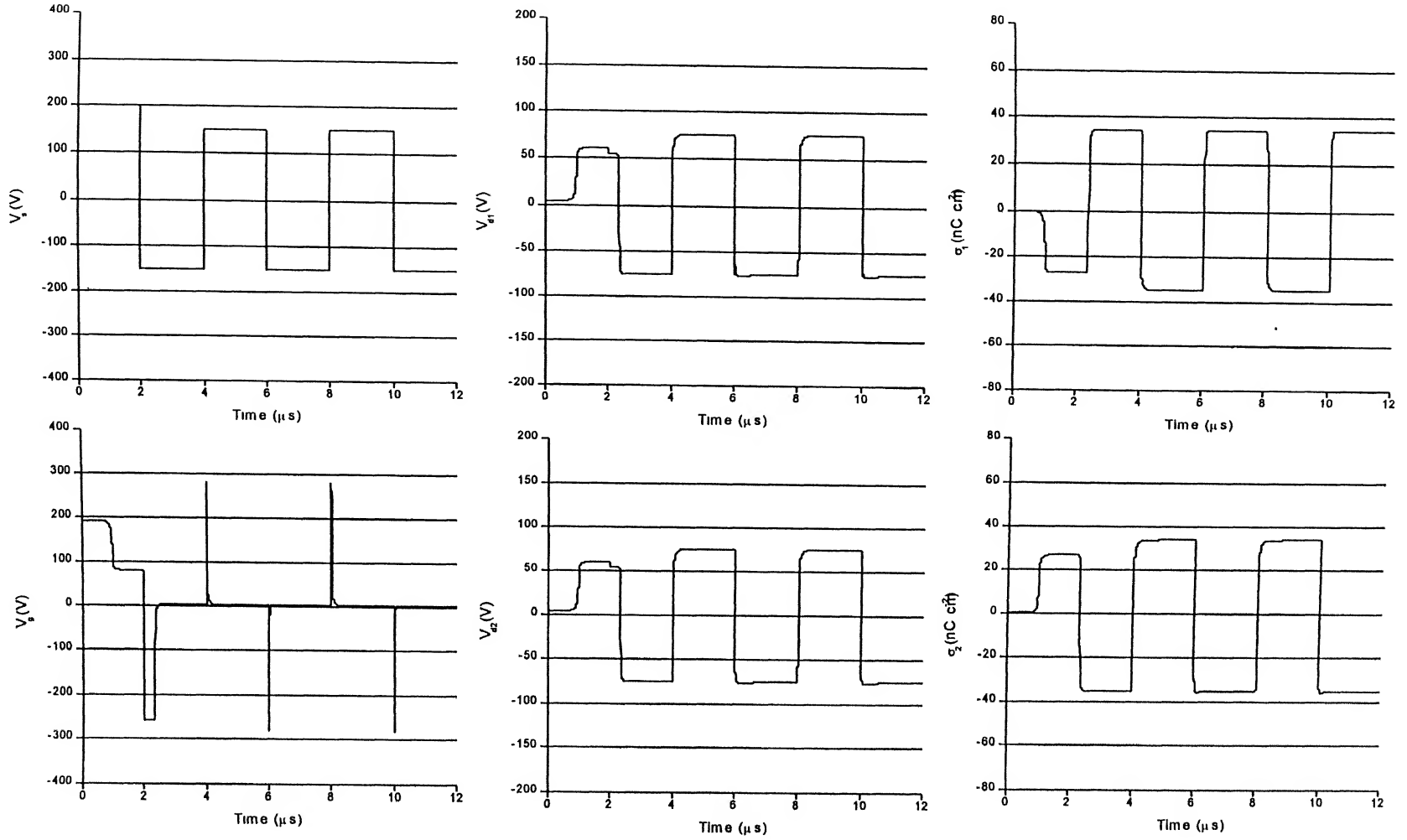

Fig 5.8(f): Various properties of PDP cell for V_a= 200 V and V_s = 150 V

5.9 Distribution of secondary electron flux

The time evolution of secondary electron flux is shown in figure 5.8.

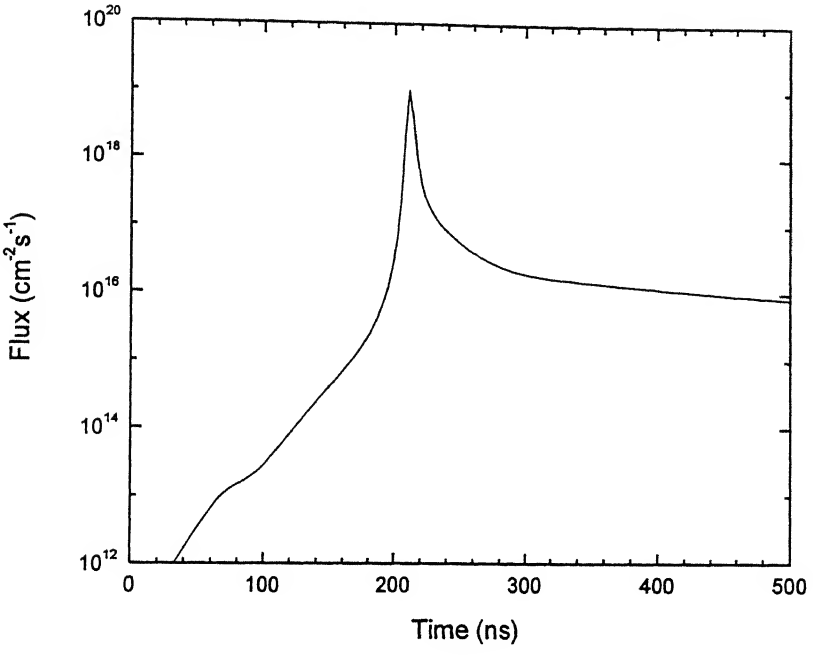

Fig 5.9: Total flux of secondary electrons as a function of time.

Before time t=200 ns there is exponential rise in secondary electron flux because of electron multiplication in a uniform field, which results in formation of positive ions. These positive ions form secondary electrons. Then there is sharp increase in the secondary electron flux, corresponding to formation of discharge in the gas gap. Then flux decreases, because of the charging of dielectric layer and formation of sheath on the dielectric.

5.10 Effect of Firing Voltage

Figure 5.10 shows the effect of different firing voltage on voltage across the cell.

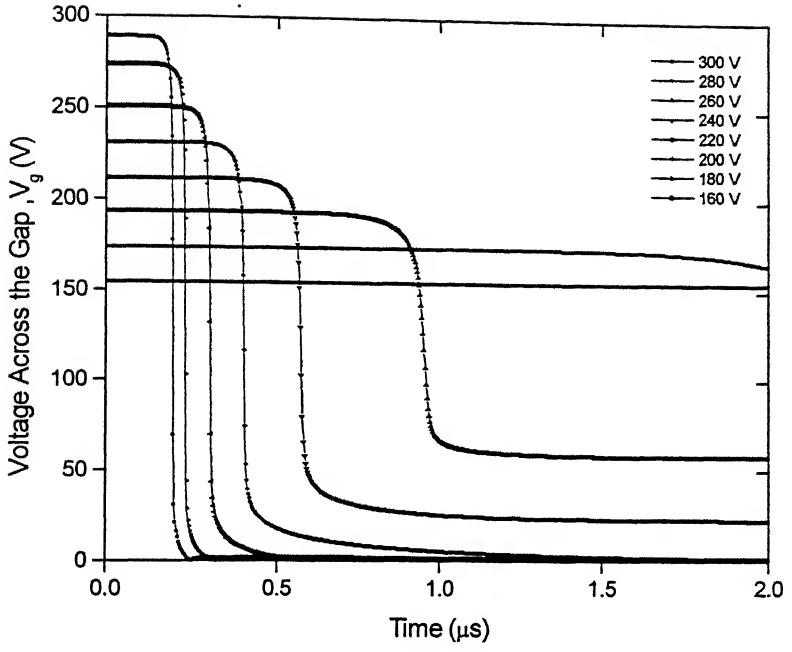

Fig 5.10: Effect of varying Firing Voltage on Voltage across the cell (V_g)

From the figure it is clear that the onset of discharge is delayed, as the firing voltage is decreased. For the voltages lower then 240 V, the voltage across the gap is not reduced to zero. From this we can infer that at voltages lower then 240 V, complete redistribution of charge does not takes place.

5.11 Effect of secondary electron emission coefficient

Figure 5.11 shows the effect on varying Ne^+ and Xe^+ ion secondary electron emission coefficient on voltage across the cell.

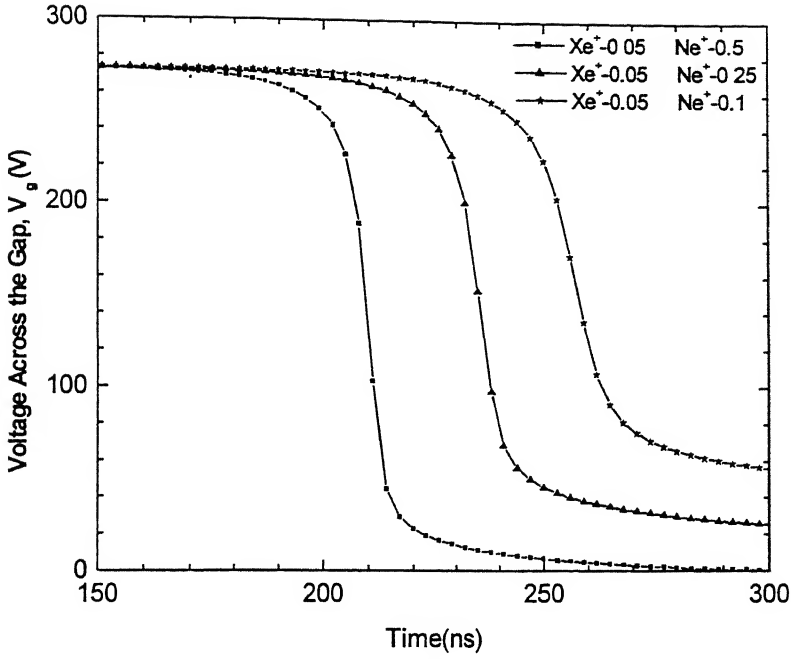

Fig 5.11(a): Effect of varying Ne^+ ion secondary electron emission coefficient on Voltage across the cell (V_g)

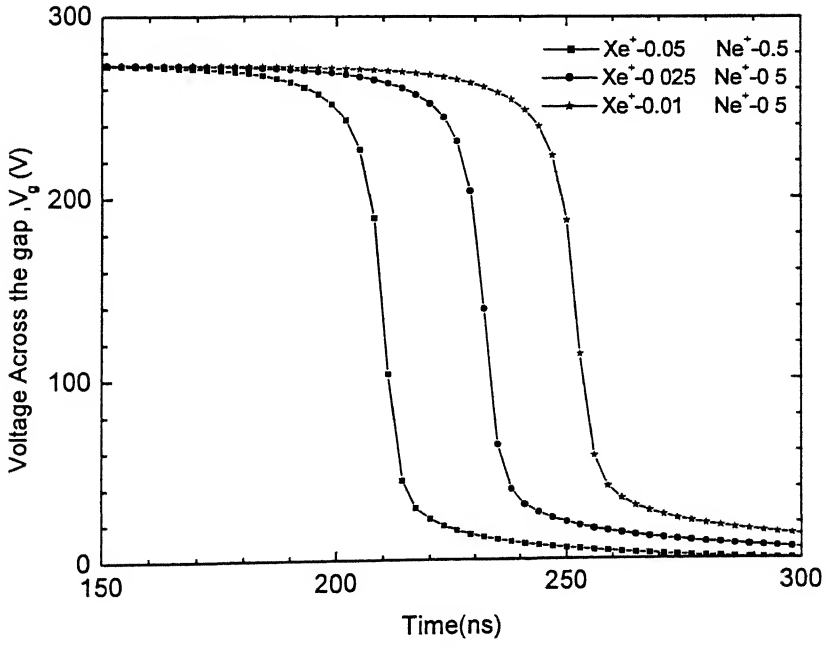

Fig 5.11(b): Effect of varying Xe^+ ion secondary electron emission coefficient on Voltage across the cell (V_g)

From the figure it is clear that varying secondary electron emission coefficient(γ), greatly affects the onset of the discharge. If γ is decreased, the occurrence of discharge is delayed. This clearly shows that γ plays an important role in defining breakdown of gas.

Chapter 6

Conclusions

A one dimensional model of the discharge occurring in the alternating current plasma display panel cell is developed. We have used this model to study the properties of a discharge pulse in a neon-xenon (90-10) mixture, for a 100 μm gap length at 560 Torr. The model results are found to be in good agreement with the published literature. In section 6.1 various conclusions that can be derived from the work are discussed, whereas section 6.2 deals with the scope of future work.

6.1 Conclusions

The conclusions of the present study are

1) The results show that the discharge current pulse under these conditions has a peak value close to 8.3 A/cm^{-2}. The current then decreases rapidly and reaches a value close to zero in less then 10 ns. However, 100 ns are needed to transfer all the charges to the dielectric layer.
2) The neutral density does not affect the results obtained in the simulation work. So in order to reduce the time of simulation, the neutral density can be treated as constant.
3) Using voltage transfer curve, range of bistability is determined. For the case studied in the thesis, it is found to be in the range of 120 V to 160 V. This implies that for any V_s less than 120 volts the cell will never be switched ON, whatever the writing voltage is, and for V_s greater than 160, the cell can never be switched OFF.
4) When multipulse simulation is done, it is found that the discharge is not a function of firing voltage, but it depends on the sustain voltage. Thus in order to optimize the PDP working, low firing voltage and high sustain voltage, defined by bistability margin, can be used.

6.2 Suggestions for Future Work

The following additional works can be carried out

1) In this thesis only electric part of the model is considered. If excited species kinetics and photon transport can be included in the work, UV emission can also be studied.
2) One Dimensional hybrid model can be used, in which the electrons are treated with the Monte Carlo simulation.
3) Two dimensional, and even three dimensional, simulation can be used to properly understand the discharge characteristics.

Appendix 1

Analytical solution of Poisson's Equation

Consider a simple PDP cell, as shown in figure A.1

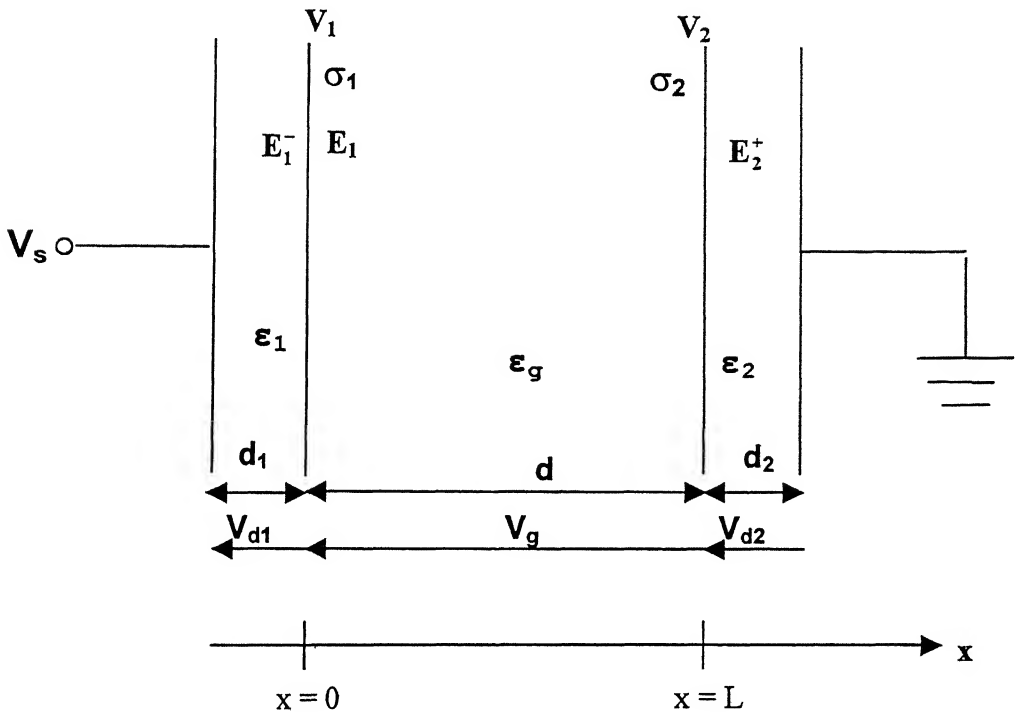

Fig A.1: Simple PDP cell

V_s is the applied voltage

σ_1 and σ_2 are the charge density on the left and right electrodes respectively.

ε_1, ε_2 and ε_g are the dielectric of left dielectric, right dielectric and gas gap, respectively.

d_1, d_2 and d are the thickness of left dielectric, right dielectric and gas gap, respectively.

V_{d1} and V_{d2} is the voltage drop across the left and right dielectric, respectively.

V_g is the voltage across the gas gap

V_1 and V_2 are the voltages at x=0 and x=L, respectively.

In the gas gap, the Poisson's equation can be written as

$$\nabla.\mathbf{E} = \frac{\rho}{\varepsilon_g}$$

(A1.1)

For the one dimensional case, it becomes

$$\frac{\partial \mathbf{E}}{\partial x} = \frac{\rho}{\varepsilon_g}$$

This can be written as

$$\partial \mathbf{E} = \frac{1}{\varepsilon_g}\rho \partial x$$

Integrating it, we get

$$\mathbf{E}(x) = \frac{1}{\varepsilon_g}\int_0^x \rho dx + C$$

where, C is the constant of integration.

At x = 0, $\mathbf{E}(0) = \mathbf{E}_1$

Thus,

$$\mathbf{E}(x) = \frac{1}{\varepsilon_g}\int_0^x \rho dx + \mathbf{E}_1$$

(A1.2)

Consider $\mathbf{E}_1^-$ and $\mathbf{E}_2^+$, electric field in the two dielectrics.

According to Gauss law

$$\varepsilon_g \mathbf{E}_1 - \varepsilon_1 \mathbf{E}_1^- = \sigma_1$$

$$\mathbf{E}_1^- = \frac{\varepsilon_g}{\varepsilon_1}\mathbf{E}_1 - \frac{\sigma_1}{\varepsilon_1}$$

(A1.3)

If charge neutrality is assumed, then

$$\varepsilon_2 \mathbf{E}_2^+ = \varepsilon_1 \mathbf{E}_1^-$$

Thus we get,

$$\mathbf{E}_2^+ = \frac{\varepsilon_g}{\varepsilon_2}\mathbf{E}_1 - \frac{\sigma_1}{\varepsilon_2}$$

(A1.4)

Inside dielectrics,

$$\mathbf{E}_1^- = \frac{V_s - V_1}{d_1}, \text{ and}$$

$$\mathbf{E}_2^+ = \frac{V_2}{d_2}$$

Thus

$$V_s - V_1 = \left(\frac{\varepsilon_g}{\varepsilon_1}\mathbf{E}_1 - \frac{\sigma_1}{\varepsilon_1}\right)d_1$$

(A1.5)

$$V_2 = \left(\frac{\varepsilon_g}{\varepsilon_2}\mathbf{E}_1 - \frac{\sigma_1}{\varepsilon_2}\right)d_2$$

(A1.6)

We know that,

$$\frac{d(V(x))}{dx} = -\mathbf{E}(x)$$

$$d(V(x)) = -\mathbf{E}(x)dx$$

Integrating

$$V_1 - V_2 = \int_1^2 \mathbf{E}(x)dx$$

(A1.7)

Adding equation A1.5, A1.6 and A1.7

$$V_s = \left(\frac{\varepsilon_g}{\varepsilon_1}\mathbf{E}_1 - \frac{\sigma_1}{\varepsilon_1}\right)d_1 + \left(\frac{\varepsilon_g}{\varepsilon_2}\mathbf{E}_1 - \frac{\sigma_1}{\varepsilon_2}\right)d_2 + \int_0^d \mathbf{E}(x)dx$$

$$V_s = \left(\frac{\varepsilon_g}{\varepsilon_1}\mathbf{E}_1 - \frac{\sigma_1}{\varepsilon_1}\right)d_1 + \left(\frac{\varepsilon_g}{\varepsilon_2}\mathbf{E}_1 - \frac{\sigma_1}{\varepsilon_2}\right)d_2 + \int_0^d \left(\frac{1}{\varepsilon_g}\int_0^x (\rho dx)\right)dx + \int_0^d \mathbf{E}_1 dx$$

Thus we get,

$$\mathbf{E}_1 = \frac{V_s - A + \frac{\sigma_1}{\varepsilon_1}d_1 + \frac{\sigma_1}{\varepsilon_2}d_2}{\frac{\varepsilon_g}{\varepsilon_1}d_1 + \frac{\varepsilon_g}{\varepsilon_2}d_2 + d} \qquad \text{(A.1.8)}$$

Appendix 2

BOLSIG output file, rates.out[27]

```
------------------------------------------------------------------------
------------
Xe_10+Ne              Xe   Ne     ( 10.0 % - 90.0 %)
 ------------------------------------------------------------------------
-------------
    5.00000        V/cm/torr   (    15.5280     Td)
 COLLISION FREQUENCIES in s-1.torr-1 (at 300 K)
 ------------------------------------------------------------------------
-------------
  0.813E+09             0.00   (eV)          elastique
  0.515E+06             8.31   (eV)          EXC
  0.395E+06             8.44   (eV)          EXC
  0.557E+06             9.69   (eV)          EXC
  0.641E+06            10.00   (eV)          EXC
  0.568E+05            11.00   (eV)          EXC
  0.185E+05            11.70   (eV)          EXC
  0.000E+00             3.44   (eV)          EXE
  0.879E+05            12.12   (eV)          ionisation
  0.717E+09             0.00   (eV)          elastique
  0.128E+03            16.62   (eV)          EXC
  0.156E+02            16.67   (eV)          EXC
  0.286E+02            16.84   (eV)          EXC
  0.501E+01            18.72   (eV)          EXC
  0.161E+00            20.00   (eV)          EXC
  0.110E-01            20.65   (eV)          EXC
  0.000E+00             4.90   (eV)          EXC
  0.153E-04            21.56   (eV)          ionisation
 ------------------------------------------------------------------------
-------------
   10.0000        V/cm/torr   (    31.0559     Td)
 COLLISION FREQUENCIES in s-1.torr-1 (at 300 K)
 ------------------------------------------------------------------------
-------------
  0.862E+09             0.00   (eV)          elastique
  0.968E+06             8.31   (eV)          EXC
  0.111E+07             8.44   (eV)          EXC
  0.181E+07             9.69   (eV)          EXC
  0.245E+07            10.00   (eV)          EXC
  0.278E+06            11.00   (eV)          EXC
  0.172E+06            11.70   (eV)          EXC
  0.000E+00             3.44   (eV)          EXE
  0.957E+06            12.12   (eV)          ionisation
  0.789E+09             0.00   (eV)          elastique
  0.139E+05            16.62   (eV)          EXC
```

```
  0.205E+04          16.67   (eV)          EXC
  0.529E+04          16.84   (eV)          EXC
  0.273E+04          18.72   (eV)          EXC
  0.319E+03          20.00   (eV)          EXC
  0.812E+02          20.65   (eV)          EXC
  0.000E+00           4.90   (eV)          EXC
  0.239E+03          21.56   (eV)          ionisation
 ------------------------------------------------------------------------
-------------
    15.0000       V/cm/torr   (    46.5839     Td)
 COLLISION FREQUENCIES in s-1.torr-1 (at 300 K)
 ------------------------------------------------------------------------
-------------
  0.890E+09           0.00   (eV)          elastique
  0.136E+07           8.31   (eV)          EXC
  0.203E+07           8.44   (eV)          EXC
  0.334E+07           9.69   (eV)          EXC
  0.484E+07          10.00   (eV)          EXC
  0.594E+06          11.00   (eV)          EXC
  0.518E+06          11.70   (eV)          EXC
  0.000E+00           3.44   (eV)          EXE
  0.296E+07          12.12   (eV)          ionisation
  0.854E+09           0.00   (eV)          elastique
  0.875E+05          16.62   (eV)          EXC
  0.142E+05          16.67   (eV)          EXC
  0.458E+05          16.84   (eV)          EXC
  0.300E+05          18.72   (eV)          EXC
  0.501E+04          20.00   (eV)          EXC
  0.158E+04          20.65   (eV)          EXC
  0.000E+00           4.90   (eV)          EXC
  0.656E+04          21.56   (eV)          ionisation
 ------------------------------------------------------------------------
-------------
    20.0000       V/cm/torr   (    62.1118     Td)
 COLLISION FREQUENCIES in s-1.torr-1 (at 300 K)
 ------------------------------------------------------------------------
-------------
  0.901E+09           0.00   (eV)          elastique
  0.166E+07           8.31   (eV)          EXC
  0.302E+07           8.44   (eV)          EXC
  0.485E+07           9.69   (eV)          EXC
  0.735E+07          10.00   (eV)          EXC
  0.926E+06          11.00   (eV)          EXC
  0.102E+07          11.70   (eV)          EXC
  0.000E+00           3.44   (eV)          EXE
  0.584E+07          12.12   (eV)          ionisation
  0.908E+09           0.00   (eV)          elastique
  0.242E+06          16.62   (eV)          EXC
  0.416E+05          16.67   (eV)          EXC
  0.158E+06          16.84   (eV)          EXC
  0.110E+06          18.72   (eV)          EXC
  0.220E+05          20.00   (eV)          EXC
```

```
  0.771E+04          20.65   (eV)          EXC
  0.000E+00           4.90   (eV)          EXC
  0.399E+05          21.56   (eV)          ionisation
 ------------------------------------------------------------------------
-------------
    25.0000       V/cm/torr   (    77.6398     Td)
 COLLISION FREQUENCIES in s-1.torr-1 (at 300 K)
 ------------------------------------------------------------------------
-------------
  0.908E+09           0.00   (eV)          elastique
  0.192E+07           8.31   (eV)          EXC
  0.413E+07           8.44   (eV)          EXC

  0.642E+07           9.69   (eV)          EXC
  0.100E+08          10.00   (eV)          EXC
  0.127E+07          11.00   (eV)          EXC
  0.168E+07          11.70   (eV)          EXC
  0.000E+00           3.44   (eV)          EXE
  0.959E+07          12.12   (eV)          ionisation
  0.963E+09           0.00   (eV)          elastique
  0.482E+06          16.62   (eV)          EXC
  0.866E+05          16.67   (eV)          EXC
  0.373E+06          16.84   (eV)          EXC
  0.263E+06          18.72   (eV)          EXC
  0.587E+05          20.00   (eV)          EXC
  0.218E+05          20.65   (eV)          EXC
  0.000E+00           4.90   (eV)          EXC
  0.133E+06          21.56   (eV)          ionisation
 ------------------------------------------------------------------------
-------------
    30.0000       V/cm/torr   (    93.1677     Td)
 COLLISION FREQUENCIES in s-1.torr-1 (at 300 K)
 ------------------------------------------------------------------------
-------------
  0.910E+09           0.00   (eV)          elastique
  0.214E+07           8.31   (eV)          EXC
  0.528E+07           8.44   (eV)          EXC
  0.795E+07           9.69   (eV)          EXC
  0.127E+08          10.00   (eV)          EXC
  0.162E+07          11.00   (eV)          EXC
  0.248E+07          11.70   (eV)          EXC
  0.000E+00           3.44   (eV)          EXE
  0.140E+08          12.12   (eV)          ionisation
  0.101E+10           0.00   (eV)          elastique
  0.793E+06          16.62   (eV)          EXC
  0.148E+06          16.67   (eV)          EXC
  0.704E+06          16.84   (eV)          EXC
  0.489E+06          18.72   (eV)          EXC
  0.118E+06          20.00   (eV)          EXC
  0.454E+05          20.65   (eV)          EXC
  0.000E+00           4.90   (eV)          EXC
  0.319E+06          21.56   (eV)          ionisation
```

```
------------------------------------------------------------------------
------------
    35.0000        V/cm/torr    (     108.696      Td)
 COLLISION FREQUENCIES in s-1.torr-1 (at 300 K)
 ------------------------------------------------------------------------
------------
  0.910E+09             0.00    (eV)          elastique
  0.233E+07             8.31    (eV)          EXC
  0.647E+07             8.44    (eV)          EXC
  0.945E+07             9.69    (eV)          EXC
  0.154E+08            10.00    (eV)          EXC
  0.195E+07            11.00    (eV)          EXC
  0.338E+07            11.70    (eV)          EXC
  0.000E+00             3.44    (eV)          EXE
  0.190E+08            12.12    (eV)          ionisation
  0.106E+10             0.00    (eV)          elastique
  0.116E+07            16.62    (eV)          EXC
  0.225E+06            16.67    (eV)          EXC
  0.116E+07            16.84    (eV)          EXC
  0.782E+06            18.72    (eV)          EXC
  0.202E+06            20.00    (eV)          EXC
  0.793E+05            20.65    (eV)          EXC
  0.000E+00             4.90    (eV)          EXC
  0.626E+06            21.56    (eV)          ionisation
 ------------------------------------------------------------------------
------------
    40.0000        V/cm/torr    (     124.224      Td)
 COLLISION FREQUENCIES in s-1.torr-1 (at 300 K)
 ------------------------------------------------------------------------
------------
  0.908E+09             0.00    (eV)          elastique
  0.249E+07             8.31    (eV)          EXC
  0.767E+07             8.44    (eV)          EXC
  0.109E+08             9.69    (eV)          EXC
  0.181E+08            10.00    (eV)          EXC
  0.227E+07            11.00    (eV)          EXC
  0.437E+07            11.70    (eV)          EXC
  0.000E+00             3.44    (eV)          EXE
  0.244E+08            12.12    (eV)          ionisation
  0.111E+10             0.00    (eV)          elastique
  0.158E+07            16.62    (eV)          EXC
  0.314E+06            16.67    (eV)          EXC
  0.173E+07            16.84    (eV)          EXC
  0.114E+07            18.72    (eV)          EXC
  0.309E+06            20.00    (eV)          EXC
  0.123E+06            20.65    (eV)          EXC
  0.000E+00             4.90    (eV)          EXC
  0.108E+07            21.56    (eV)          ionisation
 ------------------------------------------------------------------------
------------
```

45.0000 V/cm/torr (139.752 Td)
COLLISION FREQUENCIES in s-1.torr-1 (at 300 K)

0.904E+09	0.00	(eV)	elastique
0.262E+07	8.31	(eV)	EXC
0.888E+07	8.44	(eV)	EXC
0.123E+08	9.69	(eV)	EXC
0.207E+08	10.00	(eV)	EXC
0.257E+07	11.00	(eV)	EXC
0.543E+07	11.70	(eV)	EXC
0.000E+00	3.44	(eV)	EXE
0.302E+08	12.12	(eV)	ionisation
0.116E+10	0.00	(eV)	elastique
0.202E+07	16.62	(eV)	EXC
0.415E+06	16.67	(eV)	EXC
0.241E+07	16.84	(eV)	EXC
0.155E+07	18.72	(eV)	EXC
0.437E+06	20.00	(eV)	EXC
0.175E+06	20.65	(eV)	EXC
0.000E+00	4.90	(eV)	EXC
0.169E+07	21.56	(eV)	ionisation

50.0000 V/cm/torr (155.280 Td)
COLLISION FREQUENCIES in s-1.torr-1 (at 300 K)

0.899E+09	0.00	(eV)	elastique
0.273E+07	8.31	(eV)	EXC
0.101E+08	8.44	(eV)	EXC
0.136E+08	9.69	(eV)	EXC
0.232E+08	10.00	(eV)	EXC
0.285E+07	11.00	(eV)	EXC
0.656E+07	11.70	(eV)	EXC
0.000E+00	3.44	(eV)	EXE
0.363E+08	12.12	(eV)	ionisation
0.120E+10	0.00	(eV)	elastique
0.249E+07	16.62	(eV)	EXC
0.524E+06	16.67	(eV)	EXC
0.320E+07	16.84	(eV)	EXC
0.201E+07	18.72	(eV)	EXC
0.584E+06	20.00	(eV)	EXC
0.236E+06	20.65	(eV)	EXC
0.000E+00	4.90	(eV)	EXC
0.248E+07	21.56	(eV)	ionisation

60.0000 V/cm/torr (186.335 Td)
COLLISION FREQUENCIES in s-1.torr-1 (at 300 K)

```
 ------------------------------------------------------------------------
-------------
  0.888E+09            0.00   (eV)          elastique
  0.291E+07            8.31   (eV)          EXC
  0.125E+08            8.44   (eV)          EXC
  0.161E+08            9.69   (eV)          EXC
  0.280E+08           10.00   (eV)          EXC
  0.336E+07           11.00   (eV)          EXC
  0.895E+07           11.70   (eV)          EXC
  0.000E+00            3.44   (eV)          EXE
  0.493E+08           12.12   (eV)          ionisation
  0.129E+10            0.00   (eV)          elastique
  0.347E+07           16.62   (eV)          EXC
  0.766E+06           16.67   (eV)          EXC
  0.507E+07           16.84   (eV)          EXC
  0.302E+07           18.72   (eV)          EXC
  0.929E+06           20.00   (eV)          EXC
  0.376E+06           20.65   (eV)          EXC
  0.000E+00            4.90   (eV)          EXC
  0.461E+07           21.56   (eV)          ionisation
 ------------------------------------------------------------------------
-------------
    70.0000       V/cm/torr   (    217.391     Td)
 COLLISION FREQUENCIES in s-1.torr-1 (at 300 K)
 ------------------------------------------------------------------------
-------------
  0.874E+09            0.00   (eV)          elastique
  0.303E+07            8.31   (eV)          EXC
  0.149E+08            8.44   (eV)          EXC
  0.184E+08            9.69   (eV)          EXC
  0.325E+08           10.00   (eV)          EXC
  0.380E+07           11.00   (eV)          EXC
  0.115E+08           11.70   (eV)          EXC
  0.000E+00            3.44   (eV)          EXE
  0.629E+08           12.12   (eV)          ionisation
  0.137E+10            0.00   (eV)          elastique
  0.447E+07           16.62   (eV)          EXC
  0.103E+07           16.67   (eV)          EXC
  0.726E+07           16.84   (eV)          EXC
  0.411E+07           18.72   (eV)          EXC
  0.132E+07           20.00   (eV)          EXC
  0.535E+06           20.65   (eV)          EXC
  0.000E+00            4.90   (eV)          EXC
  0.752E+07           21.56   (eV)          ionisation
 ------------------------------------------------------------------------
-------------
    80.0000       V/cm/torr   (    248.447     Td)
 COLLISION FREQUENCIES in s-1.torr-1 (at 300 K)
 ------------------------------------------------------------------------
-------------
  0.860E+09            0.00   (eV)          elastique
  0.311E+07            8.31   (eV)          EXC
```

```
  0.172E+08            8.44   (eV)          EXC
  0.205E+08            9.69   (eV)          EXC
  0.368E+08           10.00   (eV)          EXC
  0.418E+07           11.00   (eV)          EXC
  0.141E+08           11.70   (eV)          EXC
  0.000E+00            3.44   (eV)          EXE
  0.769E+08           12.12   (eV)          ionisation
  0.144E+10            0.00   (eV)          elastique
  0.546E+07           16.62   (eV)          EXC
  0.130E+07           16.67   (eV)          EXC
  0.970E+07           16.84   (eV)          EXC
  0.526E+07           18.72   (eV)          EXC
  0.176E+07           20.00   (eV)          EXC
  0.708E+06           20.65   (eV)          EXC
  0.000E+00            4.90   (eV)          EXC
  0.112E+08           21.56   (eV)          ionisation
 ------------------------------------------------------------------
-------------
    90.0000       V/cm/torr   (    279.503     Td)
 COLLISION FREQUENCIES in s-1.torr-1 (at 300 K)
 ------------------------------------------------------------------
-------------
  0.846E+09            0.00   (eV)          elastique
  0.316E+07            8.31   (eV)          EXC
  0.194E+08            8.44   (eV)          EXC
  0.224E+08            9.69   (eV)          EXC
  0.407E+08           10.00   (eV)          EXC
  0.451E+07           11.00   (eV)          EXC
  0.167E+08           11.70   (eV)          EXC
  0.000E+00            3.44   (eV)          EXE
  0.912E+08           12.12   (eV)          ionisation
  0.151E+10            0.00   (eV)          elastique
  0.642E+07           16.62   (eV)          EXC
  0.159E+07           16.67   (eV)          EXC
  0.123E+08           16.84   (eV)          EXC
  0.643E+07           18.72   (eV)          EXC
  0.222E+07           20.00   (eV)          EXC
  0.887E+06           20.65   (eV)          EXC
  0.000E+00            4.90   (eV)          EXC
  0.157E+08           21.56   (eV)          ionisation
 ------------------------------------------------------------------
-------------
    100.000       V/cm/torr   (    310.559     Td)
 COLLISION FREQUENCIES in s-1.torr-1 (at 300 K)
 ------------------------------------------------------------------
-------------
  0.832E+09            0.00   (eV)          elastique
  0.319E+07            8.31   (eV)          EXC
  0.215E+08            8.44   (eV)          EXC
  0.242E+08            9.69   (eV)          EXC
  0.444E+08           10.00   (eV)          EXC
  0.479E+07           11.00   (eV)          EXC
```

```
  0.194E+08          11.70   (eV)          EXC
  0.000E+00           3.44   (eV)          EXE
  0.106E+09          12.12   (eV)          ionisation
  0.157E+10           0.00   (eV)          elastique
  0.736E+07          16.62   (eV)          EXC
  0.188E+07          16.67   (eV)          EXC
  0.151E+08          16.84   (eV)          EXC
  0.761E+07          18.72   (eV)          EXC
  0.271E+07          20.00   (eV)          EXC
  0.107E+07          20.65   (eV)          EXC
  0.000E+00           4.90   (eV)          EXC
  0.208E+08          21.56   (eV)          ionisation
 ------------------------------------------------------------------
-------------
    150.000       V/cm/torr   (    465.839     Td)
 COLLISION FREQUENCIES in s-1.torr-1 (at 300 K)
 ------------------------------------------------------------------
-------------
  0.770E+09           0.00   (eV)          elastique
  0.309E+07           8.31   (eV)          EXC
  0.309E+08           8.44   (eV)          EXC
  0.310E+08           9.69   (eV)          EXC
  0.591E+08          10.00   (eV)          EXC
  0.564E+07          11.00   (eV)          EXC
  0.322E+08          11.70   (eV)          EXC
  0.000E+00           3.44   (eV)          EXE
  0.177E+09          12.12   (eV)          ionisation
  0.184E+10           0.00   (eV)          elastique
  0.113E+08          16.62   (eV)          EXC
  0.329E+07          16.67   (eV)          EXC
  0.301E+08          16.84   (eV)          EXC
  0.131E+08          18.72   (eV)          EXC
  0.523E+07          20.00   (eV)          EXC
  0.197E+07          20.65   (eV)          EXC
  0.000E+00           4.90   (eV)          EXC
  0.563E+08          21.56   (eV)          ionisation
 ------------------------------------------------------------------
-------------
    200.000       V/cm/torr   (    621.118     Td)
 COLLISION FREQUENCIES in s-1.torr-1 (at 300 K)
 ------------------------------------------------------------------
-------------
  0.720E+09           0.00   (eV)          elastique
  0.281E+07           8.31   (eV)          EXC
  0.384E+08           8.44   (eV)          EXC
  0.354E+08           9.69   (eV)          EXC
  0.694E+08          10.00   (eV)          EXC
  0.593E+07          11.00   (eV)          EXC
  0.439E+08          11.70   (eV)          EXC
  0.000E+00           3.44   (eV)          EXE
  0.246E+09          12.12   (eV)          ionisation
  0.204E+10           0.00   (eV)          elastique
```

0.143E+08	16.62	(eV)	EXC
0.456E+07	16.67	(eV)	EXC
0.451E+08	16.84	(eV)	EXC
0.176E+08	18.72	(eV)	EXC
0.767E+07	20.00	(eV)	EXC
0.274E+07	20.65	(eV)	EXC
0.000E+00	4.90	(eV)	EXC
0.104E+09	21.56	(eV)	ionisation

250.000 V/cm/torr (776.398 Td)

COLLISION FREQUENCIES in s-1.torr-1 (at 300 K)

0.681E+09	0.00	(eV)	elastique
0.254E+07	8.31	(eV)	EXC
0.446E+08	8.44	(eV)	EXC
0.384E+08	9.69	(eV)	EXC
0.766E+08	10.00	(eV)	EXC
0.592E+07	11.00	(eV)	EXC
0.540E+08	11.70	(eV)	EXC
0.000E+00	3.44	(eV)	EXE
0.310E+09	12.12	(eV)	ionisation
0.218E+10	0.00	(eV)	elastique
0.165E+08	16.62	(eV)	EXC
0.568E+07	16.67	(eV)	EXC
0.590E+08	16.84	(eV)	EXC
0.211E+08	18.72	(eV)	EXC
0.992E+07	20.00	(eV)	EXC
0.337E+07	20.65	(eV)	EXC
0.000E+00	4.90	(eV)	EXC
0.160E+09	21.56	(eV)	ionisation

300.000 V/cm/torr (931.677 Td)

COLLISION FREQUENCIES in s-1.torr-1 (at 300 K)

0.650E+09	0.00	(eV)	elastique
0.224E+07	8.31	(eV)	EXC
0.496E+08	8.44	(eV)	EXC
0.404E+08	9.69	(eV)	EXC
0.816E+08	10.00	(eV)	EXC
0.575E+07	11.00	(eV)	EXC
0.628E+08	11.70	(eV)	EXC
0.000E+00	3.44	(eV)	EXE
0.370E+09	12.12	(eV)	ionisation
0.228E+10	0.00	(eV)	elastique
0.181E+08	16.62	(eV)	EXC
0.664E+07	16.67	(eV)	EXC
0.717E+08	16.84	(eV)	EXC
0.239E+08	18.72	(eV)	EXC

```
  0.119E+08            20.00   (eV)          EXC
  0.387E+07            20.65   (eV)          EXC
  0.000E+00             4.90   (eV)          EXC
  0.222E+09            21.56   (eV)          ionisation
 ------------------------------------------------------------------------
-------------
    350.000       V/cm/torr   (    1086.96     Td)
 COLLISION FREQUENCIES in s-1.torr-1 (at 300 K)
 ------------------------------------------------------------------------
-------------
  0.625E+09             0.00   (eV)          elastique
  0.200E+07             8.31   (eV)          EXC
  0.536E+08             8.44   (eV)          EXC
  0.417E+08             9.69   (eV)          EXC
  0.851E+08            10.00   (eV)          EXC
  0.548E+07            11.00   (eV)          EXC
  0.703E+08            11.70   (eV)          EXC
  0.000E+00             3.44   (eV)          EXE
  0.427E+09            12.12   (eV)          ionisation
  0.235E+10             0.00   (eV)          elastique
  0.193E+08            16.62   (eV)          EXC
  0.747E+07            16.67   (eV)          EXC
  0.829E+08            16.84   (eV)          EXC
  0.259E+08            18.72   (eV)          EXC
  0.137E+08            20.00   (eV)          EXC
  0.426E+07            20.65   (eV)          EXC
  0.000E+00             4.90   (eV)          EXC
  0.286E+09            21.56   (eV)          ionisation
 ------------------------------------------------------------------------
-------------
    400.000       V/cm/torr   (    1242.24     Td)
 COLLISION FREQUENCIES in s-1.torr-1 (at 300 K)
 ------------------------------------------------------------------------
-------------
  0.605E+09             0.00   (eV)          elastique
  0.177E+07             8.31   (eV)          EXC
  0.569E+08             8.44   (eV)          EXC
  0.426E+08             9.69   (eV)          EXC
  0.876E+08            10.00   (eV)          EXC
  0.519E+07            11.00   (eV)          EXC
  0.767E+08            11.70   (eV)          EXC
  0.000E+00             3.44   (eV)          EXE
  0.479E+09            12.12   (eV)          ionisation
  0.239E+10             0.00   (eV)          elastique
  0.202E+08            16.62   (eV)          EXC
  0.817E+07            16.67   (eV)          EXC
  0.928E+08            16.84   (eV)          EXC
  0.275E+08            18.72   (eV)          EXC
  0.152E+08            20.00   (eV)          EXC
  0.456E+07            20.65   (eV)          EXC
  0.000E+00             4.90   (eV)          EXC
  0.352E+09            21.56   (eV)          ionisation
```

```
 ------------------------------------------------------------------------
-------------
    450.000       V/cm/torr   (    1397.52     Td)
 COLLISION FREQUENCIES in s-1.torr-1 (at 300 K)
 ------------------------------------------------------------------------
-------------
  0.587E+09            0.00   (eV)          elastique
  0.157E+07            8.31   (eV)          EXC
  0.595E+08            8.44   (eV)          EXC
  0.431E+08            9.69   (eV)          EXC
  0.892E+08           10.00   (eV)          EXC
  0.487E+07           11.00   (eV)          EXC
  0.823E+08           11.70   (eV)          EXC
  0.000E+00            3.44   (eV)          EXE
  0.531E+09           12.12   (eV)          ionisation
  0.242E+10            0.00   (eV)          elastique
  0.208E+08           16.62   (eV)          EXC
  0.880E+07           16.67   (eV)          EXC
  0.102E+09           16.84   (eV)          EXC
  0.287E+08           18.72   (eV)          EXC
  0.165E+08           20.00   (eV)          EXC
  0.480E+07           20.65   (eV)          EXC
  0.000E+00            4.90   (eV)          EXC
  0.420E+09           21.56   (eV)          ionisation
 ------------------------------------------------------------------------
-------------
    500.000       V/cm/torr   (    1552.80     Td)
 COLLISION FREQUENCIES in s-1.torr-1 (at 300 K)
 ------------------------------------------------------------------------
-------------
  0.572E+09            0.00   (eV)          elastique
  0.142E+07            8.31   (eV)          EXC
  0.614E+08            8.44   (eV)          EXC
  0.434E+08            9.69   (eV)          EXC
  0.902E+08           10.00   (eV)          EXC
  0.457E+07           11.00   (eV)          EXC
  0.868E+08           11.70   (eV)          EXC
  0.000E+00            3.44   (eV)          EXE
  0.577E+09           12.12   (eV)          ionisation
  0.243E+10            0.00   (eV)          elastique
  0.212E+08           16.62   (eV)          EXC
  0.931E+07           16.67   (eV)          EXC
  0.109E+09           16.84   (eV)          EXC
  0.296E+08           18.72   (eV)          EXC
  0.176E+08           20.00   (eV)          EXC
  0.498E+07           20.65   (eV)          EXC
  0.000E+00            4.90   (eV)          EXC
  0.484E+09           21.56   (eV)          ionisation
 ------------------------------------------------------------------------
-------------
    550.000       V/cm/torr   (    1708.07     Td)
 COLLISION FREQUENCIES in s-1.torr-1 (at 300 K)
```

```
 ------------------------------------------------------------------------
-------------
  0.559E+09            0.00   (eV)          elastique
  0.127E+07            8.31   (eV)          EXC
  0.629E+08            8.44   (eV)          EXC
  0.434E+08            9.69   (eV)          EXC
  0.908E+08           10.00   (eV)          EXC
  0.426E+07           11.00   (eV)          EXC
  0.907E+08           11.70   (eV)          EXC
  0.000E+00            3.44   (eV)          EXE
  0.622E+09           12.12   (eV)          ionisation
  0.242E+10            0.00   (eV)          elastique
  0.214E+08           16.62   (eV)          EXC
  0.977E+07           16.67   (eV)          EXC
  0.116E+09           16.84   (eV)          EXC
  0.302E+08           18.72   (eV)          EXC
  0.186E+08           20.00   (eV)          EXC
  0.512E+07           20.65   (eV)          EXC
  0.000E+00            4.90   (eV)          EXC
  0.551E+09           21.56   (eV)          ionisation
 ------------------------------------------------------------------------
-------------
    600.000       V/cm/torr   (    1863.35     Td)
 COLLISION FREQUENCIES in s-1.torr-1 (at 300 K)
 ------------------------------------------------------------------------
-------------
  0.548E+09            0.00   (eV)          elastique
  0.114E+07            8.31   (eV)          EXC
  0.638E+08            8.44   (eV)          EXC
  0.434E+08            9.69   (eV)          EXC
  0.910E+08           10.00   (eV)          EXC
  0.396E+07           11.00   (eV)          EXC
  0.939E+08           11.70   (eV)          EXC
  0.000E+00            3.44   (eV)          EXE
  0.663E+09           12.12   (eV)          ionisation
  0.241E+10            0.00   (eV)          elastique
  0.215E+08           16.62   (eV)          EXC
  0.102E+08           16.67   (eV)          EXC
  0.122E+09           16.84   (eV)          EXC
  0.307E+08           18.72   (eV)          EXC

  0.194E+08           20.00   (eV)          EXC
  0.522E+07           20.65   (eV)          EXC
  0.000E+00            4.90   (eV)          EXC
  0.615E+09           21.56   (eV)          ionisation
 ------------------------------------------------------------------------
-------------
    650.000       V/cm/torr   (    2018.63     Td)
 COLLISION FREQUENCIES in s-1.torr-1 (at 300 K)
 ------------------------------------------------------------------------
-------------
  0.538E+09            0.00   (eV)          elastique
```

```
  0.102E+07            8.31   (eV)          EXC
  0.644E+08            8.44   (eV)          EXC
  0.432E+08            9.69   (eV)          EXC
  0.909E+08           10.00   (eV)          EXC
  0.368E+07           11.00   (eV)          EXC
  0.967E+08           11.70   (eV)          EXC
  0.000E+00            3.44   (eV)          EXE
  0.702E+09           12.12   (eV)          ionisation
  0.239E+10            0.00   (eV)          elastique
  0.215E+08           16.62   (eV)          EXC
  0.105E+08           16.67   (eV)          EXC
  0.127E+09           16.84   (eV)          EXC
  0.310E+08           18.72   (eV)          EXC
  0.201E+08           20.00   (eV)          EXC
  0.529E+07           20.65   (eV)          EXC
  0.000E+00            4.90   (eV)          EXC
  0.678E+09           21.56   (eV)          ionisation
 ------------------------------------------------------------------
------------
    700.000       V/cm/torr   (    2173.91     Td)
 COLLISION FREQUENCIES in s-1.torr-1 (at 300 K)
 ------------------------------------------------------------------
------------
  0.529E+09            0.00   (eV)          elastique
  0.926E+06            8.31   (eV)          EXC
  0.644E+08            8.44   (eV)          EXC
  0.429E+08            9.69   (eV)          EXC
  0.906E+08           10.00   (eV)          EXC
  0.342E+07           11.00   (eV)          EXC
  0.988E+08           11.70   (eV)          EXC
  0.000E+00            3.44   (eV)          EXE
  0.739E+09           12.12   (eV)          ionisation
  0.236E+10            0.00   (eV)          elastique
  0.214E+08           16.62   (eV)          EXC
  0.108E+08           16.67   (eV)          EXC
  0.132E+09           16.84   (eV)          EXC
  0.311E+08           18.72   (eV)          EXC
  0.207E+08           20.00   (eV)          EXC
  0.534E+07           20.65   (eV)          EXC
  0.000E+00            4.90   (eV)          EXC
  0.739E+09           21.56   (eV)          ionisation
 ------------------------------------------------------------------
------------
    750.000       V/cm/torr   (    2329.19     Td)
 COLLISION FREQUENCIES in s-1.torr-1 (at 300 K)
 ------------------------------------------------------------------
------------
  0.522E+09            0.00   (eV)          elastique
  0.841E+06            8.31   (eV)          EXC
  0.642E+08            8.44   (eV)          EXC
  0.426E+08            9.69   (eV)          EXC
  0.901E+08           10.00   (eV)          EXC
```

```
  0.319E+07          11.00   (eV)          EXC
  0.101E+09          11.70   (eV)          EXC
  0.000E+00           3.44   (eV)          EXE
  0.773E+09          12.12   (eV)          ionisation
  0.232E+10           0.00   (eV)          elastique
  0.212E+08          16.62   (eV)          EXC
  0.110E+08          16.67   (eV)          EXC
  0.135E+09          16.84   (eV)          EXC
  0.312E+08          18.72   (eV)          EXC
  0.212E+08          20.00   (eV)          EXC
  0.537E+07          20.65   (eV)          EXC
  0.000E+00           4.90   (eV)          EXC
  0.797E+09          21.56   (eV)          ionisation
 ------------------------------------------------------------------
-------------
    800.000       V/cm/torr   (    2484.47     Td)
 COLLISION FREQUENCIES in s-1.torr-1 (at 300 K)
 ------------------------------------------------------------------
-------------
  0.514E+09           0.00   (eV)          elastique
  0.773E+06           8.31   (eV)          EXC
  0.638E+08           8.44   (eV)          EXC
  0.422E+08           9.69   (eV)          EXC
  0.895E+08          10.00   (eV)          EXC
  0.296E+07          11.00   (eV)          EXC
  0.102E+09          11.70   (eV)          EXC
  0.000E+00           3.44   (eV)          EXE
  0.805E+09          12.12   (eV)          ionisation
  0.229E+10           0.00   (eV)          elastique
  0.209E+08          16.62   (eV)          EXC
  0.112E+08          16.67   (eV)          EXC
  0.139E+09          16.84   (eV)          EXC
  0.312E+08          18.72   (eV)          EXC
  0.216E+08          20.00   (eV)          EXC
  0.538E+07          20.65   (eV)          EXC
  0.000E+00           4.90   (eV)          EXC
  0.853E+09          21.56   (eV)          ionisation
 ------------------------------------------------------------------
-------------
    850.000       V/cm/torr   (    2639.75     Td)
 COLLISION FREQUENCIES in s-1.torr-1 (at 300 K)
 ------------------------------------------------------------------
-------------
  0.508E+09           0.00   (eV)          elastique
  0.707E+06           8.31   (eV)          EXC
  0.629E+08           8.44   (eV)          EXC
  0.418E+08           9.69   (eV)          EXC
  0.888E+08          10.00   (eV)          EXC
  0.276E+07          11.00   (eV)          EXC
  0.103E+09          11.70   (eV)          EXC
  0.000E+00           3.44   (eV)          EXE
  0.834E+09          12.12   (eV)          ionisation
```

```
  0.224E+10            0.00   (eV)          elastique
  0.206E+08           16.62   (eV)          EXC
  0.114E+08           16.67   (eV)          EXC
  0.141E+09           16.84   (eV)          EXC
  0.311E+08           18.72   (eV)          EXC
  0.218E+08           20.00   (eV)          EXC
  0.538E+07           20.65   (eV)          EXC
  0.000E+00            4.90   (eV)          EXC
  0.906E+09           21.56   (eV)          ionisation
 ------------------------------------------------------------------------
-------------
    900.000       V/cm/torr   (    2795.03     Td)
 COLLISION FREQUENCIES in s-1.torr-1 (at 300 K)
 ------------------------------------------------------------------------
-------------
  0.503E+09            0.00   (eV)          elastique
  0.648E+06            8.31   (eV)          EXC
  0.620E+08            8.44   (eV)          EXC
  0.413E+08            9.69   (eV)          EXC
  0.880E+08           10.00   (eV)          EXC
  0.258E+07           11.00   (eV)          EXC
  0.104E+09           11.70   (eV)          EXC
  0.000E+00            3.44   (eV)          EXE
  0.861E+09           12.12   (eV)          ionisation
  0.220E+10            0.00   (eV)          elastique
  0.202E+08           16.62   (eV)          EXC
  0.115E+08           16.67   (eV)          EXC
  0.144E+09           16.84   (eV)          EXC
  0.310E+08           18.72   (eV)          EXC
  0.220E+08           20.00   (eV)          EXC
  0.537E+07           20.65   (eV)          EXC
  0.000E+00            4.90   (eV)          EXC
  0.956E+09           21.56   (eV)          ionisation
 ------------------------------------------------------------------------
-------------
    950.000       V/cm/torr   (    2950.31     Td)
 COLLISION FREQUENCIES in s-1.torr-1 (at 300 K)
 ------------------------------------------------------------------------
-------------
  0.497E+09            0.00   (eV)          elastique
  0.594E+06            8.31   (eV)          EXC
  0.609E+08            8.44   (eV)          EXC
  0.409E+08            9.69   (eV)          EXC
  0.871E+08           10.00   (eV)          EXC
  0.241E+07           11.00   (eV)          EXC
  0.104E+09           11.70   (eV)          EXC
  0.000E+00            3.44   (eV)          EXE
  0.885E+09           12.12   (eV)          ionisation
  0.216E+10            0.00   (eV)          elastique
  0.198E+08           16.62   (eV)          EXC
  0.116E+08           16.67   (eV)          EXC
  0.145E+09           16.84   (eV)          EXC
```

```
  0.308E+08            18.72   (eV)          EXC
  0.222E+08            20.00   (eV)          EXC
  0.535E+07            20.65   (eV)          EXC
  0.000E+00             4.90   (eV)          EXC
  0.100E+10            21.56   (eV)          ionisation
 ------------------------------------------------------------------------
-------------
    1000.00       V/cm/torr   (    3105.59     Td)
 COLLISION FREQUENCIES in s-1.torr-1 (at 300 K)
 ------------------------------------------------------------------------
-------------
  0.493E+09             0.00   (eV)          elastique
  0.546E+06             8.31   (eV)          EXC
  0.596E+08             8.44   (eV)          EXC
  0.404E+08             9.69   (eV)          EXC
  0.862E+08            10.00   (eV)          EXC
  0.225E+07            11.00   (eV)          EXC
  0.105E+09            11.70   (eV)          EXC
  0.000E+00             3.44   (eV)          EXE
  0.909E+09            12.12   (eV)          ionisation
  0.211E+10             0.00   (eV)          elastique
  0.194E+08            16.62   (eV)          EXC
  0.116E+08            16.67   (eV)          EXC
  0.147E+09            16.84   (eV)          EXC
  0.306E+08            18.72   (eV)          EXC
  0.223E+08            20.00   (eV)          EXC
  0.532E+07            20.65   (eV)          EXC
  0.000E+00             4.90   (eV)          EXC
  0.105E+10            21.56   (eV)          ionisation
 ------------------------------------------------------------------------
-------------
    1050.00       V/cm/torr   (    3260.87     Td)
 COLLISION FREQUENCIES in s-1.torr-1 (at 300 K)

 ------------------------------------------------------------------------
-------------
  0.491E+09             0.00   (eV)          elastique
  0.527E+06             8.31   (eV)          EXC
  0.592E+08             8.44   (eV)          EXC
  0.402E+08             9.69   (eV)          EXC
  0.858E+08            10.00   (eV)          EXC
  0.224E+07            11.00   (eV)          EXC
  0.104E+09            11.70   (eV)          EXC
  0.000E+00             3.44   (eV)          EXE
  0.911E+09            12.12   (eV)          ionisation
  0.210E+10             0.00   (eV)          elastique
  0.192E+08            16.62   (eV)          EXC
  0.116E+08            16.67   (eV)          EXC
  0.147E+09            16.84   (eV)          EXC
  0.304E+08            18.72   (eV)          EXC
  0.223E+08            20.00   (eV)          EXC
  0.529E+07            20.65   (eV)          EXC
```

0.000E+00	4.90	(eV)	EXC
0.106E+10	21.56	(eV)	ionisation

Appendix 3

BOLSIG output file, swarm.out[27]

```
 ------------------------------------------------------------------------
-------------
Xe_10+Ne              Xe    Ne     ( 10.0 % - 90.0 %)
 ------------------------------------------------------------------------
-------------
 Mobility: torr.cm2/V/s; Diffusion: torr.cm2/s; Energy: eV  alpha/p,
eta/p: cm-1.torr-1
 ------------------------------------------------------------------------
-------------
            2            0
 ------------------------------------------------------------------------
-------------
 E/p V/cm/torr  E/n (Td)   Mobility      Diffusion   Energy
alpha/p       al/p         al/p
 ------------------------------------------------------------------------
-------------
   0.5000E+01  0.1553E+02  0.8747E+06  0.3403E+07  0.4502E+01
0.2009E-01   0.2009E-01  0.3493E-11
   0.1000E+02  0.3106E+02  0.8184E+06  0.3535E+07  0.5159E+01
0.1170E+00   0.1170E+00  0.2922E-04
   0.1500E+02  0.4658E+02  0.7790E+06  0.3673E+07  0.5767E+01
0.2537E+00   0.2532E+00  0.5614E-03
   0.2000E+02  0.6211E+02  0.7522E+06  0.3801E+07  0.6291E+01
0.3910E+00   0.3883E+00  0.2649E-02
   0.2500E+02  0.7764E+02  0.7273E+06  0.3930E+07  0.6823E+01
0.5350E+00   0.5276E+00  0.7310E-02
   0.3000E+02  0.9317E+02  0.7055E+06  0.4056E+07  0.7342E+01
0.6773E+00   0.6622E+00  0.1505E-01
   0.3500E+02  0.1087E+03  0.6860E+06  0.4177E+07  0.7851E+01
0.8172E+00   0.7912E+00  0.2606E-01
   0.4000E+02  0.1242E+03  0.6683E+06  0.4295E+07  0.8353E+01
0.9541E+00   0.9138E+00  0.4029E-01
   0.4500E+02  0.1398E+03  0.6520E+06  0.4409E+07  0.8849E+01
0.1088E+01   0.1030E+01  0.5760E-01
   0.5000E+02  0.1553E+03  0.6370E+06  0.4519E+07  0.9339E+01
0.1219E+01   0.1141E+01  0.7779E-01
   0.6000E+02  0.1863E+03  0.6101E+06  0.4730E+07  0.1031E+02
0.1472E+01   0.1346E+01  0.1260E+00
   0.7000E+02  0.2174E+03  0.5866E+06  0.4931E+07  0.1126E+02
0.1715E+01   0.1532E+01  0.1832E+00
   0.8000E+02  0.2484E+03  0.5657E+06  0.5123E+07  0.1221E+02
0.1948E+01   0.1700E+01  0.2477E+00
   0.9000E+02  0.2795E+03  0.5470E+06  0.5307E+07  0.1315E+02
0.2171E+01   0.1853E+01  0.3181E+00
   0.1000E+03  0.3106E+03  0.5301E+06  0.5486E+07  0.1409E+02
0.2386E+01   0.1993E+01  0.3930E+00
```

```
   0.1500E+03  0.4658E+03  0.4665E+06  0.6321E+07  0.1875E+02
0.3339E+01  0.2534E+01  0.8051E+00
   0.2000E+03  0.6211E+03  0.4249E+06  0.7126E+07  0.2348E+02
0.4116E+01  0.2890E+01  0.1226E+01
   0.2500E+03  0.7764E+03  0.3962E+06  0.7951E+07  0.2836E+02
0.4745E+01  0.3128E+01  0.1617E+01
   0.3000E+03  0.9317E+03  0.3758E+06  0.8827E+07  0.3348E+02
0.5250E+01  0.3284E+01  0.1966E+01
   0.3500E+03  0.1087E+04  0.3613E+06  0.9773E+07  0.3886E+02
0.5637E+01  0.3375E+01  0.2263E+01
   0.4000E+03  0.1242E+04  0.3507E+06  0.1080E+08  0.4452E+02
0.5924E+01  0.3418E+01  0.2506E+01
   0.4500E+03  0.1398E+04  0.3427E+06  0.1196E+08  0.5073E+02
0.6163E+01  0.3441E+01  0.2722E+01
   0.5000E+03  0.1553E+04  0.3371E+06  0.1319E+08  0.5704E+02
0.6297E+01  0.3423E+01  0.2874E+01
   0.5500E+03  0.1708E+04  0.3331E+06  0.1460E+08  0.6407E+02
0.6403E+01  0.3395E+01  0.3009E+01
   0.6000E+03  0.1863E+04  0.3304E+06  0.1612E+08  0.7143E+02
0.6450E+01  0.3346E+01  0.3104E+01
   0.6500E+03  0.2019E+04  0.3287E+06  0.1777E+08  0.7917E+02
0.6460E+01  0.3288E+01  0.3172E+01
   0.7000E+03  0.2174E+04  0.3280E+06  0.1966E+08  0.8775E+02
0.6440E+01  0.3220E+01  0.3220E+01
   0.7500E+03  0.2329E+04  0.3280E+06  0.2166E+08  0.9657E+02
0.6383E+01  0.3143E+01  0.3240E+01
   0.8000E+03  0.2484E+04  0.3283E+06  0.2384E+08  0.1059E+03
0.6310E+01  0.3064E+01  0.3246E+01
   0.8500E+03  0.2640E+04  0.3296E+06  0.2626E+08  0.1161E+03
0.6209E+01  0.2976E+01  0.3233E+01
   0.9000E+03  0.2795E+04  0.3311E+06  0.2886E+08  0.1266E+03
0.6096E+01  0.2888E+01  0.3208E+01
   0.9500E+03  0.2950E+04  0.3329E+06  0.3175E+08  0.1378E+03
0.5974E+01  0.2800E+01  0.3174E+01
   0.1000E+04  0.3106E+04  0.3351E+06  0.3484E+08  0.1497E+03
0.5842E+01  0.2711E+01  0.3131E+01
   0.1050E+04  0.3261E+04  0.3371E+06  0.3870E+08  0.1596E+03
0.5558E+01  0.2573E+01  0.2985E+01
 ------------------------------------------------------------------
-------------

 ------------------------------------------------------------------
-------------
 ------------------------------------------------------------------
-------------
 Energy Deposition (%)
          18    collision processes
 ------------------------------------------------------------------
-------------
     Electric Field (V/cm/torr)
```

```
    0.5000E+01    0.1000E+02    0.1500E+02    0.2000E+02    0.2500E+02
0.3000E+02
    0.3500E+02    0.4000E+02    0.4500E+02    0.5000E+02    0.6000E+02
0.7000E+02
    0.8000E+02    0.9000E+02    0.1000E+03    0.1500E+03    0.2000E+03
0.2500E+03
    0.3000E+03    0.3500E+03    0.4000E+03    0.4500E+03    0.5000E+03
0.5500E+03
    0.6000E+03    0.6500E+03    0.7000E+03    0.7500E+03    0.8000E+03
0.8500E+03
    0.9000E+03    0.9500E+03    0.1000E+04    0.1050E+04

        0 Process: elastique
    0.1839E+00    0.5689E-01    0.2933E-01    0.1823E-01    0.1276E-01
0.9579E-02
    0.7540E-02    0.6145E-02    0.5142E-02    0.4392E-02    0.3360E-02
0.2691E-02
    0.2230E-02    0.1896E-02    0.1645E-02    0.9779E-03    0.6958E-03
0.5436E-03
    0.4493E-03    0.3852E-03    0.3387E-03    0.3051E-03    0.2774E-03
0.2565E-03
    0.2390E-03    0.2242E-03    0.2123E-03    0.2016E-03    0.1923E-03
0.1843E-03
    0.1770E-03    0.1705E-03    0.1648E-03    0.1560E-03

        1 Process: EXC
    0.1957E+02    0.9832E+01    0.6448E+01    0.4580E+01    0.3507E+01
0.2801E+01
    0.2301E+01    0.1932E+01    0.1649E+01    0.1425E+01    0.1100E+01
0.8765E+00
    0.7140E+00    0.5922E+00    0.4995E+00    0.2444E+00    0.1376E+00
0.8534E-01
    0.5507E-01    0.3747E-01    0.2620E-01    0.1886E-01    0.1396E-01
0.1046E-01
    0.7974E-02    0.6130E-02    0.4790E-02    0.3789E-02    0.3056E-02
0.2468E-02
    0.2006E-02    0.1643E-02    0.1353E-02    0.1178E-02

        1 Process: EXC
    0.1524E+02    0.1141E+02    0.9778E+01    0.8482E+01    0.7662E+01
0.7018E+01
    0.6495E+01    0.6055E+01    0.5679E+01    0.5351E+01    0.4806E+01
0.4364E+01
    0.3998E+01    0.3688E+01    0.3421E+01    0.2483E+01    0.1909E+01
0.1520E+01
    0.1238E+01    0.1023E+01    0.8551E+00    0.7234E+00    0.6152E+00
0.5265E+00
    0.4526E+00    0.3912E+00    0.3383E+00    0.2938E+00    0.2563E+00
0.2230E+00
    0.1951E+00    0.1709E+00    0.1501E+00    0.1343E+00

        1 Process: EXC
```

```
    0.2466E+02    0.2144E+02    0.1844E+02    0.1561E+02    0.1368E+02
0.1214E+02
    0.1090E+02    0.9876E+01    0.9019E+01    0.8290E+01    0.7117E+01
0.6211E+01
    0.5493E+01    0.4908E+01    0.4423E+01    0.2859E+01    0.2019E+01
0.1503E+01
    0.1158E+01    0.9133E+00    0.7348E+00    0.6014E+00    0.4985E+00
0.4176E+00
    0.3531E+00    0.3014E+00    0.2587E+00    0.2236E+00    0.1946E+00
0.1699E+00
    0.1493E+00    0.1318E+00    0.1168E+00    0.1049E+00

        1 Process: EXC
    0.2930E+02    0.2993E+02    0.2764E+02    0.2443E+02    0.2206E+02
0.2005E+02
    0.1835E+02    0.1690E+02    0.1565E+02    0.1456E+02    0.1276E+02
0.1133E+02
    0.1016E+02    0.9194E+01    0.8376E+01    0.5635E+01    0.4082E+01
0.3093E+01
    0.2414E+01    0.1924E+01    0.1561E+01    0.1286E+01    0.1071E+01
0.9008E+00
    0.7647E+00    0.6548E+00    0.5635E+00    0.4884E+00    0.4261E+00
0.3727E+00
    0.3280E+00    0.2899E+00    0.2573E+00    0.2309E+00

        1 Process: EXC
    0.2857E+01    0.3738E+01    0.3725E+01    0.3385E+01    0.3085E+01
0.2805E+01
    0.2556E+01    0.2334E+01    0.2139E+01    0.1967E+01    0.1681E+01
0.1453E+01
    0.1270E+01    0.1119E+01    0.9932E+00    0.5913E+00    0.3836E+00
0.2629E+00
    0.1869E+00    0.1363E+00    0.1018E+00    0.7716E-01    0.5961E-01
0.4645E-01
    0.3666E-01    0.2918E-01    0.2343E-01    0.1901E-01    0.1551E-01
0.1277E-01
    0.1059E-01    0.8825E-02    0.7396E-02    0.6620E-02

        1 Process: EXC
    0.9880E+00    0.2465E+01    0.3459E+01    0.3971E+01    0.4336E+01
0.4563E+01
    0.4701E+01    0.4778E+01    0.4813E+01    0.4817E+01    0.4768E+01
0.4671E+01
    0.4549E+01    0.4415E+01    0.4275E+01    0.3593E+01    0.3019E+01
0.2553E+01
    0.2173E+01    0.1859E+01    0.1599E+01    0.1387E+01    0.1205E+01
0.1053E+01
    0.9239E+00    0.8146E+00    0.7194E+00    0.6377E+00    0.5681E+00
0.5058E+00
    0.4524E+00    0.4058E+00    0.3649E+00    0.3281E+00

        1 Process: EXE
```

```
    0.0000E+00    0.0000E+00    0.0000E+00    0.0000E+00    0.0000E+00
0.0000E+00
    0.0000E+00    0.0000E+00    0.0000E+00    0.0000E+00    0.0000E+00
0.0000E+00
    0.0000E+00    0.0000E+00    0.0000E+00    0.0000E+00    0.0000E+00
0.0000E+00
    0.0000E+00    0.0000E+00    0.0000E+00    0.0000E+00    0.0000E+00
0.0000E+00
    0.0000E+00    0.0000E+00    0.0000E+00    0.0000E+00    0.0000E+00
0.0000E+00
    0.0000E+00    0.0000E+00    0.0000E+00    0.0000E+00

        2 Process: ionisation
    0.6678E+01    0.2021E+02    0.3019E+02    0.3575E+02    0.3998E+02
0.4296E+02
    0.4514E+02    0.4677E+02    0.4801E+02    0.4896E+02    0.5032E+02
0.5116E+02
    0.5171E+02    0.5205E+02    0.5225E+02    0.5214E+02    0.5144E+02
0.5065E+02
    0.4992E+02    0.4916E+02    0.4839E+02    0.4807E+02    0.4734E+02
0.4703E+02
    0.4660E+02    0.4618E+02    0.4594E+02    0.4554E+02    0.4522E+02
0.4489E+02
    0.4451E+02    0.4419E+02    0.4386E+02    0.4208E+02

        0 Process: elastique
    0.1003E+01    0.3429E+00    0.1961E+00    0.1342E+00    0.1030E+00
0.8418E-01
    0.7171E-01    0.6287E-01    0.5630E-01    0.5122E-01    0.4389E-01
0.3882E-01
    0.3510E-01    0.3223E-01    0.2994E-01    0.2282E-01    0.1884E-01
0.1611E-01
    0.1405E-01    0.1238E-01    0.1099E-01    0.9863E-02    0.8853E-02
0.8010E-02
    0.7264E-02    0.6614E-02    0.6041E-02    0.5527E-02    0.5077E-02
0.4666E-02
    0.4299E-02    0.3970E-02    0.3674E-02    0.3331E-02

        1 Process: EXC
    0.9744E-02    0.2817E+00    0.8294E+00    0.1336E+01    0.1761E+01
0.2076E+01
    0.2301E+01    0.2452E+01    0.2548E+01    0.2601E+01    0.2629E+01
0.2585E+01
    0.2507E+01    0.2410E+01    0.2306E+01    0.1796E+01    0.1399E+01
0.1108E+01
    0.8910E+00    0.7250E+00    0.5977E+00    0.4979E+00    0.4177E+00
0.3532E+00
    0.3005E+00    0.2574E+00    0.2210E+00    0.1907E+00    0.1656E+00
0.1436E+00
    0.1252E+00    0.1095E+00    0.9600E-01    0.8587E-01
```

```
        1 Process: EXC

    0.1187E-02   0.4166E-01   0.1349E+00   0.2305E+00   0.3177E+00
0.3892E+00
    0.4457E+00   0.4897E+00   0.5234E+00   0.5486E+00   0.5810E+00
0.5963E+00
    0.6005E+00   0.5975E+00   0.5899E+00   0.5221E+00   0.4477E+00
0.3824E+00
    0.3275E+00   0.2813E+00   0.2427E+00   0.2113E+00   0.1842E+00
0.1616E+00
    0.1423E+00   0.1259E+00   0.1116E+00   0.9934E-01   0.8887E-01
0.7945E-01
    0.7133E-01   0.6421E-01   0.5795E-01   0.5215E-01

        1 Process: EXC
    0.2204E-02   0.1089E+00   0.4397E+00   0.8840E+00   0.1381E+01
0.1867E+01
    0.2317E+01   0.2721E+01   0.3078E+01   0.3389E+01   0.3890E+01
0.4254E+01
    0.4512E+01   0.4689E+01   0.4803E+01   0.4824E+01   0.4464E+01
0.4014E+01
    0.3569E+01   0.3155E+01   0.2785E+01   0.2470E+01   0.2185E+01
0.1942E+01
    0.1728E+01   0.1544E+01   0.1380E+01   0.1236E+01   0.1112E+01
0.9996E+00
    0.9016E+00   0.8151E+00   0.7383E+00   0.6647E+00

        1 Process: EXC
    0.4290E-03   0.6234E-01   0.3206E+00   0.6857E+00   0.1082E+01
0.1442E+01
    0.1741E+01   0.1993E+01   0.2196E+01   0.2361E+01   0.2572E+01
0.2678E+01
    0.2721E+01   0.2718E+01   0.2688E+01   0.2332E+01   0.1937E+01
0.1598E+01
    0.1321E+01   0.1097E+01   0.9182E+00   0.7752E+00   0.6569E+00
0.5613E+00
    0.4825E+00   0.4179E+00   0.3627E+00   0.3166E+00   0.2780E+00
0.2444E+00
    0.2161E+00   0.1918E+00   0.1707E+00   0.1533E+00

        1 Process: EXC
    0.1475E-04   0.7785E-02   0.5713E-01   0.1465E+00   0.2582E+00
0.3730E+00
    0.4812E+00   0.5780E+00   0.6622E+00   0.7338E+00   0.8455E+00
0.9219E+00
    0.9724E+00   0.1004E+01   0.1021E+01   0.9958E+00   0.9029E+00
0.8009E+00
    0.7051E+00   0.6179E+00   0.5412E+00   0.4765E+00   0.4188E+00
0.3696E+00
    0.3268E+00   0.2901E+00   0.2576E+00   0.2294E+00   0.2051E+00
0.1833E+00
    0.1644E+00   0.1479E+00   0.1333E+00   0.1199E+00
```

```
        1 Process: EXC
    0.1035E-05   0.2049E-02   0.1864E-01   0.5295E-01   0.9883E-01
0.1478E+00
    0.1948E+00   0.2373E+00   0.2743E+00   0.3056E+00   0.3534E+00
0.3847E+00
    0.4036E+00   0.4136E+00   0.4171E+00   0.3866E+00   0.3324E+00
0.2808E+00
    0.2362E+00   0.1987E+00   0.1678E+00   0.1429E+00   0.1221E+00
0.1049E+00
    0.9062E-01   0.7872E-01   0.6858E-01   0.6006E-01   0.5290E-01
0.4662E-01
    0.4131E-01   0.3674E-01   0.3277E-01   0.2942E-01

        1 Process: EXC
    0.0000E+00   0.0000E+00   0.0000E+00   0.0000E+00   0.0000E+00
0.0000E+00
    0.0000E+00   0.0000E+00   0.0000E+00   0.0000E+00   0.0000E+00
0.0000E+00
    0.0000E+00   0.0000E+00   0.0000E+00   0.0000E+00   0.0000E+00
0.0000E+00
    0.0000E+00   0.0000E+00   0.0000E+00   0.0000E+00   0.0000E+00
0.0000E+00
    0.0000E+00   0.0000E+00   0.0000E+00   0.0000E+00   0.0000E+00
0.0000E+00
    0.0000E+00   0.0000E+00   0.0000E+00   0.0000E+00

        2 Process: ionisation
    0.1821E-08   0.7807E-02   0.1023E+00   0.3689E+00   0.8299E+00
0.1450E+01
    0.2190E+01   0.3013E+01   0.3892E+01   0.4807E+01   0.6693E+01
0.8589E+01
    0.1046E+02   0.1227E+02   0.1401E+02   0.2163E+02   0.2762E+02
0.3229E+02
    0.3608E+02   0.3907E+02   0.4140E+02   0.4373E+02   0.4518E+02
0.4684E+02
    0.4810E+02   0.4915E+02   0.5028E+02   0.5103E+02   0.5173E+02
0.5236E+02
    0.5281E+02   0.5325E+02   0.5362E+02   0.5150E+02

 ------------------------------------------------------------------
------------
 ------------------------------------------------------------------
------------
 Collision Frequencies (s-1.torr-1)
          18     collision processes

 ------------------------------------------------------------------
------------
     Electric Field (V/cm/torr)
    0.5000E+01   0.1000E+02   0.1500E+02   0.2000E+02   0.2500E+02
0.3000E+02
```

```
    0.3500E+02   0.4000E+02   0.4500E+02   0.5000E+02   0.6000E+02
0.7000E+02
    0.8000E+02   0.9000E+02   0.1000E+03   0.1500E+03   0.2000E+03
0.2500E+03
    0.3000E+03   0.3500E+03   0.4000E+03   0.4500E+03   0.5000E+03
0.5500E+03
    0.6000E+03   0.6500E+03   0.7000E+03   0.7500E+03   0.8000E+03
0.8500E+03
    0.9000E+03   0.9500E+03   0.1000E+04   0.1050E+04

 elastique
    0.8126E+09   0.8623E+09   0.8897E+09   0.9009E+09   0.9078E+09
0.9104E+09
    0.9102E+09   0.9079E+09   0.9041E+09   0.8993E+09   0.8875E+09
0.8742E+09
    0.8602E+09   0.8461E+09   0.8322E+09   0.7697E+09   0.7203E+09
0.6813E+09
    0.6503E+09   0.6253E+09   0.6046E+09   0.5868E+09   0.5722E+09
0.5592E+09
    0.5481E+09   0.5382E+09   0.5295E+09   0.5218E+09   0.5145E+09
0.5084E+09
    0.5027E+09   0.4974E+09   0.4926E+09   0.4912E+09

 EXC
    0.5150E+06   0.9683E+06   0.1360E+07   0.1658E+07   0.1918E+07
0.2140E+07
    0.2327E+07   0.2485E+07   0.2620E+07   0.2731E+07   0.2906E+07
0.3032E+07
    0.3110E+07   0.3157E+07   0.3186E+07   0.3087E+07   0.2814E+07
0.2543E+07
    0.2241E+07   0.1995E+07   0.1769E+07   0.1575E+07   0.1416E+07
0.1269E+07
    0.1142E+07   0.1024E+07   0.9265E+06   0.8413E+06   0.7729E+06
0.7073E+06
    0.6475E+06   0.5939E+06   0.5458E+06   0.5268E+06

 EXC
    0.3950E+06   0.1107E+07   0.2031E+07   0.3024E+07   0.4127E+07
0.5280E+07
    0.6467E+07   0.7671E+07   0.8884E+07   0.1010E+08   0.1251E+08
0.1486E+08
    0.1715E+08   0.1936E+08   0.2149E+08   0.3088E+08   0.3845E+08
0.4459E+08
    0.4960E+08   0.5363E+08   0.5685E+08   0.5949E+08   0.6142E+08
0.6286E+08
    0.6379E+08   0.6436E+08   0.6443E+08   0.6421E+08   0.6380E+08
0.6294E+08
    0.6198E+08   0.6085E+08   0.5958E+08   0.5915E+08

 EXC
    0.5565E+06   0.1811E+07   0.3336E+07   0.4848E+07   0.6416E+07
0.7955E+07
```

```
    0.9452E+07   0.1090E+08   0.1229E+08   0.1362E+08   0.1613E+08
0.1842E+08
    0.2052E+08   0.2244E+08   0.2420E+08   0.3097E+08   0.3542E+08
0.3840E+08
    0.4041E+08   0.4172E+08   0.4255E+08   0.4308E+08   0.4336E+08
0.4342E+08
    0.4335E+08   0.4319E+08   0.4290E+08   0.4258E+08   0.4220E+08
0.4177E+08
    0.4133E+08   0.4088E+08   0.4040E+08   0.4024E+08

 EXC
    0.6406E+06   0.2449E+07   0.4845E+07   0.7350E+07   0.1003E+08
0.1273E+08
    0.1542E+08   0.1807E+08   0.2066E+08   0.2319E+08   0.2803E+08
0.3255E+08
    0.3679E+08   0.4073E+08   0.4440E+08   0.5915E+08   0.6939E+08
0.7659E+08
    0.8165E+08   0.8514E+08   0.8757E+08   0.8923E+08   0.9024E+08
0.9078E+08
    0.9097E+08   0.9093E+08   0.9057E+08   0.9010E+08   0.8954E+08
0.8877E+08
    0.8798E+08   0.8712E+08   0.8621E+08   0.8583E+08

 EXC
    0.5680E+05   0.2781E+06   0.5935E+06   0.9260E+06   0.1275E+07
0.1619E+07
    0.1952E+07   0.2269E+07   0.2568E+07   0.2848E+07   0.3357E+07
0.3797E+07
    0.4179E+07   0.4506E+07   0.4787E+07   0.5643E+07   0.5927E+07
0.5917E+07
    0.5746E+07   0.5485E+07   0.5191E+07   0.4868E+07   0.4567E+07
0.4255E+07
    0.3965E+07   0.3683E+07   0.3423E+07   0.3188E+07   0.2964E+07
0.2765E+07
    0.2581E+07   0.2411E+07   0.2253E+07   0.2237E+07

 EXC
    0.1847E+05   0.1725E+06   0.5183E+06   0.1021E+07   0.1685E+07
0.2476E+07
    0.3376E+07   0.4366E+07   0.5431E+07   0.6556E+07   0.8951E+07
0.1147E+08
    0.1408E+08   0.1672E+08   0.1937E+08   0.3224E+08   0.4385E+08
0.5403E+08
    0.6283E+08   0.7033E+08   0.7668E+08   0.8227E+08   0.8680E+08
0.9071E+08
    0.9394E+08   0.9668E+08   0.9883E+08   0.1006E+09   0.1020E+09
0.1030E+09
    0.1037E+09   0.1042E+09   0.1045E+09   0.1042E+09

 EXE
    0.0000E+00   0.0000E+00   0.0000E+00   0.0000E+00   0.0000E+00
0.0000E+00
```

```
    0.0000E+00    0.0000E+00    0.0000E+00    0.0000E+00    0.0000E+00
0.0000E+00
    0.0000E+00    0.0000E+00    0.0000E+00    0.0000E+00    0.0000E+00
0.0000E+00
    0.0000E+00    0.0000E+00    0.0000E+00    0.0000E+00    0.0000E+00
0.0000E+00
    0.0000E+00    0.0000E+00    0.0000E+00    0.0000E+00    0.0000E+00
0.0000E+00
    0.0000E+00    0.0000E+00    0.0000E+00    0.0000E+00

 ionisation
    0.8785E+05    0.9574E+06    0.2958E+07    0.5842E+07    0.9594E+07
0.1402E+08
    0.1900E+08    0.2443E+08    0.3023E+08    0.3634E+08    0.4928E+08
0.6289E+08
    0.7694E+08    0.9124E+08    0.1057E+09    0.1773E+09    0.2456E+09
0.3098E+09
    0.3702E+09    0.4267E+09    0.4794E+09    0.5308E+09    0.5769E+09
0.6219E+09
    0.6635E+09    0.7025E+09    0.7394E+09    0.7730E+09    0.8050E+09
0.8339E+09
    0.8606E+09    0.8855E+09    0.9085E+09    0.9108E+09

 elastique
    0.7173E+09    0.7890E+09    0.8539E+09    0.9085E+09    0.9629E+09
0.1015E+10
    0.1065E+10    0.1113E+10    0.1159E+10    0.1203E+10    0.1288E+10
0.1367E+10
    0.1440E+10    0.1509E+10    0.1574E+10    0.1840E+10    0.2035E+10
0.2177E+10
    0.2278E+10    0.2347E+10    0.2391E+10    0.2416E+10    0.2426E+10
0.2421E+10
    0.2407E+10    0.2387E+10    0.2356E+10    0.2322E+10    0.2286E+10
0.2243E+10
    0.2201E+10    0.2156E+10    0.2111E+10    0.2096E+10

 EXC
    0.1282E+03    0.1387E+05    0.8747E+05    0.2418E+06    0.4818E+06
0.7932E+06
    0.1163E+07    0.1577E+07    0.2024E+07    0.2493E+07    0.3474E+07
0.4470E+07
    0.5460E+07    0.6423E+07    0.7356E+07    0.1134E+08    0.1431E+08
0.1651E+08
    0.1813E+08    0.1931E+08    0.2018E+08    0.2079E+08    0.2118E+08
0.2141E+08
    0.2151E+08    0.2150E+08    0.2137E+08    0.2117E+08    0.2094E+08
0.2058E+08
    0.2021E+08    0.1980E+08    0.1936E+08    0.1920E+08

 EXC
    0.1557E+02    0.2045E+04    0.1419E+05    0.4160E+05    0.8665E+05
0.1482E+06
```

```
    0.2247E+06   0.3141E+06   0.4145E+06   0.5241E+06   0.7655E+06
0.1028E+07
    0.1304E+07   0.1588E+07   0.1876E+07   0.3288E+07   0.4565E+07
0.5680E+07
    0.6644E+07   0.7467E+07   0.8170E+07   0.8795E+07   0.9311E+07
0.9768E+07
    0.1015E+08   0.1049E+08   0.1076E+08   0.1099E+08   0.1120E+08
0.1135E+08
    0.1148E+08   0.1157E+08   0.1165E+08   0.1163E+08

 EXC
    0.2862E+02   0.5291E+04   0.4576E+05   0.1579E+06   0.3728E+06
0.7038E+06
    0.1156E+07   0.1728E+07   0.2414E+07   0.3205E+07   0.5073E+07
0.7260E+07
    0.9701E+07   0.1234E+08   0.1512E+08   0.3007E+08   0.4505E+08
0.5902E+08
    0.7169E+08   0.8292E+08   0.9280E+08   0.1018E+09   0.1093E+09
0.1162E+09
    0.1221E+09   0.1273E+09   0.1317E+09   0.1354E+09   0.1388E+09
0.1414E+09
    0.1436E+09   0.1454E+09   0.1469E+09   0.1467E+09

 EXC
    0.5011E+01   0.2726E+04   0.3002E+05   0.1102E+06   0.2628E+06
0.4890E+06
    0.7816E+06   0.1139E+07   0.1549E+07   0.2008E+07   0.3018E+07
0.4112E+07
    0.5262E+07   0.6433E+07   0.7613E+07   0.1308E+08   0.1759E+08
0.2113E+08
    0.2387E+08   0.2594E+08   0.2752E+08   0.2874E+08   0.2957E+08
0.3021E+08
    0.3066E+08   0.3100E+08   0.3114E+08   0.3120E+08   0.3121E+08
0.3110E+08
    0.3096E+08   0.3078E+08   0.3057E+08   0.3043E+08

 EXC
    0.1612E+00   0.3186E+03   0.5007E+04   0.2204E+05   0.5868E+05
0.1184E+06
    0.2022E+06   0.3090E+06   0.4372E+06   0.5843E+06   0.9285E+06
0.1325E+07
    0.1760E+07   0.2223E+07   0.2706E+07   0.5227E+07   0.7674E+07
0.9916E+07
    0.1192E+08   0.1367E+08   0.1518E+08   0.1653E+08   0.1765E+08
0.1862E+08
    0.1944E+08   0.2014E+08   0.2071E+08   0.2116E+08   0.2155E+08
0.2182E+08
    0.2205E+08   0.2221E+08   0.2233E+08   0.2228E+08

 EXC
    0.1096E-01   0.8120E+02   0.1582E+04   0.7715E+04   0.2176E+05
0.4544E+05
```

```
    0.7929E+05   0.1229E+06   0.1754E+06   0.2357E+06   0.3759E+06
0.5354E+06
    0.7076E+06   0.8873E+06   0.1071E+07   0.1965E+07   0.2737E+07
0.3367E+07
    0.3869E+07   0.4258E+07   0.4560E+07   0.4802E+07   0.4983E+07
0.5120E+07
    0.5221E+07   0.5293E+07   0.5338E+07   0.5366E+07   0.5383E+07
0.5377E+07
    0.5366E+07   0.5346E+07   0.5319E+07   0.5295E+07

 EXC
    0.0000E+00   0.0000E+00   0.0000E+00   0.0000E+00   0.0000E+00
0.0000E+00
    0.0000E+00   0.0000E+00   0.0000E+00   0.0000E+00   0.0000E+00
0.0000E+00
    0.0000E+00   0.0000E+00   0.0000E+00   0.0000E+00   0.0000E+00
0.0000E+00
    0.0000E+00   0.0000E+00   0.0000E+00   0.0000E+00   0.0000E+00
0.0000E+00
    0.0000E+00   0.0000E+00   0.0000E+00   0.0000E+00   0.0000E+00
0.0000E+00
    0.0000E+00   0.0000E+00   0.0000E+00   0.0000E+00

 ionisation
    0.1528E-04   0.2391E+03   0.6561E+04   0.3985E+05   0.1329E+06
0.3185E+06
    0.6257E+06   0.1077E+07   0.1690E+07   0.2478E+07   0.4613E+07
0.7521E+07
    0.1121E+08   0.1566E+08   0.2084E+08   0.5634E+08   0.1042E+09
0.1602E+09
    0.2217E+09   0.2861E+09   0.3515E+09   0.4198E+09   0.4844E+09
0.5512E+09
    0.6153E+09   0.6775E+09   0.7393E+09   0.7970E+09   0.8526E+09
0.9059E+09
    0.9560E+09   0.1004E+10   0.1049E+10   0.1057E+10

 ------------------------------------------------------------------
-------------
 ------------------------------------------------------------------
-------------
 Collision Coefficients (cm-1.torr-1)
          18     collision processes
 ------------------------------------------------------------------
-------------
     Electric Field (V/cm/torr)
    0.5000E+01   0.1000E+02   0.1500E+02   0.2000E+02   0.2500E+02
0.3000E+02
    0.3500E+02   0.4000E+02   0.4500E+02   0.5000E+02   0.6000E+02
0.7000E+02
    0.8000E+02   0.9000E+02   0.1000E+03   0.1500E+03   0.2000E+03
0.2500E+03
```

```
    0.3000E+03   0.3500E+03   0.4000E+03   0.4500E+03   0.5000E+03
0.5500E+03
    0.6000E+03   0.6500E+03   0.7000E+03   0.7500E+03   0.8000E+03
0.8500E+03
    0.9000E+03   0.9500E+03   0.1000E+04   0.1050E+04

 elastique
    0.1858E+03   0.1054E+03   0.7614E+02   0.5988E+02   0.4992E+02
0.4302E+02
    0.3791E+02   0.3396E+02   0.3081E+02   0.2823E+02   0.2425E+02
0.2129E+02
    0.1901E+02   0.1719E+02   0.1570E+02   0.1100E+02   0.8475E+01
0.6878E+01
    0.5768E+01   0.4945E+01   0.4310E+01   0.3805E+01   0.3395E+01
0.3052E+01
    0.2764E+01   0.2519E+01   0.2306E+01   0.2121E+01   0.1959E+01
0.1814E+01
    0.1687E+01   0.1573E+01   0.1470E+01   0.1387E+01

 EXC
    0.1177E+00   0.1183E+00   0.1164E+00   0.1102E+00   0.1055E+00
0.1011E+00
    0.9691E-01   0.9298E-01   0.8928E-01   0.8573E-01   0.7939E-01
0.7384E-01
    0.6874E-01   0.6414E-01   0.6010E-01   0.4411E-01   0.3311E-01
0.2568E-01
    0.1988E-01   0.1578E-01   0.1261E-01   0.1021E-01   0.8400E-02
0.6924E-02
    0.5758E-02   0.4795E-02   0.4035E-02   0.3420E-02   0.2942E-02
0.2524E-02
    0.2173E-02   0.1878E-02   0.1629E-02   0.1488E-02

 EXC
    0.9031E-01   0.1352E+00   0.1738E+00   0.2010E+00   0.2269E+00
0.2495E+00
    0.2693E+00   0.2870E+00   0.3028E+00   0.3170E+00   0.3416E+00
0.3619E+00
    0.3790E+00   0.3933E+00   0.4054E+00   0.4412E+00   0.4524E+00
0.4502E+00
    0.4399E+00   0.4241E+00   0.4053E+00   0.3857E+00   0.3644E+00
0.3431E+00
    0.3217E+00   0.3013E+00   0.2806E+00   0.2610E+00   0.2429E+00
0.2246E+00
    0.2080E+00   0.1924E+00   0.1778E+00   0.1671E+00

 EXC
    0.1272E+00   0.2212E+00   0.2854E+00   0.3222E+00   0.3529E+00
0.3758E+00
    0.3937E+00   0.4077E+00   0.4188E+00   0.4277E+00   0.4407E+00
0.4487E+00
    0.4535E+00   0.4559E+00   0.4564E+00   0.4426E+00   0.4167E+00
0.3877E+00
```

```
    0.3584E+00   0.3299E+00   0.3033E+00   0.2793E+00   0.2572E+00
0.2370E+00
    0.2187E+00   0.2022E+00   0.1869E+00   0.1731E+00   0.1607E+00
0.1491E+00
    0.1387E+00   0.1292E+00   0.1206E+00   0.1137E+00

 EXC
    0.1465E+00   0.2993E+00   0.4146E+00   0.4885E+00   0.5515E+00
0.6015E+00
    0.6423E+00   0.6760E+00   0.7041E+00   0.7280E+00   0.7656E+00
0.7928E+00
    0.8129E+00   0.8274E+00   0.8376E+00   0.8452E+00   0.8164E+00
0.7732E+00
    0.7242E+00   0.6733E+00   0.6242E+00   0.5785E+00   0.5354E+00
0.4955E+00
    0.4588E+00   0.4256E+00   0.3945E+00   0.3663E+00   0.3409E+00
0.3168E+00
    0.2952E+00   0.2754E+00   0.2573E+00   0.2424E+00

 EXC

    0.1299E-01   0.3398E-01   0.5079E-01   0.6155E-01   0.7011E-01
0.7649E-01
    0.8132E-01   0.8488E-01   0.8752E-01   0.8941E-01   0.9171E-01
0.9248E-01
    0.9234E-01   0.9153E-01   0.9029E-01   0.8063E-01   0.6974E-01
0.5974E-01
    0.5097E-01   0.4337E-01   0.3700E-01   0.3156E-01   0.2709E-01
0.2323E-01
    0.2000E-01   0.1724E-01   0.1491E-01   0.1296E-01   0.1128E-01
0.9867E-02
    0.8661E-02   0.7622E-02   0.6724E-02   0.6319E-02

 EXC
    0.4222E-02   0.2107E-01   0.4435E-01   0.6787E-01   0.9264E-01
0.1170E+00
    0.1406E+00   0.1634E+00   0.1851E+00   0.2059E+00   0.2445E+00
0.2794E+00
    0.3111E+00   0.3396E+00   0.3654E+00   0.4607E+00   0.5160E+00
0.5454E+00
    0.5573E+00   0.5562E+00   0.5466E+00   0.5334E+00   0.5150E+00
0.4951E+00
    0.4738E+00   0.4526E+00   0.4304E+00   0.4088E+00   0.3884E+00
0.3675E+00
    0.3480E+00   0.3295E+00   0.3119E+00   0.2944E+00

 EXE
    0.0000E+00   0.0000E+00   0.0000E+00   0.0000E+00   0.0000E+00
0.0000E+00
    0.0000E+00   0.0000E+00   0.0000E+00   0.0000E+00   0.0000E+00
0.0000E+00
```

```
    0.0000E+00    0.0000E+00    0.0000E+00    0.0000E+00    0.0000E+00
0.0000E+00
    0.0000E+00    0.0000E+00    0.0000E+00    0.0000E+00    0.0000E+00
0.0000E+00
    0.0000E+00    0.0000E+00    0.0000E+00    0.0000E+00    0.0000E+00
0.0000E+00
    0.0000E+00    0.0000E+00    0.0000E+00    0.0000E+00

 ionisation
    0.2009E-01    0.1170E+00    0.2532E+00    0.3883E+00    0.5276E+00
0.6622E+00
    0.7912E+00    0.9138E+00    0.1030E+01    0.1141E+01    0.1346E+01
0.1532E+01
    0.1700E+01    0.1853E+01    0.1993E+01    0.2534E+01    0.2890E+01
0.3128E+01
    0.3284E+01    0.3375E+01    0.3418E+01    0.3441E+01    0.3423E+01
0.3395E+01
    0.3346E+01    0.3288E+01    0.3220E+01    0.3143E+01    0.3064E+01
0.2976E+01
    0.2888E+01    0.2800E+01    0.2711E+01    0.2573E+01

 elastique
    0.1640E+03    0.9640E+02    0.7307E+02    0.6039E+02    0.5296E+02
0.4795E+02
    0.4435E+02    0.4163E+02    0.3950E+02    0.3778E+02    0.3518E+02
0.3328E+02
    0.3183E+02    0.3066E+02    0.2969E+02    0.2630E+02    0.2394E+02
0.2198E+02
    0.2021E+02    0.1856E+02    0.1705E+02    0.1567E+02    0.1439E+02
0.1322E+02
    0.1214E+02    0.1117E+02    0.1026E+02    0.9441E+01    0.8703E+01
0.8006E+01
    0.7385E+01    0.6818E+01    0.6298E+01    0.5921E+01

 EXC
    0.2931E-04    0.1695E-02    0.7486E-02    0.1607E-01    0.2650E-01
0.3747E-01
    0.4845E-01    0.5901E-01    0.6899E-01    0.7826E-01    0.9489E-01
0.1089E+00
    0.1207E+00    0.1305E+00    0.1388E+00    0.1621E+00    0.1684E+00
0.1667E+00
    0.1608E+00    0.1527E+00    0.1438E+00    0.1348E+00    0.1257E+00
0.1169E+00
    0.1085E+00    0.1006E+00    0.9306E-01    0.8607E-01    0.7970E-01
0.7345E-01
    0.6782E-01    0.6260E-01    0.5776E-01    0.5425E-01

 EXC
    0.3561E-05    0.2499E-03    0.1214E-02    0.2765E-02    0.4765E-02
0.7004E-02
    0.9358E-02    0.1175E-01    0.1413E-01    0.1645E-01    0.2091E-01
0.2504E-01
```

0.2882E-01 0.3226E-01 0.3539E-01 0.4698E-01 0.5371E-01
0.5734E-01
0.5893E-01 0.5905E-01 0.5824E-01 0.5703E-01 0.5524E-01
0.5331E-01
0.5121E-01 0.4908E-01 0.4687E-01 0.4469E-01 0.4265E-01
0.4051E-01
0.3851E-01 0.3659E-01 0.3476E-01 0.3285E-01

EXC
0.6544E-05 0.6465E-03 0.3916E-02 0.1050E-01 0.2050E-01
0.3325E-01
0.4816E-01 0.6464E-01 0.8226E-01 0.1006E+00 0.1386E+00
0.1768E+00
0.2144E+00 0.2506E+00 0.2852E+00 0.4297E+00 0.5301E+00
0.5959E+00
0.6359E+00 0.6558E+00 0.6615E+00 0.6600E+00 0.6488E+00
0.6342E+00
0.6158E+00 0.5958E+00 0.5736E+00 0.5506E+00 0.5284E+00
0.5045E+00
0.4818E+00 0.4598E+00 0.4384E+00 0.4145E+00

EXC
0.1146E-05 0.3330E-03 0.2569E-02 0.7326E-02 0.1445E-01
0.2310E-01
0.3255E-01 0.4260E-01 0.5278E-01 0.6305E-01 0.8245E-01
0.1002E+00
0.1163E+00 0.1307E+00 0.1436E+00 0.1869E+00 0.2069E+00
0.2134E+00
0.2117E+00 0.2052E+00 0.1962E+00 0.1863E+00 0.1754E+00
0.1649E+00
0.1546E+00 0.1451E+00 0.1356E+00 0.1268E+00 0.1188E+00
0.1110E+00
0.1039E+00 0.9732E-01 0.9121E-01 0.8596E-01

EXC
0.3687E-07 0.3893E-04 0.4285E-03 0.1465E-02 0.3227E-02
0.5595E-02
0.8420E-02 0.1156E-01 0.1490E-01 0.1834E-01 0.2537E-01
0.3227E-01
0.3890E-01 0.4517E-01 0.5104E-01 0.7468E-01 0.9029E-01
0.1001E+00
0.1058E+00 0.1081E+00 0.1082E+00 0.1072E+00 0.1047E+00
0.1017E+00
0.9803E-01 0.9429E-01 0.9018E-01 0.8604E-01 0.8205E-01
0.7789E-01
0.7399E-01 0.7023E-01 0.6663E-01 0.6294E-01

EXC
0.2506E-08 0.9921E-05 0.1354E-03 0.5128E-03 0.1197E-02
0.2147E-02
0.3302E-02 0.4596E-02 0.5977E-02 0.7399E-02 0.1027E-01
0.1304E-01

```
    0.1564E-01   0.1803E-01   0.2020E-01   0.2808E-01   0.3220E-01
0.3400E-01
    0.3431E-01   0.3367E-01   0.3251E-01   0.3114E-01   0.2956E-01
0.2795E-01
    0.2633E-01   0.2478E-01   0.2325E-01   0.2181E-01   0.2049E-01
0.1919E-01
    0.1801E-01   0.1690E-01   0.1587E-01   0.1496E-01

 EXC
    0.0000E+00   0.0000E+00   0.0000E+00   0.0000E+00   0.0000E+00
0.0000E+00
    0.0000E+00   0.0000E+00   0.0000E+00   0.0000E+00   0.0000E+00
0.0000E+00
    0.0000E+00   0.0000E+00   0.0000E+00   0.0000E+00   0.0000E+00
0.0000E+00
    0.0000E+00   0.0000E+00   0.0000E+00   0.0000E+00   0.0000E+00
0.0000E+00
    0.0000E+00   0.0000E+00   0.0000E+00   0.0000E+00   0.0000E+00
0.0000E+00
    0.0000E+00   0.0000E+00   0.0000E+00   0.0000E+00

 ionisation
    0.3493E-11   0.2922E-04   0.5614E-03   0.2649E-02   0.7310E-02
0.1505E-01
    0.2606E-01   0.4029E-01   0.5760E-01   0.7779E-01   0.1260E+00
0.1832E+00
    0.2477E+00   0.3181E+00   0.3930E+00   0.8051E+00   0.1226E+01
0.1617E+01
    0.1966E+01   0.2263E+01   0.2506E+01   0.2722E+01   0.2874E+01
0.3009E+01
    0.3104E+01   0.3172E+01   0.3220E+01   0.3240E+01   0.3246E+01
0.3233E+01
    0.3208E+01   0.3174E+01   0.3131E+01   0.2985E+01
 ------------------------------------------------------------------
-------------
```

Appendix 4

Mobility of atomic xenon in pure xenon[23]

E/N(V-cm^2)	Mobility(cm^{2}s^{-1}V^{-1})
50e-17	0.5083
60e-17	0.5016
70e-17	0.4953
80e-17	0.4889
100e-17	0.4763
120e-17	0.4642
150e-17	0.4450
190e-17	0.4232
220e-17	0.4090
250e-17	0.3957
300e-17	0.3762
350e-17	0.3589
400e-17	0.3443

Appendix 5

Mobility of atomic xenon in pure neon[25]

E/N (V-cm^2)	Mobility (cm^{2}s^{-1}V^{-1})
15e-17	5.75
20e-17	5.75
30e-17	5.75
40e-17	5.70
50e-17	5.63
60e-17	5.51
80e-17	5.22
100e-17	4.94
120e-17	4.70
140e-17	4.40

Appendix 6

Calculation of Current Density

Consider a simple PDP cell, given in Appendix 1.

We know that, $E_1^- = \frac{V_s - V_1}{d_1}$.

Applying Gauss law in the left dielectric we get.

$$\varepsilon_1 E_1^- = \sigma_1$$

$$\text{Current density } (I) = \frac{d\sigma_1}{dt}$$

Thus we get,

$$I = \frac{d\left(\varepsilon_1 E_1^-\right)}{dt}$$

References

1. A. Von Engel, "**Electric Plasmas: Their nature and uses**"
2. J.P.Boeuf , "**Physics and Modeling of Plasma Displays**", *http://cpat.ups-tlse.fr*
3. Roger L. Johnson, Donald L. Bitzer and H. Gene Slottow "**The device characteristics of the Plasma Display Element**", *IEEE Transactions on Electron Devices vol. ED-18, No, 9,642(September 1971)*
4. H. Gene Slottow and William D. Petty "**Stability of discharge Series in the Plasma Display Panel**", *IEEE Transactions on Electron Devices vol. ED-18, No, 9,650(September 1971)*
5. William D. Petty and H. Gene Slottow "**Multiple States and Variable intensity in the Plasma Display Panel**", *IEEE Transactions on Electron Devices vol. ED-18, No. 9,654 (September 1971)*
6. H. Gene Slottow, "**The Voltage Transfer curve and stability criteria in the theory of the AC Plasma Display**", *IEEE Transactions on Electron Devices vol. ED-24, No, 7,848(July 1977)*
7. J. Meunier, Ph. Belenguer and J.P.Boeuf, "**Numerical model of an plasma display panel cell in neon xenon mixtures**", *J. Appl. Physics, 78 (2), 731(15 July 1995)*
8. Younghyun Kin, Rakhwan Kim, Hee Jae Kim, Hyeongtag Jeon and Jong-Wan Park, "**Effect of TiO_2 addition on the Secondary Electron Emission and Discharge Properties of MgO protective layer**", *Mat. Res. Soc. Symp. Proc. Vol 621 (2002)*
9. P. K. Bachmann, V. van Elsbergen, D. U. Wiechert, G. Zhong and J. Robertson, "**CVD diamond: a novel high γ-coating for plasma display**

panels", *Diamond and Related Materials, Volume 10, Issues 3-7, March-July 2001, Pages 809-817*

10. Shigeo Shionoya and William M. Yen, "**Phosphor Handbook**" *Phosphor research society*

11. Ramana Veerasingam, Robert B. Cambell and Robert T. McGrath, "**One Dimensional Single and Multipulse Simulations of the ON/OFF Voltages and the Bistable Margin for He, Xe and He/Xe filled Plasma Display Pixels",** *IEEE Transactions On Plasma Science, Vol 24, No. 6, December 1996*

12. Ramana Veerasingam, Robert B. Cambell and Robert T. McGrath, "**One Dimensional Fluid and Circuit Simulation of an AC Plasma Display Cell",** *IEEE Transactions On Plasma Science, Vol 23, No. 4, August 1995*

13. Ramana Veerasingam, Robert B. Cambell and Robert T. McGrath, "**A Two Dimensional Multispecies Fluid Model of the Plasma in an AC Plasma Display Panel",** *IEEE Transactions On Plasma Science, Vol 23, No. 4,698, August 1995*

14. Ramana Veerasingam, Robert B. Cambell and Robert T. McGrath, "**Two Dimensional Simulations of Plasma Flow ands Charge Spreading across Barrier Pixels in AC Plasma Displays",** *IEEE Transactions On Plasma Science, Vol 24, No. 6, December 1996*

15. C.Punset, J.P.Boeuf and L.C.Pitchford, "**Two Dimensional Simulation of an alternating current Matrix Plasma Display Cell: Cross Talk and other geometric effects",** *Journal of Applied Physics, Vol 83, Feb 1998*

16. Addressing and Sustaining in Alternating current Coplanar Plasma Displays Panels, "**Punset, S.Cany and J.P.Boeuf",** *Journal of Applied Physics, Vol 86 1999.*

17. G.J.M.Hagelaar, "**Modeling of Microdischarges For Display Technology",** *Proefschrift*

18. Shahid Rauf and Mark J. Kushner, **"Dynamics of a coplanar-electrode plasma display panel cell. Basic operation",** *Journal of Applied physics vol 85 no 7, April 1999,3460*

19. Shahid Rauf and Mark J. Kushner, **"Dynamics of a coplanar-electrode plasma display panel cell. Cell optimization",** *Journal of Applied physics vol 85 no 7, april 1999,3470.*

20. Byoung-Kuk Min, Hoon-Young Choi, Seok-Hyun Lee and Heung-Sik Tae, **"New combination of four-component gas He-Ne-Xe-Ar for high efficiency plasma display panel",** *Journal Vaccum Science Technology B 19(1), Jan/Feb 2001*

21. J.P.Boeuf, Th. Callegari, C. Punset, and R. Ganter, **"Modeling as a tool for Plasma Display Cell Optimization",** *Workshop Digest of the 18th International Display Research Conference, Asia Display'98 pp 209-220 (SID, 1998).*

22. E.C.Beaty and P.L.Patterson, **"Mobilities and Reaction rates of Neon ions in Neon",** *Physical Review 170, 116 (1968).*

23. P.H.Larsen and M.T.Elford, **"The mobilities of xenon ions and the derived charge transfer cross section for $Xe^{+}(^{3}P_{3/2})$ ions in xenon",** *Journal De Physics B 19 449 (1986)*

24. A.L.Ward, **"Calculation of cathode fall characteristics",** *Journal of Applied Physics, Vol 33. No. 9, September 1962*

25. H.W.Ellis, M.G. Thackston, E.W. McDaniel and E.A. Mason, **"Tranport properties of Gaseous ions",** *Atomic data and Nuclear Data tables, Vol 31, No. 1, July 1984*

26. *http://www.lexcie.zetnet.co.uk/fizzix-kinetic.htm*

27. BOLSIG, **"Boltzmann solver for the SIGLO-series 1.0"**, *CPA Toulouse and Kinema Software.*